8-2022

Development of Deep Shear Wave Velocity Profiles and an Approach to Generate Site Signature Consistent Pseudo Shear Wave Velocity Profiles in the Mississippi Embayment

Ashraf Kamal Himel
University of Arkansas, Fayetteville

Development of Deep Shear Wave Velocity Profiles and an Approach to Generate Site Signature Consistent Pseudo Shear Wave Velocity Profiles in the Mississippi Embayment

A dissertation submitted in partial fulfillment
of the requirements for the degree of
Doctor of Philosophy in Engineering with a concentration in Civil Engineering

by

Ashraf Kamal Himel
Bangladesh University of Engineering and Technology
Bachelor of Science in Civil Engineering, 2014
University of Arkansas
Masters of Science in Civil Engineering, 2018

August 2022
University of Arkansas

This dissertation is approved for recommendation to the Graduate Council.

Clinton M. Wood, PhD.
Dissertation Director

Christopher L. Liner, Ph.D.
Committee Member

Sarah V. Hernandez, Ph.D.
Committee Member

Michelle L. Barry, Ph.D.
Committee Member

Abstract

This dissertation details the development of a surface wave method (SWM) technique to generate deep shear wave velocity profiles (V_S profiles), applying this technique at 24 sites across the Mississippi embayment and developing an approach to generate pseudo site signature consistent V_S profiles from velocity functions and fundamental frequency. In the presented SWM technique, active and passive source surface wave measurements are inverted along with fundamental frequency to develop a site signature consistent V_S profile. Multiple transformation methods, including MSPAC, HRFK and FK are used to resolve experimental dispersion data from surface wave measurements. SWM V_S profile at the Central US Seismic Observatory (CUSSO) site is validated by comparing with the downhole measurements at the site. Both a-priori and blind approach parameterizations are used for the surface wave inversion. While a comparable result is found between the blind and a-priori approach, the blind approach is incapable of identifying velocity reversals. Therefore, if available, a-priori information should be used to guide the parameterization process. In the absence of a-priori information, engineering judgement, experience of local geology and iterative parameterization should be used.

Deep V_S profiles are developed at 24 sites across the Mississippi embayment utilizing the SWM technique. While the Central US Seismic Velocity Model (CUSVM) provides a continuous 3D Vs model of the embayment, significant differences in layer interfaces and shear wave velocities are observed between the measured and CUSVM modeled V_S profiles, particularly for the Memphis sand layer. Lower shear wave velocity for the deeper layers is observed in comparison to the measured SWM V_S profiles, indicating a spatial bias across the embayment. A parametric study varying the depth and velocity of the Memphis sand is conducted to observe the impact of the layer on site response. While the velocity of the Memphis sand has an impact on amplification, the depth to the Memphis sand influences both the

amplification and frequency range of the amplification. Inaccurate site characterization of the Memphis sand layer could affect the long period public infrastructures with 1 – 2 second natural period, such as highway bridges and skyscrapers.

Utilizing the 24 deep V_S profiles, velocity functions are developed for the geologic units found in the embayment. Pseudo site signature consistent deep V_S profiles are generated utilizing a layer interface model, velocity functions and fundamental frequency. Modeled V_S profiles generated using the developed approach are compared to the measured V_S profiles. While differences in the near surface characterization is observed, overall modeled V_S profiles have similar linear site response as the measured V_S profiles, i.e., capturing the site signature.

Dedication

To my parents, Abser Kamal and Hasina Zahan, and my wife, Kazi Disha. Without your support, I would not have achieved this.

And to my sisters, nephews, and in-laws. You all have been a driving force in my daily struggle.

Acknowledgements

I express my sincerest gratitude to my advisor, Dr. Clinton M. Wood. He has been a mentor, guide and friend throughout this journey. Without his support, I would not have finished my PhD. I appreciate his patience and effort to review my work and ever grateful for the financial support he has provided me throughout my PhD career. I would thank him for engaging me in numerous consultancy work as well as various academic duties. I am going to benefit from these experiences all along my professional career.

I would like to thank my committee member Dr. Hernandez for her persuasion to include more statistics into my research, Dr. Barry for her comments on geotechnical aspects of my research and Dr. Liner for his expert suggestion regarding geophysical methods. I have always benefitted from the criticisms, comments and suggestions this committee had made.

I am grateful to my fellow lab members at the geotechnical earthquake-engineering lab. Mike, Salman, Saye, Ethan, Tim, you all have been good friends and helped me learn through this whole journey.

I would like to thank Dr. Carpenter for his support by giving us access to the CUSSO site and providing us with data from the CUSSO vertical array.

Also, I am grateful to the funding agencies that made this research possible. This dissertation is based on work supported by the U.S. Geological Survey under Grant No. G18AP00078 and Arkansas department of transportation (ARDOT) grant no. TRC1603.

Above everything, I would like to thank my loving wife, Disha for her support and patience throughout this whole journey. I would also like to thank my parents, and rest of the family for their never-ending support.

Table of Contents

List of Figures

List of Tables

List of Published and Submitted Articles

Published

1.0 Himel, A. K., Wood, C. M., 2021. Developing an Updated Set of V_S Profiles for the Central United States Seismic Observatory with Estimates of Uncertainty between Different Methods, *Soil Dynamics and Earthquake Engineering* **143**. ***Chapter 2***

2.0 Himel, A. K., Wood, C. M., Rahimi, S., 2021b. Site Response Impacts of the Memphis Sand Layer within the Mississippi Embayment, in *Proceedings, Geo Extreme 2021*, Savannah, Georgia. ***Chapter 3***

3.0 Himel, A. K., Wood, C. M., 2022. Deep shear wave velocity profiles in the Mississippi embayment from surface wave measurements, *Soil Dynamics and Earthquake Engineering* **158**. ***Chapter 4***

Submitted

1.0 Himel, A. K., Wood, C. M., 2022b. An approach for developing site signature consistent deep shear wave velocity profiles for the Mississippi Embayment using generalized power-law functions, *Soil Dynamics and Earthquake Engineering* **(submitted)**. ***Chapter 5***

1. Chapter 1: Introduction

1.1 Site Characterization to Understand the Local Site Effects

September 19, 1985. A magnitude 8 (M_W=8.0) earthquake hit the coast of Mexico. Epicenter of the seismic event was registered near the coastal town Michoacán, Mexico with a VI – VII Modified Mercalli intensity scale (MMI). However, 350 km away from the epicenter, the Mexico City felt the devastation with a MMI of IX. Presence of high plasticity clay in the Mexico City basin amplified the seismic waves about 5 times of the original ground motion (Bard et al., 1988). In addition, the overall soil column structure found in the Mexico City consisting of soft lake sediments and shallow impedance boundary having a site period of 2 – 3.5 second was associated to the double resonance occurred to most 6 – 15 storied buildings (Mayoral et al., 2019). With 5000 dead and financial damage in order of billion USD, this seismic event forced engineers and seismologists to rethink about the local site effects in addition to the source and path effects of seismicity.

The series of seismic events in the Mexico City spawned more research interest centered around the site characterization methods to decipher and better understand local site effects. Much progress is made to this day to better understand site characterization. Primary focus in these research efforts have been on: (i) advancement of borehole site characterization methods, (ii) development of newer geophysics based site characterization methods without the need of boreholes known as surface wave methods (SWM), (iii) validating reliability of SWM in comparison to the borehole methods (Garofalo et al., 2016b), (iv) efforts to develop continuous/3D site characterization to better understand ground response. However, sparsity of deep site characterization to this day for many deep basin like structures, such as the Mississippi

embayment shows need to develop deep site characterization techniques to understand amplification, ground motion prediction and wave propagation studies for such geologic structures.

1.2 Research Significance

The Mississippi Embayment encompasses a large area in the central United States that covers parts of Arkansas, Missouri, Illinois, Kentucky, Tennessee, and Mississippi. The unconsolidated sedimentary deposits found in the embayment are shallow near the basin edge, being only a few meters thick near southern Illinois, but become very deep in the central and southern part of the embayment with depths up to about 1000 m near southern Memphis, Tennessee (Van Arsdale and TenBrink, 2000). Regardless of the sediment thickness, a strong impedance contrast is observed between the soil column and Paleozoic bedrock across the embayment. Local site effects, consisting of basin edge effects in the shallow portions of the embayment, which cause longer duration earthquake ground motions (Kawase, 2003; Boore, 1999), and a complex mixture of amplification/deamplification of seismic waves at different period ranges in the deeper parts of the embayment (Hashash et al., 2001; Wood et al., 2018; Woolery et al., 2016; Romero and Rix, 2005). The New Madrid Seismic Zone (NMSZ), situated in the Mississippi Embayment is a series of faults and the major source of seismicity in the embayment. Collectively, the local site effects from the deep sediments, basin edge effects from the shallow part of the embayment, and the presence of the NMSZ lead to areas in the embayment having some of the highest design ground motions in the United States (ASCE 2017). Very large earthquakes (7 – 8 M_W) occurred in the region in the past (Bakun and Hopper, 2004) and there is a 25 – 40% probability of a M_W 6+ earthquake in the next 50 years (Frankel et al., 2009). However, no large earthquake ground motions have been recorded in the embayment.

In absence of locally recorded ground motion, quality deep small strain shear wave velocity profiles (V_S) throughout the embayment provided a way to understand the future spatial variance of seismic amplifications in the embayment.

Quality V_S profiles are critical for estimating site specific hazard and are one of the most critical inputs into site response analyses with numerous site response studies demonstrating the influence of input V_S profiles on both the amplitude and frequency content of predicted surface ground motions (Bazzurro and Cornell, 2004; Rathje et al., 2010; Li and Assimaki, 2010; Grifitths et al., 2016; Teague and Cox, 2016). Despite the large variations in soil structure in the embayment, many of the seismic amplification studies in the Mississippi Embayment have used reference V_S profiles developed by Romero and Rix (2005) due to lack of proper site-specific V_S profiles in the embayment. However, these two reference V_S profiles fail to account for the changes in the basin structure in the embayment (Wood et al., 2018). The overall site-specific V_S profiles for the embayment are sparse, with majority of the available V_S profiles being 30 – 60 m deep (Liu et al., 1997; Street et al., 2004). Rosenblad et al. (2010) developed eleven deep V_S profiles extending down to 200 – 250 m to a shallow impedance boundary in the embayment but lack information down to the deep bedrock layer. The most recent study for deep V_S information in the Mississippi Embayment is the USGS Central U.S. Seismic Velocity Model (CUSVM) (Ramirez-Guzman et al., 2012). While this 3-D shear wave velocity model provides understanding of the basin structure, it was shown by Wood and Himel (2019) to have significant errors in V_S for different geologic units and depths to the shallow impedance boundary from the Memphis sand layer, which could significantly impact site response studies for the embayment. This emphasizes the need for additional site-specific deep V_S profiles to improve velocity models for the region and reduce uncertainties in site response studies.

Ever since the advent of geophysics for use in site characterization, development of seismic reflection/refraction survey (Raitt et al., 1954), Spectral Analysis of Surface Wave (SASW) (Heisey et al., 1982, Nazarian and Stokoe, 1984), Multi-channel Analysis of Surface Wave (MASW) (Park et al., 1999) have increased the accuracy and convenience of using geophysical methods. These methods have mainly contributed to more precise shallow site characterizations (30 – 60 m). Nevertheless, the seismic reflection/refraction methods can capture the velocity differences in deeper layers and infer geologic layer boundaries; they lack direct evidence of V_S for individual soil layers exceeding 150 m depth (Street et al., 2004). However, at this time, no SWM site characterization technique is available to researchers/practitioners that can be used to develop comparable deep site characterization results as the invasive methods. Moreover, available deep site characterization measurements across the embayment would be beneficial to understand the spatial change of basin geology in the embayment and consequently would be useful in developing a 3D shear wave velocity model.

1.3 Scope of Research

This dissertation details the development of a new SWM technique combining active and passive source surface wave measurements for deep site characterization. This technique utilizes a joint inversion solution of the measured experimental dispersion characteristics and site fundamental frequency, ensuring site signature consistent shear wave velocity profiles (V_S profiles). The surface wave measurements are for low strain displacements of soil; hence, V_S profiles produced are representing in-situ condition of soil. Lack of low-frequency energy, presence of effective mode dispersion data, and identification of the mode of wave propagation are a few of the issues for resolving V_S profiles using this technique. To validate the developed

technique, active and passive source surface wave measurements are made at the CUSSO site with an array of boreholes down to the bedrock, where downhole measurements are made to compare with the developed SWM V_S profiles at the location.

A parametric study to observe the effect of properly characterizing the shallow impedance boundary on site response is conducted. The shallow impedance boundary in the Mississippi embayment is due to the stiff Memphis sand layer, which is often poorly characterized. In this dissertation, a suit of pseudo V_S profiles is developed by varying the depth and formation velocity of the Memphis sand layer from a base V_S profile developed at the CUSSO site. Site response of the suit of V_S profiles are evaluated using linear and non-linear approach. Residuals between surface response spectra estimated from pseudo V_S profiles and the base V_S profile is calculated to observe differences in site response.

Utilizing the developed deep site characterization SWM technique, deep V_S profiles at 24 sites across the embayment is generated. Acquisition and processing of the active and passive source surface wave data is discussed. At each site, theoretical dispersion and ellipticity are compared to the experimental dispersion and HVSR f_0, respectively to ensure V_S profiles capturing local site signature. Developed V_S profiles are compared to existing CUSVM V_S profiles and measured V_S profiles in the embayment.

An approach for generating site signature consistent V_S profiles for the Mississippi embayment utilizing power-law velocity functions is developed. For this, power-law velocity functions for the geologic units found in the embayment is developed utilizing the 24 deep V_S profiles generated across the embayment. Initial V_S profiles at the study sites are modeled using the developed velocity functions, mean formation velocities of geologic units and layer interface information at that site location. The developed initial V_S profiles are adjusted to constrain the

theoretical transfer function peak (TF_0) and ellipticity peak (Ell_0) to match the measured HVSR f_0. Pseudo V_S profiles at 24 study locations using the developed approach is generated and compared to the measured V_S profiles at these locations. Pearson correlation coefficient between the time averaged V_S of the modeled and measured V_S profiles is calculated to evaluate the correlation between the modeled and measured V_S profiles.

1.4 Organization of the Dissertation

The organization of the dissertation is divided in six chapters. The first chapter discusses the research significance, and the scope of the research. Chapter 2 details the development of a SWM technique for deep site characterization in the Mississippi embayment. Results of this chapter are published in *Soil Dynamics and Earthquake Engineering* entitled "Developing an updated set of V_S profiles for the Central United States Seismic Observatory with estimates of uncertainty between different methods." Chapter 3 details a parametric study conducted to observe site response impacts of properly characterizing the Memphis sand layer in the Mississippi embayment. Results of this chapter are published in the conference proceedings of *Geoextreme 2021* entitled "Site response impacts of the Memphis sand layer within the Mississippi Embayment." Chapter 4 details the development of deep V_S profiles at 24 sites across the Mississippi embayment utilizing the developed SWM technique in Chapter 2. Results of the chapter four are published in *Soil Dynamics and Earthquake Engineering* entitled "Deep shear wave velocity profiles in the Mississippi embayment from surface wave measurements." Chapter 5 details the development of an approach to generate site signature consistent deep V_S profiles in the Mississippi embayment utilizing power-law velocity functions. Results of this chapter is submitted for review in *Soil Dynamics and Earthquake Engineering* entitled "An approach for developing site signature consistent deep shear wave velocity profiles for the

Mississippi Embayment using generalized power-law functions." In chapter 6, the work discussed in this dissertation are summarized, concluded and future research are presented.

2. Chapter 2: Developing an updated set of VS profiles for the central United States seismic observatory with estimates of uncertainty between different methods

2.1 Abstract

Deep dynamic site characterization was conducted at the Central United States Seismic Observatory (CUSSO), which is a 587 meter deep vertical seismic array situated in the Mississippi Embayment. This characterization included a combination of active and passive source surface wave methods and horizontal to vertical spectral ratio (HVSR). These measurements were used in a multimodal joint inversion of Rayleigh and Love dispersion data and the natural site frequency from HVSR (f_0) to develop non-invasive V_S profiles for the site. Downhole seismic measurements were also made down to 425 m to validate the surface wave method results and understand the uncertainty between the various measurements at the site. The developed V_S profiles are compared to published site specific V_S profiles from direct measurements, velocity models, and reference V_S profile for the embayment to understand the variability and uncertainty between different methods. Major differences in the Vs profiles were noticed in the top 50 meters, near the Memphis sand layer, and the Paleozoic bedrock layer. Site signatures from experimental dispersion data, HVSR f_0 and empirical transfer function (ETF) were evaluated to assess the appropriateness of the candidate V_S profiles. Comparison results indicate the developed V_S profiles in this study performed well in capturing the site signatures. However, the theoretical dispersion fits from published V_S profiles demonstrated a larger misfit

with the experimental data. Theoretical transfer function and Rayleigh ellipticity from published profiles also exhibited considerable differences with the HVSR f_0 and ETF amplification factor.

2.2 Introduction

The Mississippi Embayment encompasses a large area in the central United States covering parts of Arkansas, Missouri, Illinois, Kentucky, Tennessee, and Mississippi. The deep, unconsolidated sedimentary deposits in the embayment range from 100 m at St. Louis, Missouri to 1000 m at Shelby County, Memphis (Van Arsdale and TenBrink, 2000). This deep deposit is an important source of local site effects, causing uncertainty in the amplification of seismic waves (Hashash and Park, 2001; Romero and Rix, 2005; Wood and Baker, 2018). Seismicity in the region is caused by a series of faults collectively called the New Madrid Seismic Zone (NMSZ), which has some of the highest design ground motions in the United States (ASCE 2017). Understanding the local seismic site effects is crucial to designing seismic resistant infrastructure in the region. Rathje et al. (Rathje et al., 2010) listed four basic sources of uncertainty for site response analysis as: (1) input rock motions, (2) shear wave velocity (V_S) profiles, (3) non-linear dynamic soil properties, and (4) analysis method. Various site response studies have demonstrated the influence of V_S profiles on the amplitude and frequency content of surface ground motion (Rathje et al., 2010; Li and Assimaki, 2010; Griffiths et al., 2016; Teague and Cox, 2016). Thus, estimation of acceptable V_S profiles with associated uncertainties are significant for site response study.

Site-specific V_S profiles can be developed using either invasive tests, such as crosshole, downhole, and P-S suspension logging or non-invasive tests, such as surface wave methods. Invasive methods are considered to be more reliable than non-invasive methods as they are based

on direct measurements of V_S. However, epistemic uncertainties developed from wave arrival picking and wave path assumptions can influence these invasive tests (Griffiths et al., 2016a; Passeri et al., 2019). As the invasive tests are mostly localized measurements of a site, aleatory uncertainties could also be associated with the measurements. Epistemic uncertainties in invasive profiles are usually accounted for by the development of upper/lower bound V_S profiles from a base case profile (typically base profile±20%) (EPRI 2012), whereas the aleatory uncertainties are accounted for using statistically randomized profiles (Toro, 1995). Non-invasive methods, such as surface wave methods are cost-effective and have become very popular (Socco et al., 2010). Moreover, surface wave methods are found suitable for a variety of ground conditions (Socco et al., 2010). However, the surface wave inversion process to compute a shear wave velocity profile from dispersion data is highly non-linear and non-unique (Cox et al., 2014; Luke et al., 2003). Surface wave measurement results have been compared to borehole measurements in several studies for validation (Garofalo et al., 2016; Brown et al., 2002). Garofalo et al. (2016) showed that the non-invasive surface wave methods are capable of providing precise results comparable to invasive methods. As part of assessing the non-unique surface wave V_S profiles and statistically derived V_S profiles, the idea of the 'site signature' was developed (Griffiths et al., 2016a; Griffiths et al., 2016b; Teague et al., 2018). Griffiths et al. (Griffiths et al., 2016a; Griffiths et al., 2016b) first recognized the dispersion data as a site signature, which is a spatially averaged property of the site material that can reveal important information about wave propagation across the site. Griffiths et al. (2016b) demonstrated that upper/lower bound V_S profiles (base profile±20%) yielded a poor theoretical fit to the experimental dispersion data (i.e., not capturing the site signature). Also, very few of the randomized profiles to account for the aleatory uncertainty were found acceptable based on the dispersion fit. Later, in addition to the

experimental dispersion data, Teague et al. (2018) studied the fundamental frequency from the HVSR peak as a site signature. Regardless of the non-unique nature of the surface wave method V_S profiles, Griffiths et al. (Griffiths et al., 2016a; Griffiths et al., 2016b) and Teague et al. (2018) concluded that non-unique V_S profiles are able to match the site signature when they are carefully developed. As a result, non-unique surface wave method V_S profiles which match the site signature provide rational means to account for uncertainty and yield reasonable site response estimates (Teague et al., 2018).

In the Mississippi Embayment, different invasive and non-invasive site-specific V_S characterization techniques and generic reference V_S profiles have been used to study site effects. However, the database of site-specific V_S profiles for the region is sparse, with the majority of the available V_S profiles being only 30 – 60 m deep (Liu et al., 1997; Street et al., 2004). For deeper Vs profiles to bedrock, reference V_S profiles from Romero and Rix (2005) are typically used for site response studies in the embayment (Romero and Rix, 2005; Hashash and Park, 2001). These profiles consist of two reference V_S profiles (lowlands and highlands) and were based on compiled Vs profiles from southern Tennessee, eastern Arkansas, and northwestern Missouri. While these are commonly used, they do not well represent any single site in the embayment. Rosenblad et al. (2010) developed eleven deep V_S profiles in the region using surface wave method, but these only range from 200 – 250 m deep. Cramer et al. (2006) used P-S suspension logging to characterize down to 420 m at the Memphis light, gas, and water well site (MLGW). Gomberg et al. (2003) showed that shear wave velocity in the Mississippi Embayment is correlated with the local lithology and hence could be extrapolated without direct measurements. Based on this philosophy, Ramirez-Guzman et al. (2012) developed the Central United States Seismic Velocity Model (CUSVM), a 3-D shear wave velocity model using a

significant number of boreholes and seismic refraction profiles. However, below 100 m depth, the reference V_S profiles and the site-specific CUSVM V_S profiles for the Mississippi Embayment show more than 50% difference, increasing the uncertainty in site response studies using the generalized reference profiles for the whole embayment (Wood and Himel, 2019).

Another effort to develop a Vs profile for the Mississippi Embayment was made by Woolery et al. (Woolery et al., 2016) at the Central United States Seismic Observatory (CUSSO) (shown in Fig 2.1), which was constructed to study the effects of local geology on seismic wave propagation. The CUSSO borehole array consists of three boreholes with depths of 30 m, 259 m, and 587 m. Seismometer and accelerometer are placed at the surface and 2 m into bedrock to observe amplification of seismic waves through the soil column. Accelerometers at 30 m, 259 m, and 526 m depths were also installed to study the amplification/deamplification of seismic waves at different geological interfaces. A complex mixture of amplification/deamplification generated by the sedimentary deposits was observed (Woolery et al., 2016), emphasizing the necessity of proper dynamic site characterization of the entire soil profile to fully understand the site effects. Woolery et al. (2016) developed a seismic velocity model at CUSSO by performing: (1) walkaway seismic reflection and refraction surveys, (2) P-S suspension logging, and (3) analyzing phase arrival times from the instrumented vertical array. The shear wave velocity model developed from the suspension log and walkaway survey showed significant differences(as much as up to 300 m/sec), which was speculated to be caused by inaccuracies in the P-S suspension logging due to sediment disturbances in the borehole. This Vs inaccuracy at CUSSO provides an opportunity to better understand the Vs structure in the embayment, but also to understand the uncertainty in the Vs structure when different dynamic site characterization methods are used at a deep sedimentary basin site.

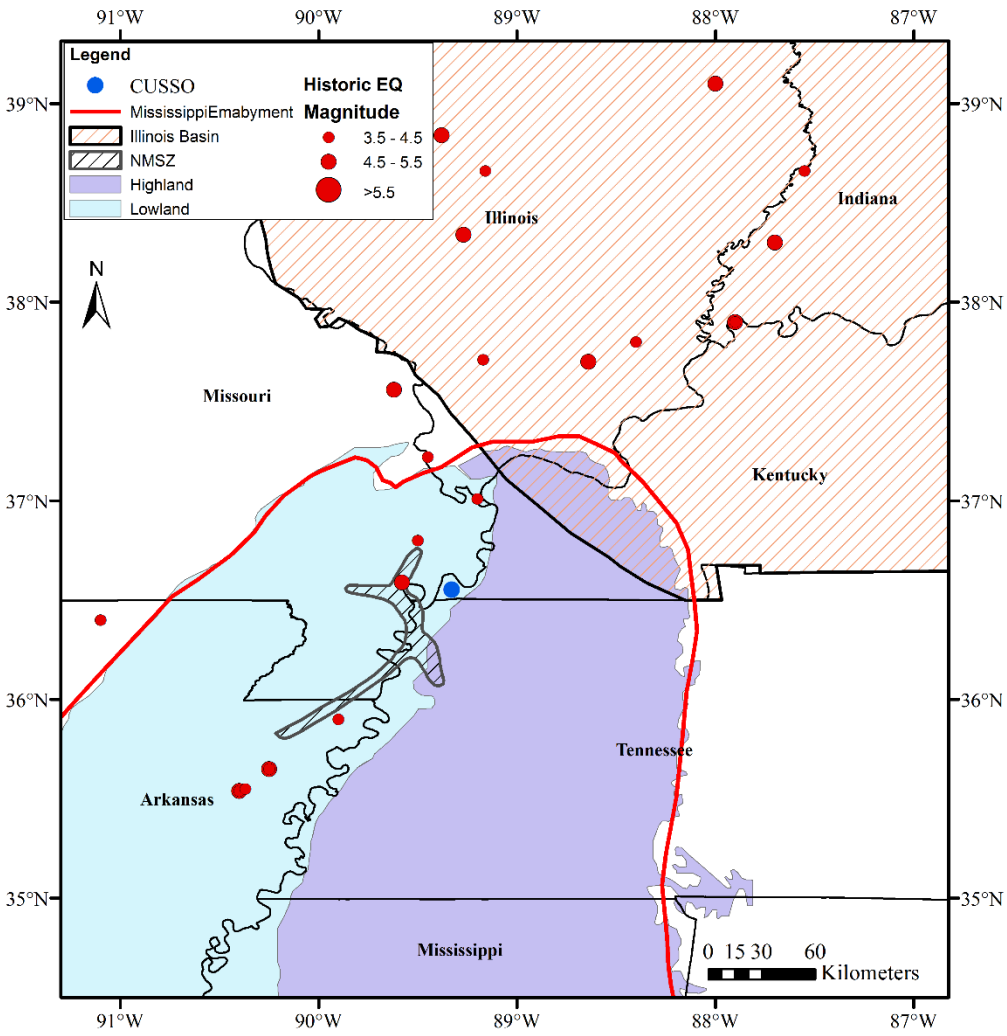

Figure 2.1 Map of the Mississippi Embayment showing the CUSSO station. The historic earthquakes occurred in the Mississippi Embayment and Illinois basin are also shown.

This study focuses on updating the shear wave velocity information at the CUSSO downhole array, validating the use of non-invasive surface wave methods for Mississippi Embayment sites, and understanding the uncertainty between Vs profiles collected by various authors at CUSSO. For this purpose, surface wave and downhole measurements were made at the CUSSO site. Both active and passive source surface wave methods were used to collect data near the CUSSO boreholes. The downhole testing was conducted down to 115 m and 425 m, respectively in the 259 m and 587 m deep boreholes. A blind analysis method, without a-priori

information on the site and a guided analysis method, are used to develop the non-invasive surface wave method V_S profiles. The developed non-invasive V_S profiles are compared with the invasive V_S profile and literature V_S profiles at the site to understand the uncertainty between Vs profiles developed using a variety of methods at a deep basin site. Next, the theoretical dispersion data from all the profiles are compared with the recorded experimental dispersion data to check the Vs profiles appropriateness at capturing the site signature. Moreover, the ellipticity peak and theoretical transfer function (TTF) peak generated from V_S profiles are compared to the experimental HVSR f_0 and empirical transfer function (ETF). The potential errors and uncertainty of each Vs profile are discussed.

2.3 Overview of the Mississippi Embayment Geology

The main constituents of the Mississippi Embayment geology are Quaternary, Upper Tertiary, Lower to Middle Claiborne, Paleocene, Cretaceous and Paleozoic era bedrock (Ramirez-Guzman et al., 2012). The surface deposits in the Quaternary layer are classified as Holocene or Pleistocene (Romero and Rix, 2005). The Holocene deposits are found in the alluvial plains of the Mississippi river floodplain, also known as the lowlands and the Pleistocene deposits are found further east on the highlands (Figure 2.1) (Romero and Rix, 2005). The Upper Tertiary layer consists of the Jackson formation and the upper Claiborne group. The Jackson formation contains clay, silt, sand and lignite (Brahana et al., 1987), whereas the upper Claiborne includes Cockfield and Cook Mountain formation, characterized by silts and clay (Van Arsdale and TenBrink, 2000). The Lower to Middle Claiborne group (LMC) below the Upper Tertiary layer contains the Memphis sand unit, also known as the “500-foot sand” (Romero and Rix, 2005). The Memphis sand is a very fine to coarse grained, light gray-white sand (Van Arsdale and TenBrink, 2000) with a thickness of 164 – 292 m and approximately 300 m deep in the

Memphis area (Brahana et al., 1987). The Paleocene layer contains the Wilcox and Midway groups, which are made up of several formations. Silt, clay, fine to coarse grained sand, and minor limestone are the main components of the Paleocene layer (Van Arsdale and TenBrink, 2000; Brahana et al., 1987). The Cretaceous layer is situated just above the bedrock, containing several forms of clays and sands. This layer contains the McNairy sand, Demopolis formation and coffee formation. The Paleozoic bedrock layer signifies the basement of the Mississippi Embayment deposits and is primarily made up of white to dark-gray, fine to coarse crystalline dolomite (Brahana et al., 1987).

The Memphis sand and Paleozoic bedrock are two major sources of impedance contrast in the embayment. The alluvial surface deposits have a low V_S of 193 ± 14 m/sec compared with the Memphis sand and the Paleozoic bedrock units, which have V_S of 685 ± 83 m/sec (Rosenblad et al., 2010) and 2000 - 3400 m/sec (Cramer et al., 2006), respectively. The low shear wave velocity of the deep deposits and two impedance boundaries make the embayment susceptible to ground motion amplification.

2.4 Testing Methodology

Non-Invasive Method

The surface wave method V_s profiles at CUSSO were developed using a combination of active source multichannel analyses of surface wave (MASW) (Park et al., 1999), passive source microtremor array measurement (MAM) (Tokimatsu, 1997), and horizontal to vertical spectral ratio (HVSR) (Nakamura, 1989). Both Rayleigh and Love wave MASW data were collected with a linear array of 24, 4.5 Hz vertical (Rayleigh) and horizontal (Love) geophones with 2 m geophone spacing (array length of 46 m). A 5.4 kg sledgehammer was used as the seismic source to create the Rayleigh and Love waves by vertical and horizontal strikes, respectively. Multiple

source offsets of 5 m, 10 m, 20 m, and 40 m were used from the first geophone to produce high quality data allowing uncertainty to be quantified and near-field effects to be minimized. At each source offset location, ten sledgehammer blows were stacked to improve the signal-to-noise ratio. Using the same MASW geophone array and a 2 m source offset, P-wave refraction data was collected to estimate the ground water table at the site.

The MAM measurements were carried out using circular and L-shaped arrays. Circular arrays of 50 m, 200 m, and 500 m diameters were used. In the circular MAM array, nine three component Trillium compact, 20 second broadband seismometers were used. These seismometers were arranged with one at the center and eight uniformly distributed around the circumference. Ambient noise was recorded for one hour for the 50 m and 200 m diameter arrays and for two hours for the 500 m diameter array. A Nanometrics Centaur digitizer was used to record the data. Exact locations of each seismometers in the field were recorded using a centimeter accurate GPS unit. The MAM data recorded using the circular array of seismometers were also used for the HVSR measurements. The L-array MAM measurements were carried out using 24, 4.5 Hz vertical geophones. A geophone spacing of 5 m was used, resulting in an approximate L-shaped array of 55 m x 60 m. Ambient noise for the L-array was recorded for one hour. A map of all the surface wave recording arrays is shown in Figure 2.2 .

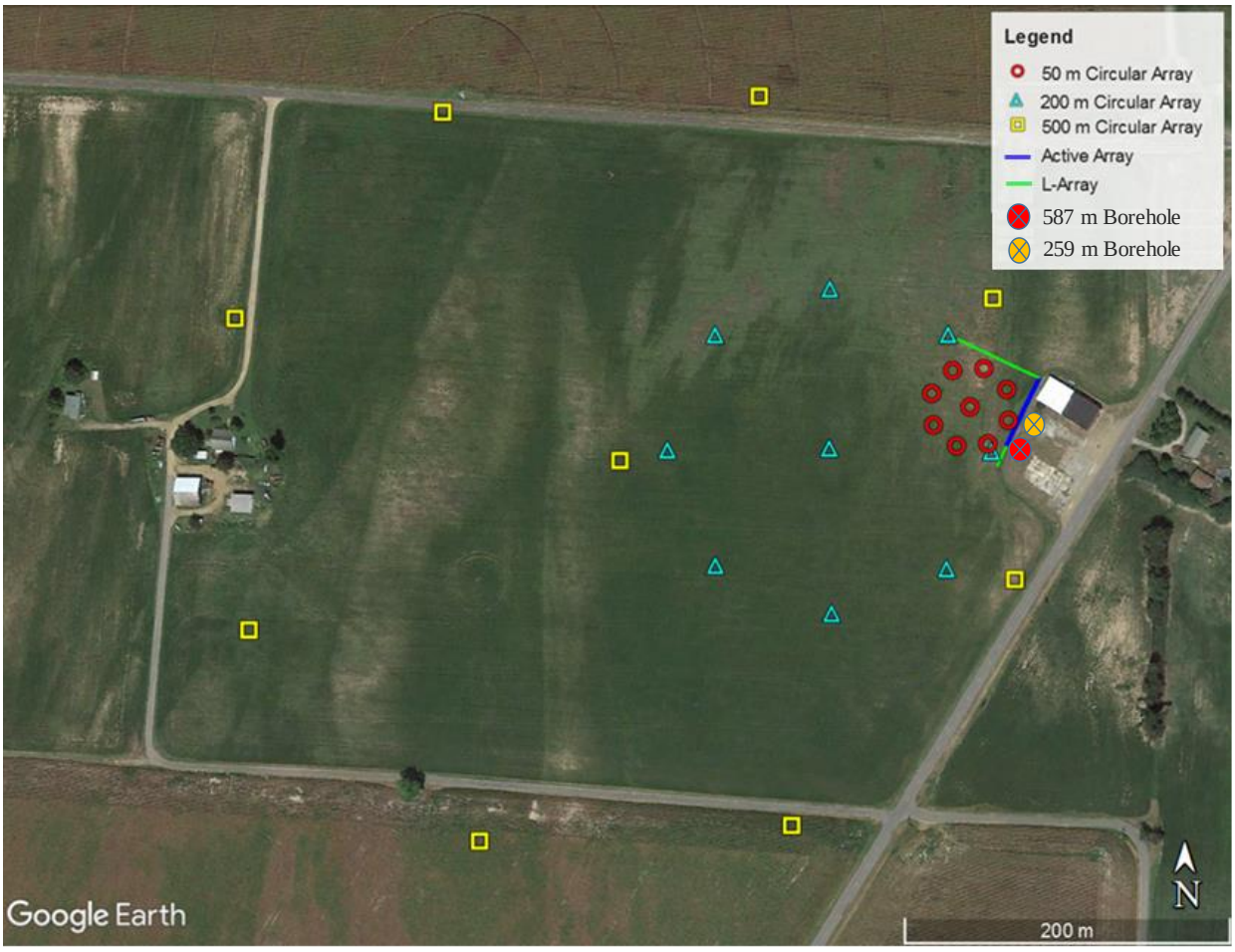

Figure 2.2 A map of the three circular MAM arrays (50 m, 200 m, and 500 diameter), active MASW array, and L-array is shown along with the adjacent CUSSO boreholes.

Invasive Method

Downhole seismic testing was conducted in the CUSSO boreholes in two stages. The preliminary shallow testing was conducted down to 115 m in the 259 m deep borehole, whereas the deep testing was conducted down to 425 m in the 587 m deep borehole. The shallow downhole testing was conducted in accordance with ASTM D7400-19 (ASTM, 2019). In both cases, a wall-lock type Geostuff BHG-3 geophone system was used (Crice, 2002). Due to the steel casings in both boreholes, the orientation mechanism in the BHG-3 could not be utilized.

To avoid the inclusion of any tube waves, the water level in the borehole was lowered to approximately 30 m prior to the testing in each stage.

For the shallow testing in the 259 m deep borehole, a 5.4 kg sledgehammer was used as a seismic source. A vehicle-on-beam traction source and steel strike plate with offset of 3.05 m from borehole were used for generating the seismic waves. Downward propagating P-waves were generated by vertical blows on the strike plate, whereas downward propagating horizontally polarized shear waves were generated by horizontal blows on the traction beam. For identifying the first arrival of the shear wave, "positive" and "negative" polarity waves were created by striking the traction beam from either side. Five sledgehammer blows were stacked at each incremental depth to increase the signal-to-noise ratio. A Data Physics Quattro dynamic signal analyzer was used for recording the signal from the receiver. Testing was performed from the top down, starting at 0.75 m below ground surface with sampling intervals of 0.75 m down to 15 m and 1.5 m interval below 15 m.

For the deep testing in the 587 m deep borehole, the University of Arkansas Vibroseis truck (Industrial Vehicles International T – 15000) was utilized as the seismic source. The center of the vibroseis plate was offset from the borehole by 3 m with the reaction mass oriented perpendicular to the borehole to generate horizontally polarized shear waves. Three to five 8 second sinusoidal sweeps with frequency ranging from 20 – 80 Hz were used at each incremental depth. The same BHG-3 geophone system was used for testing. A Data Physics Mobilyzer dynamic signal analyzer was used to record the waveforms during testing. Testing was performed from the top down, starting at 3 m below the surface with a 3 m sampling interval down to 425 m. Further details and raw data from the invasive and non-invasive testing are available in Wood and Himel (2019).

2.5 Data Processing

Non-Invasive

The active source MASW data (Rayleigh and Love) were processed using the Frequency Domain BeamFormer (FDBF) method in conjunction with the multiple source offset approach (Cox and Wood, 2011; Zywicki, 1999). The circular and L-array MAM dispersion data were processed using the high resolution frequency wavenumber method (HRFK) (Capon, 1969). In addition, the circular array Rayleigh MAM dispersion data were processed using the modified spatial auto-correlation method (MSPAC) (Bettig et al., 2001). The high resolution Rayleigh wave three component beamforming method (RTBF) was also utilized to process the circular array Rayleigh MAM data (Wathelet et al., 2018). The RTBF method offers some advantage over the conventional frequency wavenumber methods (f-k) to identify various modes, particularly at higher frequencies where the conventional f-k methods fail due to aliasing (Wathelet et al., 2018). A composite experimental dispersion curve was developed by refining the experimental data from each method and combining the resulting dispersion data.

The circular array MAM data were also used to develop HVSRs for each of the nine seismometers for all circular arrays. The peaks from all measurements were combined to determine a single HVSR peak frequency with associated standard deviation. General guidelines established by the SESAME project were followed for processing the HVSR (SESAME, 2004). The fundamental frequency from the HVSR test was later used for a joint inversion to constrain the overall stiffness of the V_S profile. For this study, the bedrock depth was constrained at 585 m deep based on borehole logs at the site (Woolery et al., 2016).

The P-wave refraction data was processed following the method in Redpath (1973). Recorded time series data from the linear geophone array were processed to identify the P-wave arrival at each receiver offset as a function of time. The time-intercept method was used to estimate the depth of water table from the receiver offset-arrival time plot.

A joint inversion of the composite experimental dispersion data and the HVSR peak frequency (f_0) was conducted to obtain the shear wave velocity profiles using the Geopsy software package, Dinver (Wathelet, 2008). The neighborhood algorithm method (Dunkin, 1965) is used in Dinver to generate numerous theoretical V_S profiles within user-defined constraints. Parameters to constrain the inversion solution contain ranges of shear wave velocity, P-wave velocity, Poisson's ratio, density and number/thickness of layers. In this study, two sets of parameterizations were used. First a generic set of 'blind' parameterizations using normally dispersive soil characteristics was developed based on knowledge from the literature (Wood and Baker, 2018; Lin et al., 2014; Ramirez-Guzman et al., 2012, Rosenblad et al., 2010). The inversion models developed using these generic parameterizations are referred to as 'SWM' throughout the paper. Second is an informed set of parameterizations where the Vs and layering information from the downhole seismic testing is used as a guide for establishing layer thickness and velocity bounds. These models are referred to as 'SWM Guided' hereafter. In both SWM and SWM Guided, two million trial V_S profiles were generated in the final inversion to ensure that the solution space was properly explored. The theoretical dispersion curves and ellipticity peaks generated from the V_S profiles were compared with the experimental dispersion data and the HVSR f_0, respectively. The overall 'closeness' between the experimental and theoretical results were quantified as the misfit (Wathelet et al., 2004). A misfit value of one indicates that the theoretical results are within one standard deviation of the experimental result (Deschenes et

al., 2018). During the iterative inversion process, the neighborhood algorithm attempts to minimize the misfit. The effective and higher mode data were identified manually by comparing the theoretical and experimental dispersion curves after each inversion run. Since Dinver cannot utilize effective modes, the identified effective mode data were removed. The detected higher mode data were assigned appropriate mode number and were utilized in the inversion run. For each circular array, most of the dispersion points beyond the array resolution limit ($k_{min}/2$) were removed (Wathelet, 2008). A representative 1000 lowest misfit V_S profiles were used to calculate a median Vs profile for the site. This provides a more reasonable solution to the inversion problem than selecting just the single lowest misfit profile (Deschenes et al., 2018). Along with the calculated median, a random selection of 1000 V_S profiles within a misfit of one were selected to represent the uncertainty in the Vs from the inversion process.

Invasive

The shallow and deep downhole datasets were both analyzed using the corrected vertical travel time versus depth analysis method (Wood, 2009). The horizontal components of the downhole tool (BGH-3) were rotated to the highest amplitude azimuth to orient one horizontal component in-line with the E-W oriented shear beam and cross-line vibroseis signal, respectively for the shallow and deep dataset. For the shallow dataset, the first arrival times were picked directly from the waterfall plot of the waveforms. For the deep dataset, the recorded raw data from the field were cross-correlated with the true reference source signal for each depth and the highest amplitude of the cross correlation was chosen as the travel time at each depth. The arrival time was corrected for the offset of the source from the borehole. The velocity and thickness of different layers are then identified from the travel time vs depth plot of the S-wave arrival times.

2.6 Results and Discussion

Downhole Results

The shear wave velocity profile obtained from the downhole analysis at CUSSO boreholes is shown in Figure 2.3a along with the P-S suspension-log shear wave velocity profile from Woolery et al. (2016) and reference V_S profiles for different soil types from Lin et al. (2014). The geologic stratigraphy at the CUSSO site from Woolery et al. (2016) is shown in Figure 2.3b with some modification. A dashed red line marks the interface between the Upper Paleocene and Early Paleocene in Figure 2.3b.

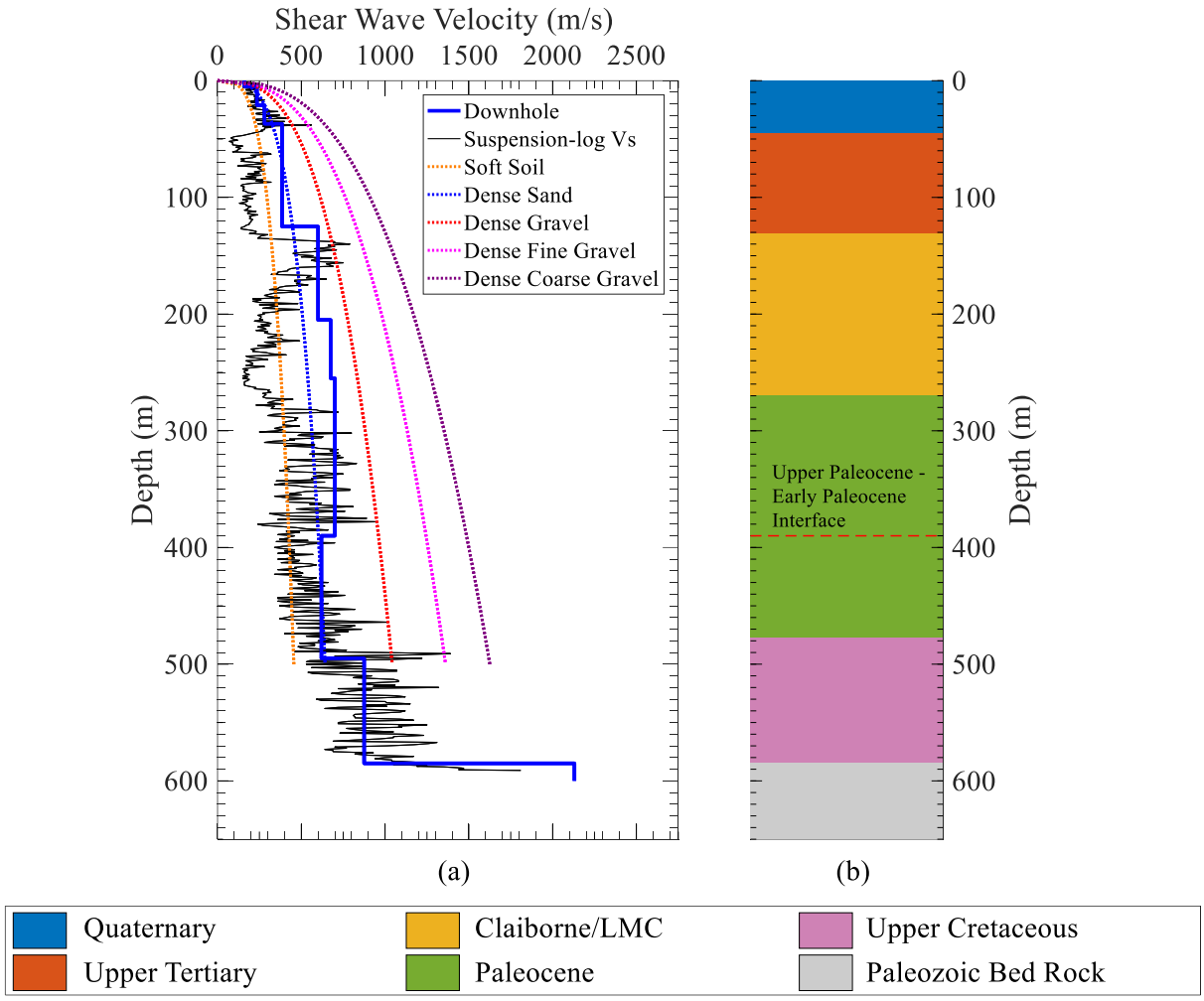

Figure 2.3 (a) Downhole VS profile obtained from the 259 m and 587 m deep borehole at CUSSO. Suspension-log shear wave profile from Woolery et al. (2016) and reference VS profiles for different soil types from Lin et al. (2014) are shown for comparison. (b) Geologic stratigraphy at CUSSO from Woolery et al. (2016) is shown.

The downhole V_S profile is in good agreement with the P-S suspension-log V_S profile down to around 40 m, representing the Quaternary layer interface. The P-S suspension-log V_S profile then exhibits an anomalously low-velocity zone from 40 – 130 m and does not match with the downhole V_S profile. This anomalous low-velocity zone is suspected to be due to sediment disturbances in the borehole (Woolery et al., 2016). The downhole V_S profile infers the Upper Tertiary layer from around 40 – 125 m, with a velocity of 385 m/sec, which is similar to a

dense sand layer reference velocity at this depth range. At 125 m, a major velocity increase to 600 m/sec is observed in the downhole V_S profile. This velocity contrast corresponds with the geologic stratigraphy for the lower middle Claiborne (LMC) or, i.e., the Memphis sand formation. The downhole profile does not clearly resolve the Paleocene formation. However, two stiffer layers are observed with V_S of 675 m/sec and 700 m/sec and extend to 255 m and 390 m, respectively. The P-S suspension-log V_S profile exhibits another anomalous low-velocity zone from around 180 – 300 m, making the suspension-log V_S profile incoherent with the downhole V_S profile in this depth range. In the downhole V_S profile, a softer layer with velocity reversal is observed at 390 m with a velocity of 620 m/sec, which is in the vicinity of upper Paleocene and early Paleocene interface, extending below 425 m. The suspension-log V_S profile also exhibits softer layers in this depth range. To complete the downhole V_S profile to bedrock, the V_S profile from Woolery et al. (2016) is used to include the Cretaceous layer with a V_S of 875 m/sec starting at 495 m and extending down to the bedrock at 585 m. A bedrock V_S of 2130 m/sec was presumed for the downhole profile based on the surface wave testing results discussed later in the paper.

Surface Wave Inversion Results

The composite experimental dispersion data developed from the surface wave measurements are shown in Figure 2.4a and b for the Rayleigh and Love wave data, respectively. For each data point, the mean and +/- one standard deviation are shown. The array resolution limit for the 500 m circular array ($k_{min}/2$) is also shown. In general, the active and passive dispersion data fits well together for both the Rayleigh and Love wave data. The Rayleigh wave data does extend to lower frequencies than the Love wave data with significantly more uncertainty in the data below a frequency of 1 Hz.

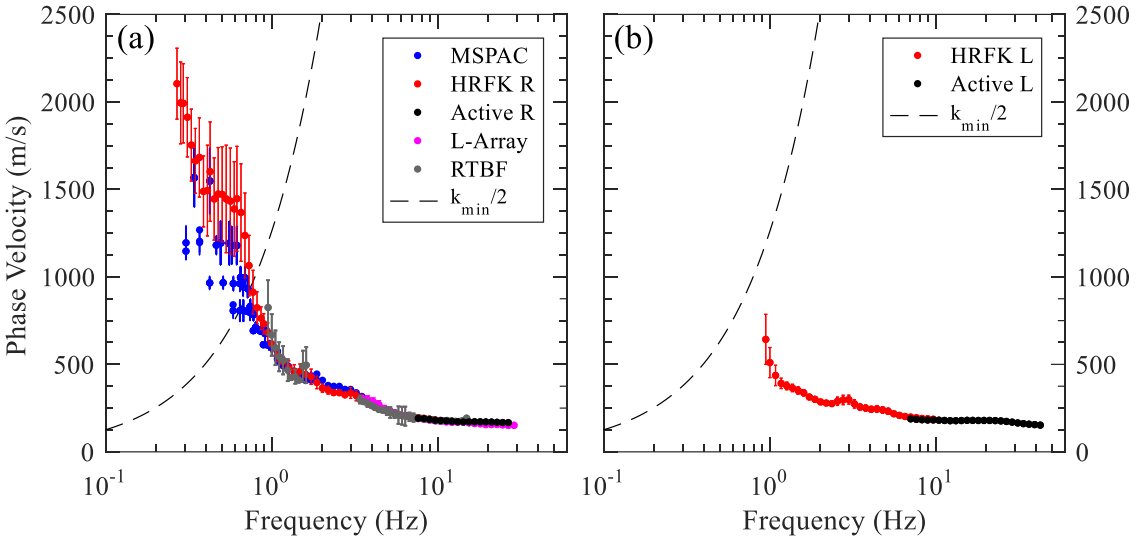

Figure 2.4 Composite experimental dispersion data from the surface wave measurements at CUSSO is shown for (a) Rayleigh wave and (b) Love wave. The array resolution limit for the 500 m circular array (kmin/2) shows the boundary for potentially less reliable data.

The theoretical dispersion curves associated with the SWM and SWM Guided V_S profiles are shown in Figure 2.5. In both cases, a theoretical fit from the median V_S profile and theoretical fits from 1000 randomly selected V_S profiles (within a misfit of 1.0) are shown. The calculated misfit between the experimental dispersion data and theoretical fit (for the median V_S profile) for the SWM and SWM Guided are 0.24 and 0.4, respectively. Visually and quantitatively, both analyses have comparable fits with the experimental data. For the Rayleigh and Love wave data, data points approximately from 0.6 – 0.8 Hz and 2.3 – 6 Hz were removed as they were identified as effective mode through numerous iterations. A few experimental dispersion points for the Rayleigh wave data (<0.6 Hz) were beyond the array resolution limit but were used to ensure enough resolution at deeper depths.

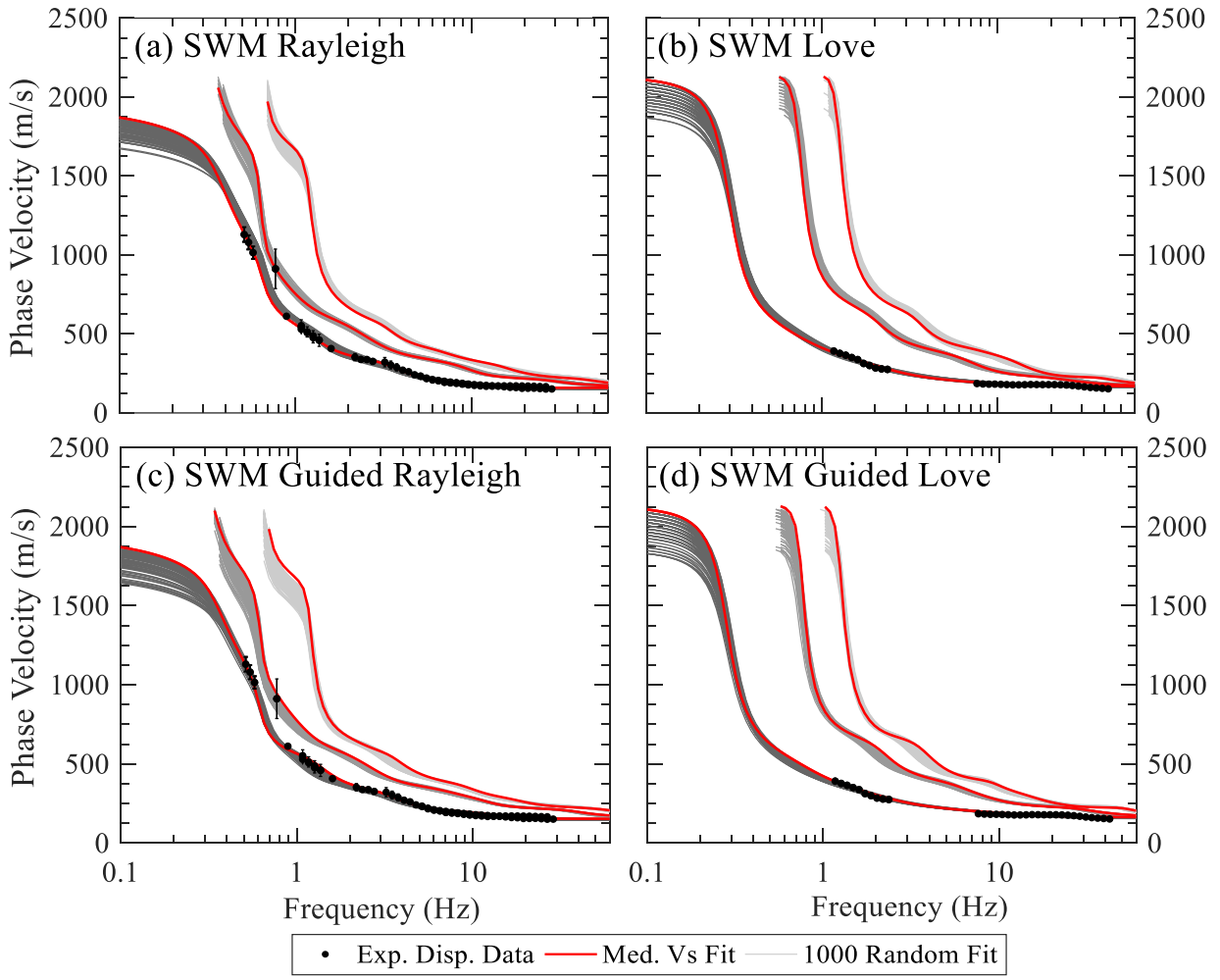

Figure 2.5 Experimental dispersion data and theoretical fits for the median VS and randomly selected 1000 VS profiles. Misfit calculated between the experimental and theoretical fit (median VS) for SWM and SWM Guided are 0.24 and 0.4, respectively.

The experimental HVSR results for the CUSSO site are shown in Figure 2.6. The natural frequency from the HVSR first peak is 0.29 ±0.01 Hz. The fundamental mode Rayleigh ellipticity curves generated from the median V_S profiles of the SWM and SWM Guided are shown along with the HVSR curve in Figure 2.6a and b, respectively. The ellipticity peaks from SWM and SWM Guided are 0.297 Hz (2.4% higher) and 0.291 Hz (0.34% higher), respectively, which are within one standard deviation of the HVSR peak. This infers that the deep impedance contrast from bedrock was accurately modeled in both of the inversion runs.

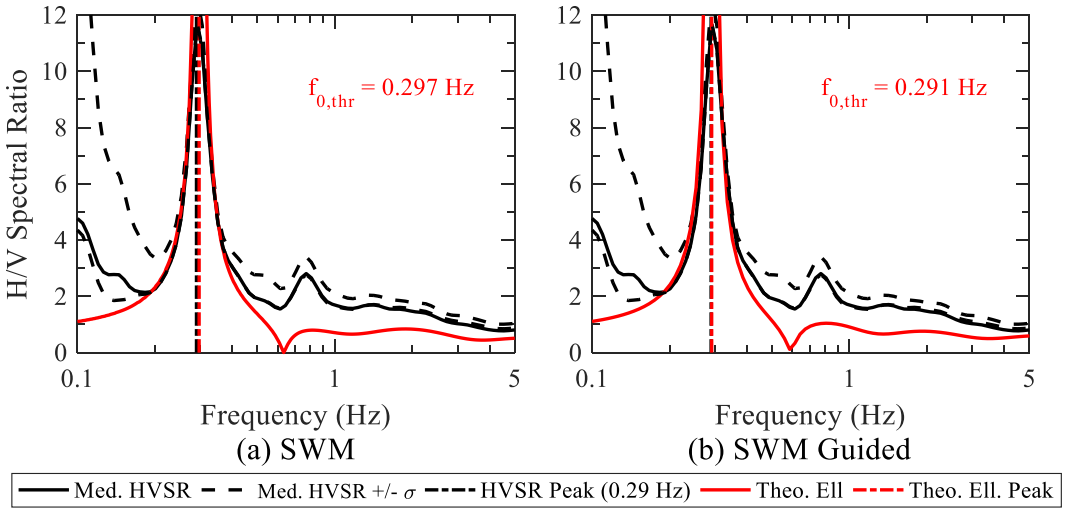

Figure 2.6 Experimental HVSR curve along with theoretical Rayleigh ellipticity curve generated from the median VS profile for (a) SWM and (b) SWM Guided.

Shear wave velocity profiles obtained from the SWM and SWM Guided are shown in Figure 2.7a and b, respectively. For each analysis method, the median V_S profile estimated from the 1000 lowest misfit V_S profiles and 1000 randomly selected V_S profiles within a misfit of 1.0 are shown. It should be noted that the median V_S profiles were not directly generated from the inversion method. Instead, they were calculated by computing the median layer depth and median V_S for each layer from the 1000 lowest misfit Vs profiles. Reference V_S profiles for different soil types from Lin et al. (2014) are shown for comparison with the SWM and SWM Guided analyses results. To demonstrate the variability among the V_S profiles, the standard deviation of the natural logarithm of V_S ($\sigma\ln(V_S)$) is shown for each analysis in Figure 2.7c. The $\sigma\ln(V_S)$ method has been commonly used as a tool to quantify the variability in V_S (Deschenes et al., 2018; Teague et al., 2018; Toro, 1995). The geologic stratigraphy at the CUSSO site from Woolery et al. (2016) is superimposed on Figure 2.7c.

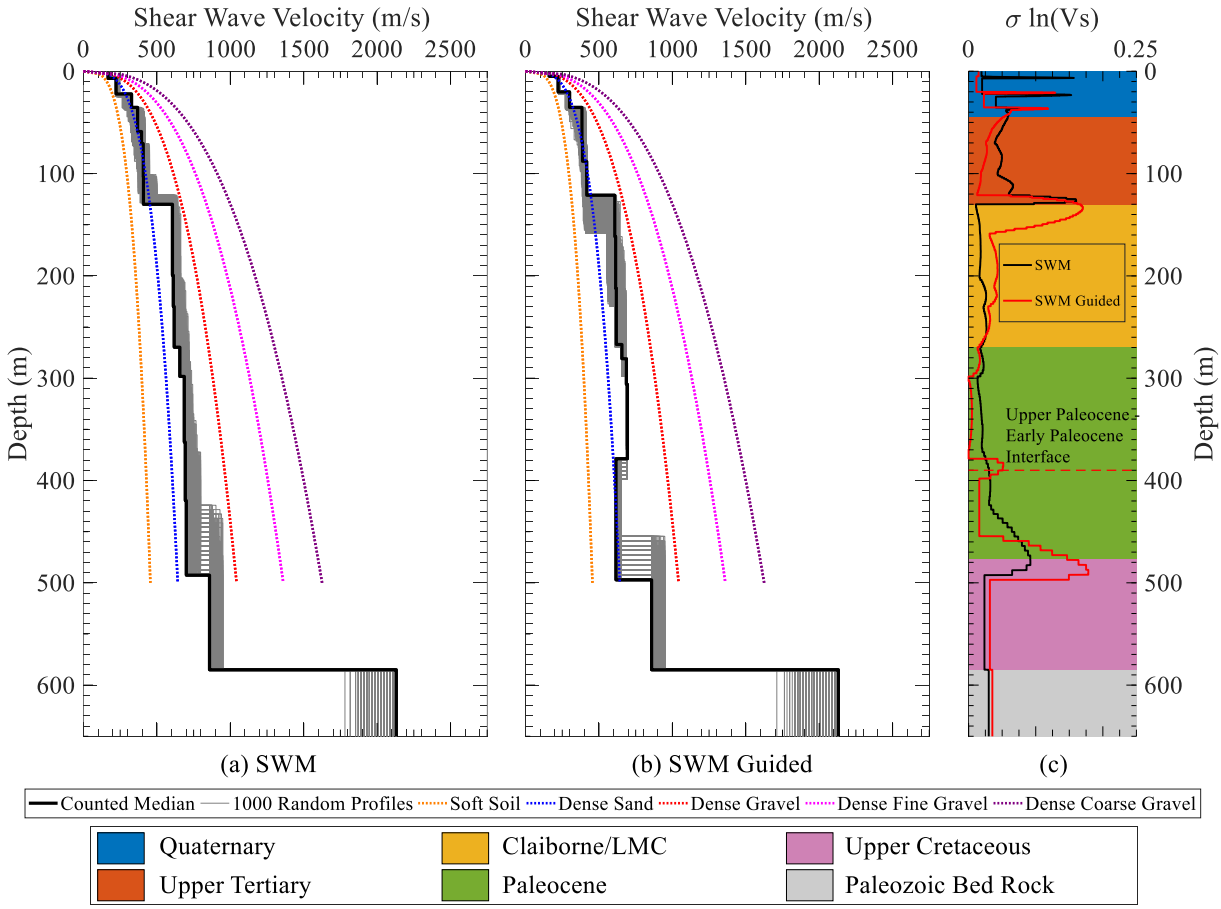

Figure 2.7 V_S profiles generated from the surface wave inversion are shown. A median V_S profile computed from the 1000 lowest misfit V_S profiles and 1000 randomly selected V_S profiles within misfit of 1 from a pool of 2 million models are shown for (a) SWM and (b) SWM Guided. Reference V_S curves from Lin et al. (2014) for different soil types are shown for comparison with each analyses methods V_S profile. Standard deviation of the natural logarithm of V_S ($\sigma \ln V_S$) for each analyses methods are shown for demonstrating the variability between the V_S profiles in (c). The geologic stratigraphy at CUSSO from Woolery et al. (2016) is superimposed on (c).

From Figure 2.7, both the SWM and SWM Guided Vs profiles resolve the Quaternary and the Upper Tertiary layer interface around similar depth. Both profiles demonstrate V_S values within the soft soil and dense sand reference V_S curves down to roughly 120 m, which is consistent with the soil types found in the Quaternary and Upper Tertiary layer in the Mississippi Embayment. A major velocity increase to around 610 m/sec is observed in both V_S profiles at

130 m and 120 m deep in the SWM and SWM Guided, respectively. This interface in both analyses is a shallow impedance contrast, having a V_S value close to the dense gravel at this depth, inferring the start of the lower middle Claiborne (LMC) or, i.e., the Memphis sand. The Claiborne/LMC in the geologic stratigraphy is around 131 m, which is in good agreement with the V_S profiles. Following this shallow impedance contrast, both analyses show uniform increases in V_S for the Paleocene layer (the SWM Guided shows this trend until the velocity reversal). At 375 - 500 m, the SWM Guided analysis was able to resolve the velocity reversal interpreted from the downhole test. The velocity reversal in the SWM Guided is in the vicinity of the Upper Paleocene-Early Paleocene interface. A sharp change in natural gamma-ray count log and single-point resistivity log is also observed at this depth in Woolery et al. (2016), indicating a change of material type. The SWM and SWM Guided demonstrate another velocity increase around 450 – 500 m deep with an average V_S value of 850 m/sec, which is similar to the Upper Cretaceous layer formation velocity suggested by Ramirez-Guzman et al. (2012) and Woolery et al. (2016). The geologic stratigraphy at CUSSO shows this layer starting at 480 m. In both analyses, the bedrock was constrained at 585 m. The bedrock V_S for SWM ranged from 2000 – 2130 m/sec and 1850 – 2130 m/sec for the SWM Guided. In both analyses, the $\sigma\ln(V_S)$ is below 0.2 and primarily shows increased uncertainty near the layer interfaces, notably for the Memphis sand and Upper Cretaceous layer around 120 m and 500 m, respectively. This demonstrates the variability and uncertainty associated with the layer interfaces.

Inter-method comparison

In this section, a comparison is made between V_S profiles in this study and CUSSO V_S profiles from the literature. In Figure 2.8a, a comparison of the V_S profiles from SWM (median), SWM Guided (median), downhole, Woolery et al. (2016), Ramirez-Guzman et al. (2012)

(CUSVM), and Romero and Rix (2005) (lowland profile) is shown down to 200 m, whereas in Figure 2.8b, a comparison down to the bedrock is shown. Two pseudo V_S profiles computed from the maximum and minimum V_S values of the SWM and SWM Guided random profiles at every 0.1 m depth, together termed as 'max/min of non-invasive', are also shown in Figure 2.8a and 8b. These two pseudo V_S profiles help understand the uncertainty and variability associated with each layer of the median surface wave Vs profiles. The geologic stratigraphy from Woolery et al. (2016) is superimposed on Figure 2.8a and b. The time average shear wave velocity ($V_{S,Z}$) (similar to Vs30 calculation) is computed at every 0.1 m depth increment for all the V_S profiles mentioned and is shown in Figure 2.8c. The $\sigma \ln V_S$ between all V_S profiles, except Romero & Rix (2005) (as this profile is not site-specific) and the pseudo V_S profiles were calculated for the actual V_S and $V_{S,Z}$ and are shown in Figure 2.8d. The geologic stratigraphy from CUSVM, which was used as one of the literature sources for creating the parameterizations for surface wave inversions are superimposed on Figure 2.8d for layer depth and thickness comparisons. In this paper, unless CUSVM geologic stratigraphy is mentioned, by default the geologic stratigraphy from Woolery et al. (2016) is inferred.

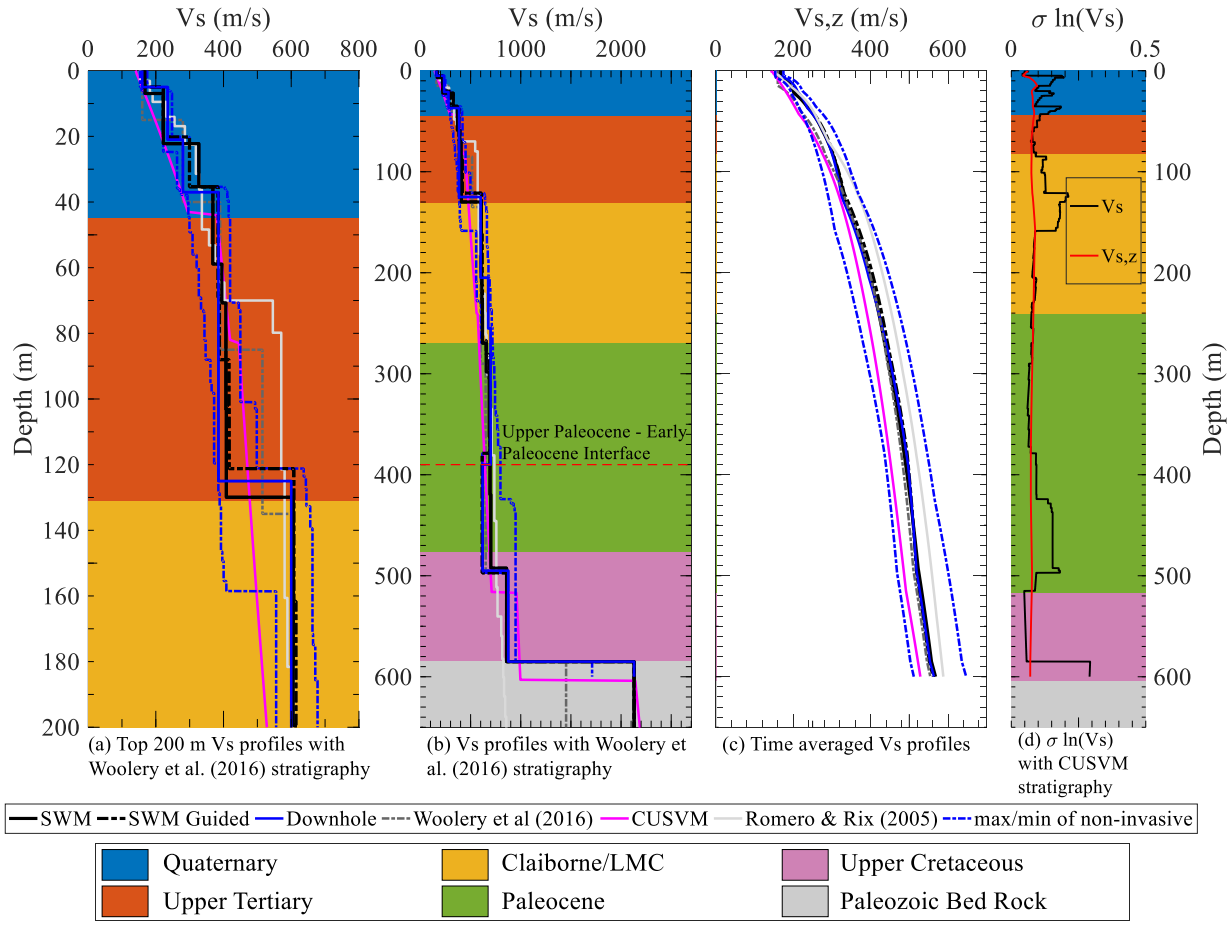

Figure 2.8 Shear wave velocity comparison between the developed V_S profiles and related V_S profiles from literature shown in (a) for the top 200 m, (b) down to the bedrock. Two pseudo V_S profiles computed from the maximum and minimum values of the random SWM and SWM Guided profiles, together termed as 'max/min of non-invasive' are shown in (a) and (b). The geologic stratigraphy from Woolery et al. (2016) is superimposed on (a) and (b) for comparing the layer thicknesses with the V_S profiles. A comparison of the time averaged V_S profiles ($V_{S,Z}$) is shown in (c). The $\sigma \ln V_S$ between all V_S profiles (except the Romero and Rix (2005) and the pseudo V_S profiles) are shown for actual V_S and $V_{S,Z}$ in (d). The geologic stratigraphy from CUSVM is superimposed on (d) for comparing the layer thicknesses and depth with the V_S profiles.

The SWM, SWM Guided, and downhole V_S profiles show similar depths to the Quaternary-Upper Tertiary interface, which approximately matches the geologic stratigraphy from Woolery et al. (2016). These V_S profiles resolve the Memphis sand at 120 – 130 m depth, within reasonable bound of the Memphis sand depth depicted by the local geology (131 m). However, the Romero and Rix (2005), Ramirez-Guzman et al. (2012), and Woolery et al. (2016)

V_S profiles have a shallower impedance contrast at 70 m, 82 m, and 85 m, respectively, inferring the probable Memphis sand, which is not in agreement with the local geology. All the V_S profiles in the comparison show similar trends from around 120 – 375 m, except the CUSVM, which is softer in this depth range and closer to the minimum of the pseudo V_S profiles. The downhole and SWM Guided V_S profiles resolved a velocity reversal layer around 380 m. The SWM V_S profile could not resolve this velocity reversal as it utilized a normally dispersive parameterizations. All the V_S profiles resolve the start of the Upper Cretaceous layer at around 470 – 520 m, except the Romero and Rix (2005), which does not resolve this layer. The local geology has this layer starting at around 480 m. The Paleozoic bedrock depth was constrained in the invasive and non-invasive V_S profiles as per the Woolery et al. (2016) bedrock depth at 585 m. However, the CUSVM V_S profile demonstrates the bedrock depth at 604 m, and the Romero and Rix (2005) does not include a bedrock layer at any specific depth. The SWM, SWM Guided and downhole V_S profiles have a bedrock V_S ranging from 2080 – 2180 m/sec. In contrast, the Woolery et al. (2016) V_S profile has a top-of-bedrock V_S of 1452 m/sec, which is likely a result of the P-S suspension log only penetrating a few meters into the bedrock layer. The CUSVM V_S profile has a bedrock V_S of 2140 m/sec, consistent with the developed V_S profiles in this study.

For the $V_{S,Z}$ comparison (Figure 2.8c), all the $V_{S,Z}$ profiles are within the bounds of the 'max/min of non-invasive' pseudo profiles. The SWM, SWM Guided, and downhole $V_{S,Z}$ profiles are in good agreement throughout the entire profile. The CUSVM V_S profile has a lower time weighted average velocity down to the bedrock, making this the softest among all profiles (except the lower bound of pseudo profiles). The Woolery et al. (2016) also has lower $V_{S,Z}$ down to around 100 m, but onwards become coherent with the V_S profiles in this study. The Romero and Rix (2005) $V_{S,Z}$ profile surpasses all the other profiles around 70 m due to the shallow

impedance contrast at 70 m depth, making this time weighted profile stiffest among all profiles (except the upper bound of the pseudo profiles). The Woolery et al. (2016) reported the average shear wave velocity from earthquake phase arrivals between the ground surface and bedrock to be 610 m/sec. The time weighted average shear wave velocity down to the bedrock for SWM, SWM Guided, downhole, Woolery et al. (2016), and CUSVM are 558, 552, 553, 546, and 526 m/sec, respectively. The developed V_S profiles in this study have average shear wave velocities in the range of 8.5 – 9.5% lower than the recorded average earthquake shear wave velocity, whereas the Woolery et al. (2016) and CUSVM profile's average shear wave velocities are respectively 10.5 and 13.5% lower. It should be noted that the time weighted average shear wave velocity for CUSVM was calculated down to the bedrock at 604 m.

The $\sigma \ln V_S$ for Vs and $V_{S,Z}$ shown in Figure 2.8d demonstrates the uncertainty between the actual V_S profiles and the time weighted profiles, respectively. The $\sigma \ln V_S$ for the actual V_S profiles is approximately 0.1 for much of the depth range. However, it jumps up to 0.2 in the near surface (top 50 m) and at depths associated with major impedance contrasts (e.g., Claiborne/Memphis Sand (80-160 m), and Upper Cretaceous (420-500)). Moreover, the bedrock $\sigma \ln V_S$ Jumps up to 0.36.This is mainly due to the bedrock V_S deviation of Woolery et al. (2016) V_S profile from all other profiles. Garofalo et al. (2016) also found similar trends of uncertainty for non-invasive V_S profiles. The coefficient of variation (COV) near the surface was found to be in the range of 0.2 – 0.4, whereas less than 0.2 COV was observed in the mid-profile depth. At depth near bedrock, COV was found to be as much as 0.8, inferring the challenge associated with resolving the bedrock depth and velocity with surface wave methods. The $\sigma \ln V_S$ for time weighted $V_{S,Z}$ profiles is generally around 0.1. Low COV value was also observed for $V_{S,Z}$ profiles in Garofalo

et al. (2016), except near the surface. Near surface COV for surface wave method $V_{S,Z}$ profiles in Garofalo et al. (2016) ranged from approximately 0.2 – 0.4 and decreased gradually with depth.

The CUSVM geologic stratigraphy is superimposed on Figure 2.8d to show the differences between the geologic stratigraphy from the Woolery et al. (2016) and CUSVM. The most noticeable differences between these two geologic stratigraphy is observed in the Claiborne/LMC layer depth and deeper layers, such as the Upper Cretaceous and bedrock depths. The developed V_S profiles in this study show more association with the local geologic stratigraphy from Woolery et al. (2016) than the geology from CUSVM. This also raises the question of utilizing the CUSVM for site specific site response studies, especially where shallow impedance contrast depths could influence the site response.

Site signature comparison

In this section, experimental site signatures from the dispersion data, HVSR, and recorded empirical transfer function (ETF) at CUSSO are used as a quantitative means of assessing the discussed V_S profile's appropriateness. The comparison between the experimental dispersion data and theoretical fits from the V_S profiles are shown in Figure 2.9. The comparison of theoretical dispersion fit with experimental dispersion data for the SWM and SWM Guided are shown in Figure 2.5in the Section 5.3. The calculated misfit between the experimental dispersion data and theoretical fit (both for Rayleigh and Love) for SWM, SWM Guided, downhole, Woolery et al. (2016), CUSVM, and Romero and Rix (2005) V_S profiles are 0.24, 0.4, 0.57, 1.0, 1.49, and 0.88, respectively. The non-invasive V_S profiles have lower misfit than the downhole. This is likely because the non-invasive V_S profiles were modeled using surface wave data. Thus, a relatively better fit is expected from the surface wave profiles than the downhole profile. The Woolery et al. (2016) theoretical fit (Figure 2.9c, 9d) has a higher misfit (misfit of

1.0) than the developed V_S profiles in this study. This is also graphically visible in Figure 2.9c as the Rayleigh theoretical fit separates from the experimental dispersion data around 2.2 Hz at a phase velocity of 372 m/sec. This point (372 m/sec, 2.2 Hz) represents a wavelength, $\lambda \approx 170$ m, and a resolution depth of approximately 85 m, which is the shallow impedance contrast depth that separated the Woolery et al. (2016) from the developed V_S profiles. For the CUSVM V_S profile, the theoretical Rayleigh and Love dispersion curves (Figure 2.9e, 9f) have a lower phase velocity than the experimental data, as a result the CUSVM has the highest misfit among all Vs profiles (1.49). Similarly the Woolery et al. (2016), Romero and Rix (2005) Rayleigh theoretical dispersion curve (Figure 2.9g) have a separation from the experimental dispersion data at around a wavelength of 140 m (pseudo depth of 70 m) due to the V_S profile's early shallow impedance contrast (Figure 2.8a, 8b, 8c). All the Love theoretical dispersion curves, except CUSVM, show similar misfits as the downhole and surface wave profiles, though the V_S profiles are quite different. This may be because Love wave experimental data did not reach to as long of a wavelength as the Rayleigh data, making it hard to observe the differences in theoretical fits. Moreover, Love waves have been shown to be less sensitive to V_S profile changes in the high frequency range (Zeng et al., 2007).

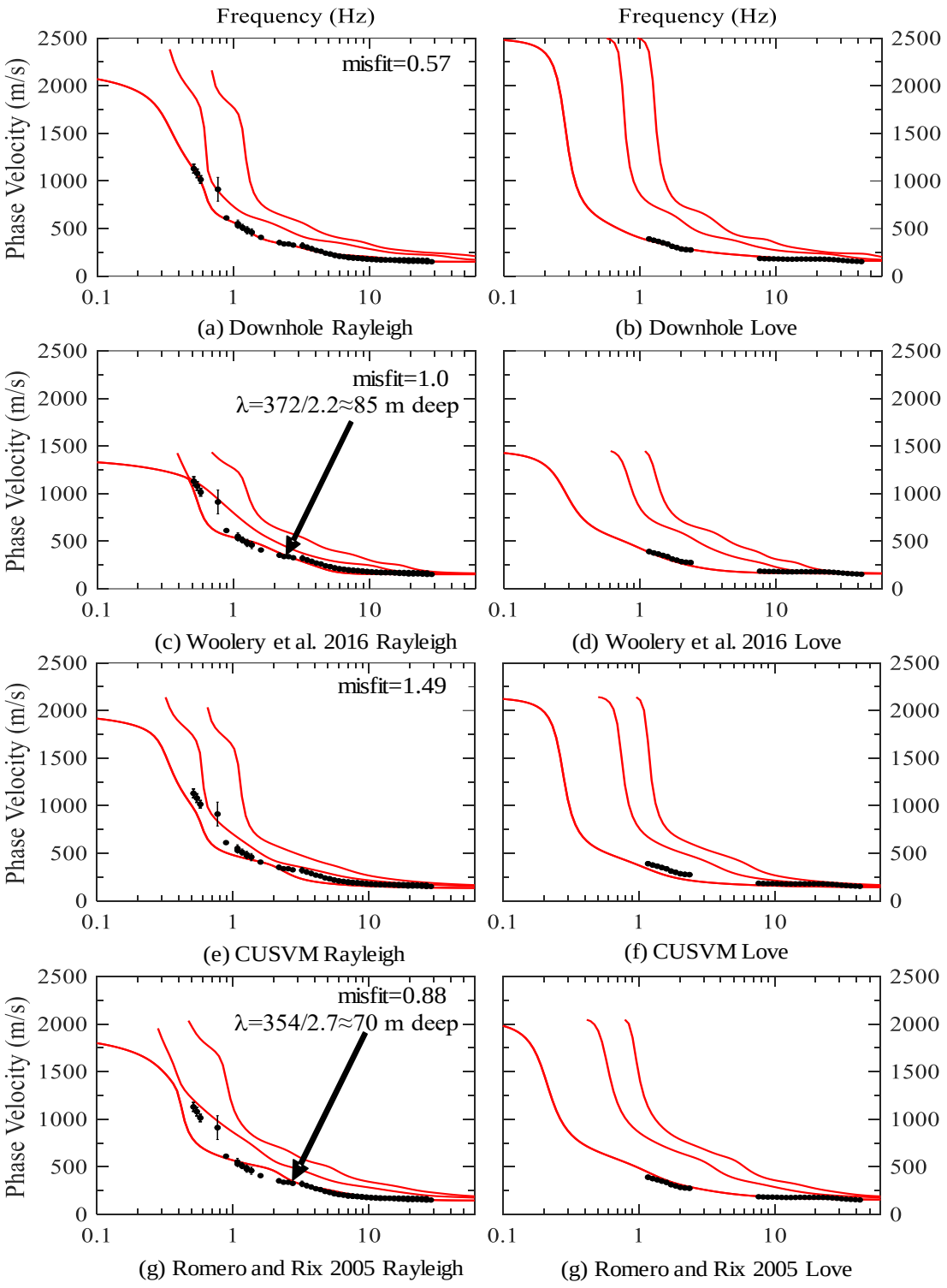

Figure 2.9 Comparison of experimental dispersion data and theoretical fit. Misfit calculated between the experimental and theoretical fit (for both Rayleigh and Love) for downhole, Woolery et al. (2016), CUSVM, and Romero and Rix (2005) V_S profiles are 0.57, 1.0, 1.49, and 0.88, respectively.

A further assessment of the V_S profiles were carried out by comparing the theoretical S_H wave transfer function (TTF) generated from the V_S profiles with empirical transfer function from the downhole array (ETF) and HVSR f_0. The fundamental mode Rayleigh wave ellipticity peaks generated from the V_S profiles were also compared with the HVSR f_0 as a crosscheck measurement. The HVSR curve is often modeled using either the S_H wave transfer function (Lermo and Chavrz-Garcia, 1993) or the Rayleigh wave ellipticity (Malischewsky and Scherbaum, 2004).

Comparisons of the TTF, ETF, and HVSR are shown in Figure 2.10a. The linear-viscoelastic TTFs were computed using the MATLAB code from Teague (Teague, 2017). The TTFs are computed between the bedrock and ground surface and computed using small strain damping ratios proposed by Darendeli (2001). The ETF at CUSSO was reported in Carpenter et al. (Carpenter et al., 2018) and is the spectral ratio of the transverse component at the ground surface to the transverse component at bedrock. The TTFs generated from the SWM, SWM Guided, downhole, Woolery et al. (2016) and CUSVM V_S profiles match well with the HVSR peak, f_0 and ETF first peak. The Romero and Rix (2005) TTF peak is situated to the left of the HVSR peak and ETF first peak, inferring a softer shear wave resonance frequency than the shear wave resonance frequency delineated by the HVSR f_0 and ETF first peak. The TTF first peak amplitude of SWM, SWM Guided, and downhole profiles correspond well with the ETF first peak amplitude and are within 3.3 – 4.1%, whereas the Woolery et al. (2016) first peak amplitude is 36% lower. This is due to the low bedrock velocity of the Woolery et al. (2016) V_S profile, causing the impedance contrast between the bedrock and overall profile to be lower and as a result generating lower amplification between the seismic waves traveling from bedrock to the ground surface.

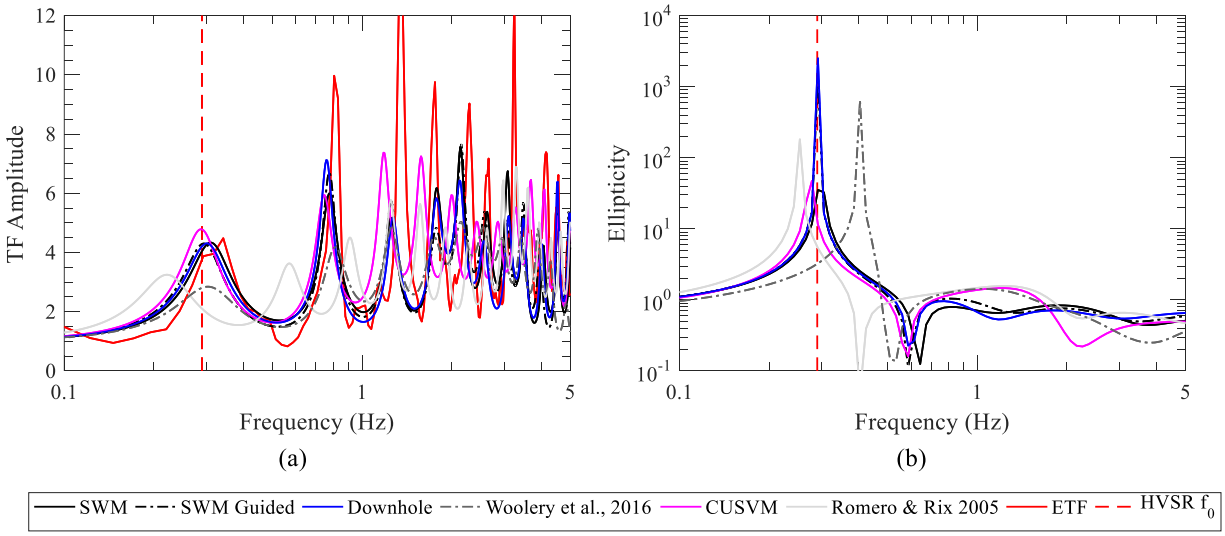

Figure 2.10 (a) Linear viscoelastic theoretical transfer functions (TTF) between surface and bedrock, generated from the V_S profiles are shown. An empirical transfer function (ETF) from Carpenter et al. (2018) and HVSR f_0 are also shown for comparison. (b) Fundamental mode Rayleigh wave ellipticity curves generated from the V_S profiles are shown. The HVSR f_0 is also shown for comparing with the ellipticity first peak, which denotes the shear wave resonance frequency in presence of seismic impedance contrast.

A comparison of Rayleigh ellipticity with the HVSR f_0 is shown in Figure 2.10b. The ellipticity peaks generated from SWM, SWM Guided, and downhole match well with the HVSR f_0, whereas the CUSVM ellipticity peak is slightly to the left of HVSR f_0. Similar to the TTF trend, the Romero and Rix [3] profile's ellipticity peak is to the left of HVSR f_0. The Woolery et al. (2016) profile's ellipticity peak is to the right of the HVSR f_0, and significantly higher (39%). This is again likely due to the bedrock Vs used by Woolery et al. (2016).

Overall, the SWM, SWM Guided, and downhole profiles exhibit better performance in capturing the site signature from dispersion data, HVSR f_0, and ETF peaks. The CUSVM profile's first peak of TTF and ellipticity are in the range of 1 – 4% of HVSR f_0. However, the theoretical dispersion fit of CUSVM profile shows a large misfit of 1.49, which is the largest among all candidate V_S profiles. As such, the CUSVM V_S profile do not appropriately capture the experimental site signature. The Romero and Rix (2005) TTF and ellipticity first peak and

Woolery et al. (2016) ellipticity first peak show noteworthy difference with the HVSR f_0, ranging from 5.2 – 39%. In addition, the Woolery et al. (2016) TTF first peak amplitude is significantly lower than the ETF first peak amplitude and is 37 % lower. The Romero and Rix (2005) and Woolery et al. (2016) profile's misfit between the theoretical fit and experimental data are substantial (0.88 – 1.0), ascertaining poor capture of experimental site signature.

2.7 Conclusions

In this study, a set of V_S profiles utilizing invasive and non-invasive methods was developed to evaluate the non-invasive method's reliability and estimate the variability with previously developed profiles at the CUSSO site. A joint inversion of the active and passive source surface wave data and HVSR fundamental frequency were used to conduct inversions to develop the non-invasive V_S profiles. Both a blind and a guided approach were utilized for surface wave inversion. Downhole measurements were carried out in the 259 m and 587 m deep boreholes using a sledgehammer and vibroseis truck as seismic sources, respectively. Even though non-invasive methods are generally considered less reliable, the non-invasive V_S profiles in this study provided comparable results to the invasive profile. However, the invasive downhole profile was able to resolve a deep low velocity layer, which is traditionally attributed to the invasive method's higher resolution at deeper depths. The blind approach non-invasive profile could not resolve this layer. Nonetheless, the guided non-invasive profile was able to resolve this deeper low velocity layer, indicating the effect of parameterization on the non-invasive method's capability to resolve deeper layers.

The developed shear wave velocity profiles were compared with the existing V_S profiles in Woolery et al. (2016), Ramirez-Guzman et al. (2012), and Romero and Rix (2005). Uncertainty ($\sigma \ln V_S$) between the Vs profiles was generally 0.1 with the uncertainty increasing up

to approximately 0.36 in the near surface layers (top 50 m), Memphis sand layer, and the Paleozoic bedrock. Several of these jumps in the uncertainty are associate with the major impedance contrasts at the site, highlighting the challenge in identifying the depth and Vs of these interfaces.

Site signatures were evaluated to assess the appropriateness of all discussed V_S profiles. The theoretical dispersion curves associated with the median of non-invasive V_S profiles and downhole V_S profile fit well with the experimental dispersion data with a reasonable misfit (0.24 – 0.57). Conversely, the theoretical dispersion curves associated with V_S profiles from previous studies have a larger misfit (0.88 – 1.49) and do not fit well with the experimental dispersion data. The better fit by the surface wave Vs profiles is expected since they were developed based on the experimental dispersion data. However, the downhole Vs profile developed in this study was developed independently of the surface wave data, indicating its higher accuracy compared to previous Vs models for the site. The site response from linear visco-elastic transfer function (TTF) associated with the developed V_S profiles demonstrated a better match with the HVSR f_0 and ETF. However, V_S profiles from previous studies show discrepancy with the HVSR f_0 and ETF, especially, the Woolery et al. (2016) TTF, which underestimated the amplification factor from ETF. Overall, the developed V_S profiles demonstrate the non-invasive method's applicability for characterizing deep sites in the Mississippi Embayment. These new measurements provided a suite of more accurate Vs profiles for modeling the recorded ground motions at the CUSSO array. The Vs profiles can be used for back analyses to reproduce ground motions at bedrock and simulation of seismic wave propagation in the Mississippi Embayment.

3. Site Response Impacts of the Memphis Sand Layer within the Mississippi Embayment

3.1 ABSTRACT

In this study, the site response impacts of accurately characterizing and resolving the Memphis sand layer at the Central United States Seismic Observatory (CUSSO) site are explored. The Memphis sand, also known as the '500 feet sand', is a major shallow impedance contrast in the Mississippi Embayment, influencing the site response estimates across the embayment. However, the Mississippi Embayment's available velocity information, including the Central United States Seismic Velocity Model, often does a poor job of properly identifying the depth and impendence contrast associated with the Memphis sand layer. To understand the impacts of the Memphis sand layer on site response estimates, a parametric study using linear visco-elastic transfer function and non-linear site response analysis is performed on a suite of shear wave velocity (V_S) profiles with varying depths to the Memphis sand and varying formation velocity of the Memphis sand. The linear and non-linear site response results indicate that varying the depth and V_S of the Memphis Sand layer within reasonable ranges can significantly impact site response results, with a variation of 10-30% observed for periods less than 1.0 sec. However, the largest variations are observed at periods between 1.0 and 2.0 secs with variations of up to 45%. This highlights the need to properly resolve shallow impedance contrast, such as the Memphis Sand in the Mississippi Embayment, for site response analyses.

3.2 Introduction

Understanding the influence of local soil conditions on earthquake ground motions (i.e., seismic site effects) is a critical aspect of the seismic design process. While many buildings or

bridges can be designed using the code based general procedure to account for seismic site effects, some sites and structures require site-specific ground motion response analyses (SSGMRA) (AASHTO 2011). One of the areas that often requires or can benefit from SSGMRA is the Mississippi Embayment. The Mississippi Embayment, situated in the central United States has deep unconsolidated sedimentary deposits ranging from 100 m to 1000 m (Van Arsdale and TenBrink, 2000) and situated in the vicinity of seismically active New Madrid Seismic Zone (NMSZ) (see Figure 3.1). This deep sediment thickness in the embayment is expected to attenuate short-period waves and amplify long period waves to a much greater extent than estimated using the general seismic design procedure (Cox et al., 2012). Therefore, SSGMRA are required for certain structures and soil conditions, especially highway bridges on liquefiable soil (AASHTO 2011). Wood and Baker (2018) showed the benefits of conducting the SSGMRA for short period bridges in the embayment, which could lead to a 7% reduction in the cost of the structure by reducing the design response spectrum in the short period range (< ~1.0 second).

To conduct a SSGMRA, the following are required: (1) input rock motions, (2) shear wave velocity (V_S) profiles, (3) non-linear dynamic soil properties, and (4) analysis method, which are also sources of uncertainty in the analysis (Idriss 2004). One of the most critical aspects is the V_S profile, preferably down to the bedrock (Hashash et al., 2001). In the Mississippi Embayment, the presence of the thick unconsolidated deposits add significant uncertainty in characterizing the V_S profile down to bedrock. Proper characterization of major impedance contrast, such as the Paleozoic bedrock and the Memphis sand in the embayment, play a critical role in SSGMRA. These two impedance boundaries in the embayment are known to influence the local site response (Wood et al., 2018; Himel 2018). Cox et al. (2012) observed almost identical site response results in their sensitivity analyses of surface response spectrum to

depth to bedrock in the Mississippi Embayment. However, the impact of the Memphis sand layer on local site response has not been studied in detail. A shallow impedance contrast in other regions has demonstrated significant influence on site response during past earthquakes, such as in the 1996 Pujili (Ecuador) earthquake. In this seismic event, most damaged buildings had a similar natural frequency to the superficial thin layer's resonant frequency (Field and Jacob, 1993).

In Gomberg et al. (2003), the upper Eocene layer (Eocene layer containing the Jackson, and Claiborne formation-Figure 3.1a) is estimated to be the source of the shallow impedance contrast. However, recent studies, conducted with stronger active source and/or low frequency passive source surface wave testing and deep downhole testing estimated the Memphis sand, which is a part of the lower to middle Claiborne group, to be the source of this shallow impedance contrast (Rosenbled et al., 2010; Wood and Himel, 2019). In spite of the borehole disturbances around 50 – 130 m, the Woolery et al. (2016) suspension log V_S profile also shows a sharp increase in velocity near the Claiborne formation (Figure 3.1a), predicting an impedance contrast. While the geologic association of the shallow impedance contrast in the Mississippi Embayment is still debated, in this paper we consider the Memphis Sand layer as the source of the impedance contrast. In this paper, the V_S profile developed by Himel and Wood (2021) is considered as the base profile (Figure 3.1), which estimates the Memphis sand as the source of shallow impedance contrast in the embayment. The Memphis sand layer is characterized throughout the embayment in previous studies with different formation velocities ranging from 445 m/sec (Central United States Seismic Velocity Model) (Ramirez-Guzman et al. 2012) to 685 m/sec (Rosenblad et al., 2010) and with different depths ranging from 50 m (Ramirez-Guzman et al. 2012) to 180 m (Wood and Himel, 2019). The resolved depth and V_S of this layer has even

been shown to vary significantly for a single site within the embayment. In a recent study at the Central United States Seismic Observatory (CUSSO) site, located in Western Kentucky (36°33'8.34"N, 89°19'46.99"W), the depth and V_S of the Memphis sand layer were provided by four research groups and was shown to vary between 70 m and 130 m with V_S between 425 m/s and 600 m/s (Himel and Wood, 2021).

In this paper, the site response impacts of properly characterizing the Memphis sand layer are explored. A suite of V_S profiles developed from a base V_S profile at CUSSO is constructed by varying the formation velocity and depth to the Memphis sand. To understand the impact of the Memphis sand on a site response analysis, both linear and non-linear site response analyses are conducted. Linear site response analyses are conducted on the V_S suite using a linear visco-elastic transfer function. The non-linear site response analyses are conducted using a suite of ten input rock motions, spectrally matched with the unified hazard target spectrum at the site. The response spectral acceleration and amplification for each V_S profile are compared and the residuals are computed to understand the impact of variations in the Memphis Sand on site response estimates.

3.3 Shear Wave Velocity Profiles

Downhole seismic measurements were conducted by Himel and Wood (2021) at the CUSSO boreholes down to 425 meters and used along with other V_S information to develop a full-depth V_S profile down to the Paleozoic bedrock at 585 m below the surface. This base profile has a Memphis sand formation velocity of 600 m/sec and a depth to the top of the Memphis sand of 125 m (V_{S30}=230 m/sec, site class D). In order to account for measurement uncertainty and spatial variability, the Memphis sand formation velocity and depth are varied as per previous studies to construct four additional pseudo V_S profiles. To account for the

uncertainty in depth to the Memphis sand layer, two V_S profiles are constructed by holding the V_S of the Memphis Sand layer at 600 m/s but varying the depth to the top of the layer from 50 m to 175 m (depth varied V_S profiles). This range of depths represent a reasonable depth range for the Memphis sand based on previous studies. In the same fashion, two V_S profiles are constructed by holding the top of the Memphis sand layer at a depth of 125 m but varying the formation velocity from 450 m/sec to 650 m/sec, which is also a reasonable range based on previous studies (velocity varied V_S profiles). The V_S profiles used in this study are shown in Figure 3.1a and 1b, respectively. While these ranges of depth and Vs may seem excessive for a single project site, site specific Vs information for most bridge projects only extends down to 30-45 m below the surface. This depth is significantly less than the typical depth of the Memphis Sand layer. Therefore, reference V_S profiles are typically used for site response. Hence, additional uncertainty is often introduced for the projects and the depth and Vs ranges used in the study are typical for various site-specific and reference Vs profiles in the region.

3.4 Linear Site Response Analysis

Linear visco-elastic theoretical transfer functions (TTF) between the surface and bedrock are computed for each of the candidate V_S profiles using a MATLAB code (D. Teague, personal comm., 2017) and shown in Figure 3.2a (depth changes) and 2b (velocity changes) for the suite of V_S profiles. Transfer function equations for damped, multiple horizontal soil layers over bedrock are used (Kramer 1996), with small strain damping ratios proposed by Darendeli, to calculate the TTFs (Darendeli, 2001). For comparison, the natural period (T_0 =3.45 sec) of the site and resonant frequency for the Memphis sand layer (T_1=1.28 sec) from Horizontal to Vertical Spectral Ratio (HVSR) measurements at the CUSSO site are plotted along with the TTFs (Wood and Himel, 2019). The HVSR peak periods are important to confirm that the V_S

profiles are correctly capturing the resonates of the site. The HVSR second peak (T_1) in the Mississippi Embayment has been shown to be caused by the shallow impedance contrast from the Memphis sand (Himel, 2018). Hence, T_1 is the resonant period for the Memphis sand layer rather than an odd harmonics of the natural period.

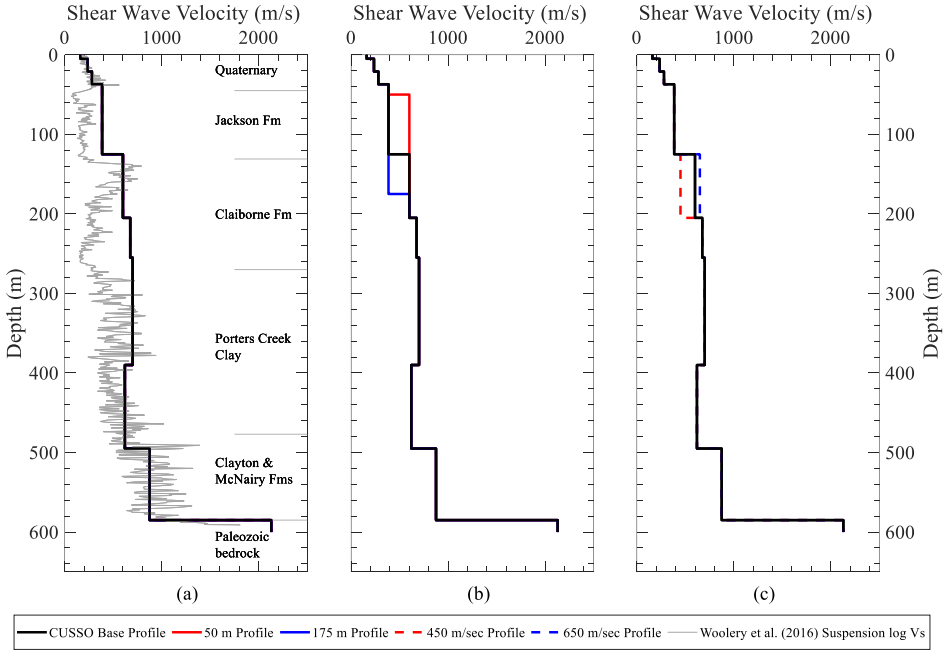

Figure 3.1 (a) Full-depth base VS profile down to bedrock from Himel and Wood (2021) along with suspension log Vs profile and geologic stratigraphy from Woolery et al. (2016). VS profiles for site response study by varying (b) the depth to the top of the Memphis sand, (c) the formation velocity of the Memphis sand.

For the depth varied V_S profiles (Figure 3.2a), the natural periods from all candidate V_S profiles' TTFs are almost identical with the HVSR natural period at the site. However, the amplitude of TTFs' at the natural period varies. The 50 m Profile's TTF has a 9% lower amplitude, whereas the 175 m Profile's TTF has a 12% higher amplitude at the natural period than the base profile's TTF. The resonant period for the Memphis sand layer from the 50 m Profile and 175 m Profile TTFs is 12% lower and 10% higher, respectively, than the base profile's resonant period for the Memphis sand, which is in good agreement with the HVSR T_1.

Around this period, the amplitude of 50 m Profile and 175 m Profile's TTFs are lower than the amplitude of the base profile's TTF. Other variations in both amplitude and peak period in the TTFs exist between 0.4-1.0 sec with variations generally being minimal below 0.4 sec. For the velocity varied V_S profiles (Figure 3.2b), the TTFs of candidate profiles do not vary significantly. All three candidate V_S profiles' TTF natural period and resonant period for Memphis sand match well with the HVSR T_0 and T_1, respectively. The amplitude of 450 m/sec Profile's TTF is 9% higher than the two other candidate profiles' TTF at the natural period.

Overall, varying the Memphis sand velocity within reasonable ranges can have approximately 9% impact on the amplitude of the linear site response analysis, but has little effect on the period ranges of amplifications. However, varying the depth to the top of the Memphis Sand layer with reasonable ranges has a larger impact on the site response results compared to the velocity varied profiles, especially around the Memphis sand's resonant period. Around this period, differences are observed for both period and amplitude between the depth-varied profile's site response and base profile's site response. Changing the Memphis sand layer's depth did not change the fundamental peak period but significantly influenced the second peak of the transfer function. This confirms that the second peak amplification is due to the shallow impedance contrast from the Memphis sand layer.

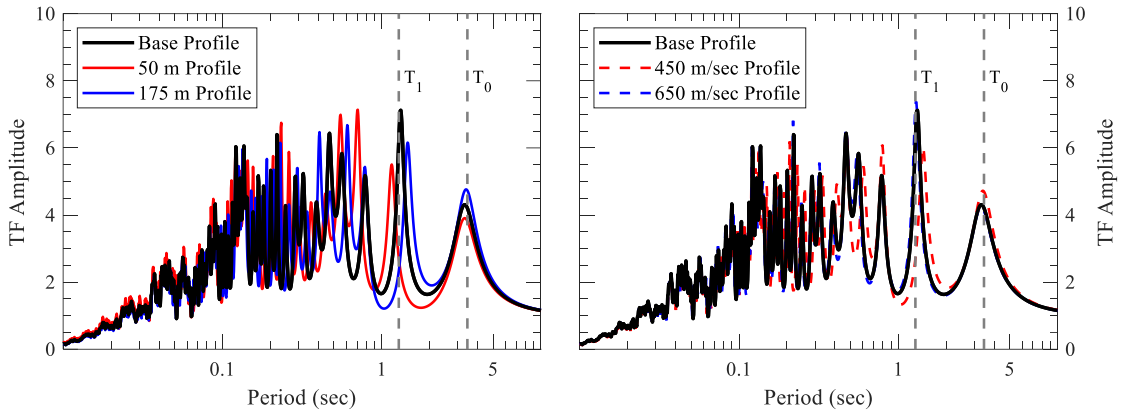

Figure 3.2 Linear visco-elastic theoretical transfer functions (TTF) between the surface and the bedrock corresponding to V_S profiles varying (a) depth to the top of the Memphis sand, (b) formation velocity of the Memphis sand. T_0=3.45 sec and T_1=1.28 sec are the fundamental period of site and resonant period of the Memphis sand, respectively.

3.5 Non-Linear Site Response Analysis

A deaggregation was performed to assess the seismic events that govern the seismic hazard at all periods at the CUSSO site. The USGS *Unified Hazard Tool, Dynamic Conterminous 2008 v 3.3 edition* was used for deaggregation. A return period of 1071 years (7% probability of exceedance in 75 years) hazard level specified by AASHTO (2011) guideline was used for the deaggregation. In this study, AASHTO (2011) code for SSGMRA is followed to prioritize the site response for bridge structures in continuation of the Wood and Baker (2018). The deaggregation results indicate a modal magnitude of 7.5~7.7 at a distance between 22 to 26 km governs the seismic hazard at all periods. It should be noted that the mean magnitude, distance pairs were close to the modal pairs, indicating a reasonably symmetric hazard sources about the mean. Using a modal magnitude of 7~7.8 at a distance of 8~40 km, a suite of ten input bedrock ground motions were selected from the Nuclear Regulatory Commission Project (NUREG) (McGuire et al., 2001). As large magnitude ground motions (GMs) at short distances have never been recorded in the central United States, earthquake time histories from other

regions are adjusted by McGuire et al. (2001) to encompass the frequency content expected from an earthquake occurring in the central and eastern United States. Using the deaggregation characteristics, the final selection of ten input ground motions are listed in Table 3.1, showing the moment magnitude, distance, PGA and duration of the seed GMs.

Table 3.1 Summary of selected input bedrock ground motions (McGuire et al., 2001).

Record	Event	Magnitude	Distance (km)	PGA (g)	Duration (sec)
SHL090	Cape Mendocino	7.1	33.8	0.585	14.6
SHL000	Cape Mendocino	7.1	33.8	0.648	14.4
GBZ000	Koacaeli, Turkey	7.4	17	0.454	7.3
DAY-TR	Tabas, Iran	7.4	17	0.947	9.7
DAY-LN	Tabas, Iran	7.4	17	0.993	8.8
GYN000	Koacaeli, Turkey	7.4	35.5	0.313	8.3
TCU128-N	Chi-Chi, Taiwan	7.6	9.7	0.305	29.9
TCU046-W	Chi-Chi, Taiwan	7.6	14.3	0.336	18.8
TCU047-W	Chi-Chi, Taiwan	7.6	33	0.7	12.9
TCU047-N	Chi-Chi, Taiwan	7.6	33	1.168	10.8

The *Unified Hazard Spectrum* (UHS) for site class A is chosen as the design target spectrum at periods between 0 and 2 sec using a return period of 1071 years. The Paleozoic bedrock in the Mississippi Embayment has a V_S > 1500 m/sec. Thus, a site class A target spectrum is used to spectrally match the input bedrock ground motions. The selected input rock ground motions must be adjusted either by scaling or spectral matching to match the seismic hazard consistent with the study site. In this study, the ten selected ground motions were adjusted by spectral matching with the design target response spectrum. RspMatch (2009 version) was used to spectrally match the selected ground motions to the design target spectrum. Though scaling is a simpler approach, previous studies have found spectral matching to be a more reliable adjustment method (Heo et al., 2011). The original and adjusted acceleration time history, and arias intensity plots were compared for all ground motions to evaluate the originality of the input ground motions after spectral adjustments (not shown here).

3.6 Simulating Shear Wave Propagation

To simulate the propagation of horizontally polarized shear wave through the soil column, the software DEEPSOIL 7.0 was utilized (Hashash et al., 2020). The Darendeli (2001) modulus reduction and damping curves were used along with the quadratic/ hyperbolic (GQ/H) model in DEEPSOIL 7.0. The modulus reduction and damping curve were fit with the University of Illinois at Urbana-Champaign reduction factor fitting procedure (MRDF-UIUC). Target shear strength values for each layer were based on Mohr-Coulomb failure criteria assuming a friction angle of 30° with no cohesion. A friction angle of 30° is a conservative estimate, given no actual laboratory test was conducted on the soil sample. These dynamic soil properties were not randomized as only the Memphis sand depth and velocity are varied to study their impact on site response. Therefore, other factors were kept as similar as possible for all the analysis.

3.7 Non-linear Site Response Analysis Results

For each candidate V_S profile, ten site response analyses were performed (using the ten input motions). Each site response analysis provided a surface acceleration time history. A 5% damped response spectra from the surface acceleration time history is calculated to obtain the surface response spectra for each analysis. A log-normal-median (LNM) surface response spectrum for each candidate V_S profile is calculated from each profile's suite of ten surface response spectra. The amplification factor (AF) is calculated from the ratio of spectral acceleration at the surface to spectral acceleration of input motion. A LNM amplification factor for each candidate V_S profile is calculated from each profile's suite of ten amplification factor curves.

The LNM surface response spectra and LNM AF calculated for each candidate V_S profile are shown in Figure 3.3a and 3b, respectively. The AASHTO design response spectrum for site

class D and two-thirds of site class D at CUSSO are also shown in Figure 3.3a for comparison with the surface response spectra.

It is observed in the surface response spectra results (Figure 3.3a) that up to 2 sec, the 50 m Profile's surface response spectra is higher (up to 32%), and the 175 m Profile's surface response spectra is lower (up to 17%) than the base profile's surface response spectra. The velocity varied 450 m/sec Profile's surface response spectra is lower than the base profile in this period range (up to 10%), whereas the 650 m/sec profile's surface response spectra is almost identical as the base profile's surface response spectra. This indicates the depth and V_S of the Memphis Sand has an effect on the site response spectrum over the peak period range (0.1-2 secs), with the largest difference observed between 1-2 secs.

For the AF results (Figure 3.3b), a similar trend as the surface response spectra results are observed. Up to a period of 2 sec, the 50 m Profile's AF is higher (up to 32%), and 175 m Profile's AF is lower (up to 17%) than the base profile's AF. All candidate V_S profiles have identical amplification peaks at approximately 4.5 second, which is higher than the HVSR T_0. Like the linear site response, the 50 m Profile has the lowest amplification around this period. All candidate V_S profiles, except the 50 m Profile, demonstrate a second amplification peak around 2.5 second, which is greater than the HVSR T_1. Similar to the linear site response TTF, the non-linear AF for the 50 m Profile demonstrates a lower second peak period than the base profile.

To demonstrate the site response difference between the base profile and other candidate V_S profiles, residuals of the varied V_S profiles' surface response spectra and AF are calculated. Considering the base profile results as measured and varied profile results as predicted, the following equation is used to calculate the residuals. The surface response spectra residuals and AF residuals are shown in Figure 3.3c and 3d, respectively.

Residual, R=ln (Sa or AF) $_{\text{base Profile}}$-ln (Sa or AF) $_{\text{varied profile}}$

The residual results for the surface response spectra and AF have similar trends. Up to a period of approximately 2 sec, the highest negative residual is observed for the 50 m Profile with a maximum of -0.28 and a residual of -0.21 between 0.1-1.0 secs. The highest positive residual is observed for the 175 m Profile, with a maximum residual of 0.18 and most residuals being between 0.05-0.18. This implies that these two profiles have the highest and lowest site response amplification in this period range, respectively. The 450 m/s Profile has positive residuals ranging from 0-0.12, while the 650 m/s Profile has almost no residual. Overall, the results for non-linear site responses are in good agreement with the linear site response analysis.

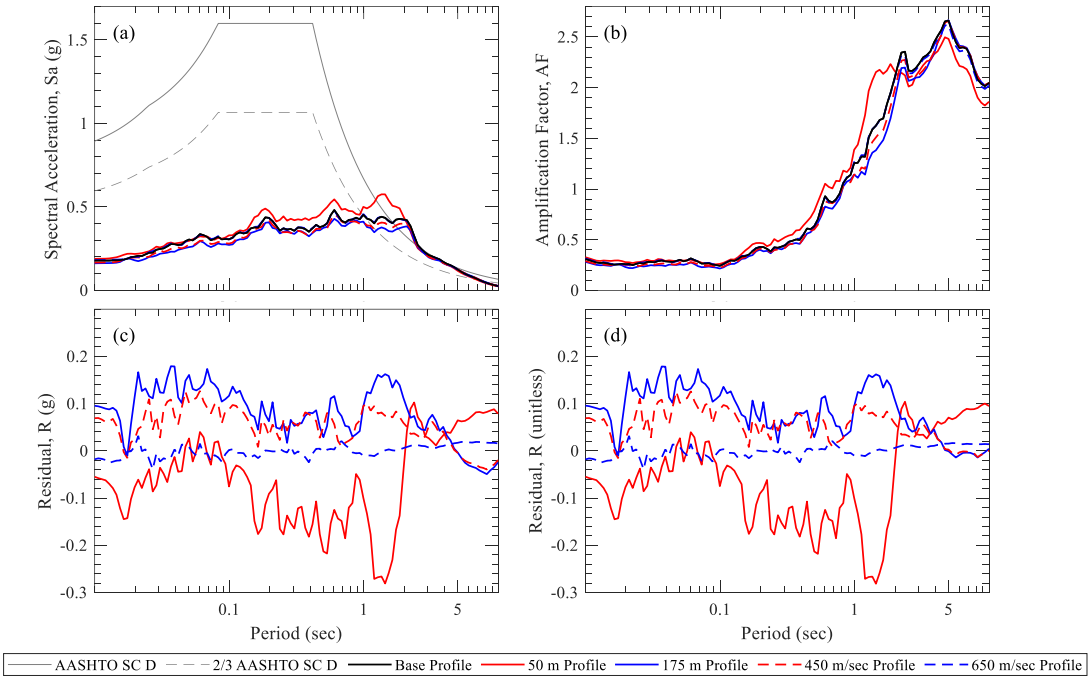

Figure 3.3 (a) LNM surface response spectra for each of the candidate V_S profiles along with AASHTO site class D general procedure response spectra, (b) LNM amplification factor for each of the candidate V_S profiles, (c) Spectral acceleration residuals for varied profiles, (d) Amplification factor residuals for varied profiles.

Finally, as per AASHTO (2011) guideline, the design response spectrum is constructed for each candidate V_S profile by multiplying the LNM AF period by period with the site class A

spectral accelerations. The delineated design response spectrum for each candidate V_S profile is shown in Figure 3.4a along with the AASHTO site class D response spectrum. As the AASHTO code allows a 33% reduction of seismic load where appropriate, delineated design response spectrum for all candidate V_S profiles is the same up to a period of approximately one second. From one to two seconds, the 50 m Profile has the highest design response spectra, and the 175 m profile has the lowest design response spectra. A percent difference in delineated design response spectra for the varied profiles with respect to the base profile's delineated design response spectra are calculated and shown in Figure 3.4b. For the 1-2 sec period range, the 50 m Profile has up to 30% higher spectral acceleration, and 175 m Profile has up to 15% lower spectral acceleration than the base profile. This infers that any bridges or buildings with natural periods of 1-2 secs could be overdesigned or under-designed, respectively, using the site response results from these two V_S profiles. The site response results demonstrate that correctly resolving the depth of the Memphis Sand layer for site response within the embayment has a significant impact. For reasonable depths to the Memphis Sand, a 45% difference in the spectral acceleration in a period range (1-2 secs) is observed and is a period range often encountered in bridge design.

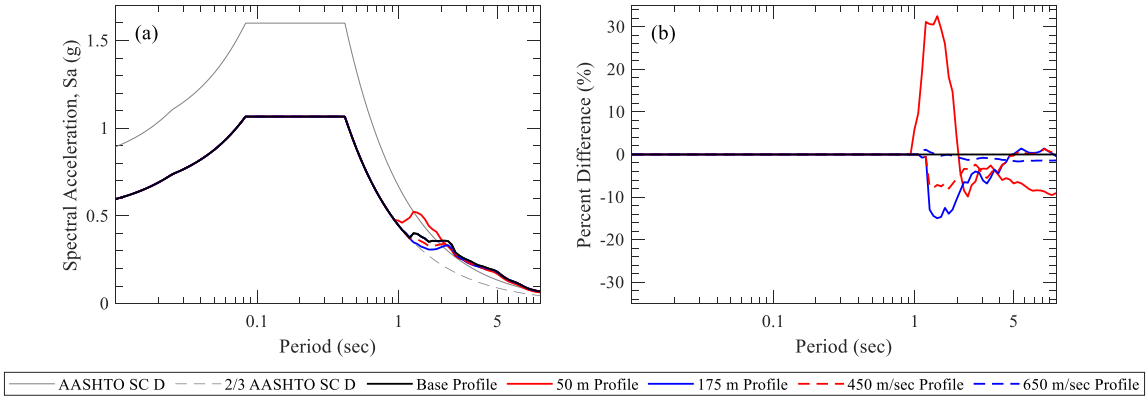

Figure 3.4 (a) Delineated design response spectrum shown for the candidate V_S profiles along with site class D design response spectrum, (b) Percent difference of delineated design response spectrum results for varied profiles with the base profile's delineated response spectrum.

3.8 Conclusion

In this study, a set of V_S profiles were constructed from the downhole profile at the CUSSO site by varying the depth and the formation velocity of the Memphis sand to observe the impacts of incorrectly resolving this shallow impedance contrast on site response results. Linear and non-linear site response analyses were conducted on all candidate V_S profiles. Both analyses methods demonstrated that varying the depth to the top of the Memphis Sand produces noteworthy difference up to a period of two secs with ranges in the spectral acceleration varying from 10 to 30% between 0 and 1.0 secs with the most significant differences occurring between 1-2 secs with a range of 45%. However, the velocity varied profiles' site response has less noteworthy differences up to a period of two second with a range of differences typically less than 10%. The delineated design response spectrums demonstrate the depth variation to the Memphis Sand has the largest impact in the 1-2 secs period range (ranges up to 45% difference). For bridges designed under the AASHTO guidelines, the differences can have a significant impact on bridges with a natural period of 1-2 secs. Inaccurately characterizing the shallow impedance contrast from the Memphis sand in the Mississippi Embayment could provide seismic loads that could lead to overdesigning or under designing of bridges or buildings. Therefore, special consideration/attention should be taken to accurately resolve the depth and velocity of the Memphis Sand layer for site response analyses.

4. Deep Shear Wave Velocity Profiles in the Mississippi Embayment from Surface Wave Measurements

4.1 Abstract

Local geology in the Mississippi embayment is a significant source of site effects due to the deep unconsolidated sediments and basin effects near the edge of the embayment. Proper characterization of the velocity structure of the embayment is crucial for site response and seismic hazard studies. In this paper, deep dynamic site characterization was conducted in the Mississippi embayment to develop shear wave velocity profiles down to bedrock at 24 sites using active and passive source surface wave methods. Study sites cover parts of Arkansas, Missouri, Kentucky, and Tennessee, with bedrock depths ranging from 250 – 1115 m. Multimodal joint inversion of surface wave data, which included both Rayleigh and Love wave dispersion and site fundamental frequency was utilized to develop the shear wave velocity profiles (V_S profiles). The developed V_S profiles provided reasonable site characterization solution and captured the site signature from experimental dispersion data and fundamental frequency. Average shear wave velocity down to bedrock range from 462 – 686 m/sec and proportionally related with the site period and depth to bedrock of the site. Average shear wave velocities estimated by previous studies using the resonance period-sediment thickness relationship tend to systematically overestimate the average shear wave velocity in the embayment by 25 – 40%. Formation velocities calculated for the commonly found geologic units in the embayment, Quaternary, Upper Tertiary, Memphis sand, Paleocene, Cretaceous, and Paleozoic bedrock are approximately 214, 418, 607, 665, 967, and 2211 m/sec, respectively. Comparison of the developed V_S profiles demonstrated better agreement with related V_S profiles

generated from direct measurements, but differences up to 30% are observed with the current velocity models of the Embayment.

4.2 Introduction

The Mississippi embayment, situated in the central United States, covers an area of about 650,000 square kilometers encompassing parts of Arkansas, Missouri, Illinois, Kentucky, Tennessee, and Mississippi. The embayment is characterized geologically by deep, unconsolidated sediments of a few meters in the upper part near southern Illinois to a depth of about 1000 m near southern Memphis, Tennessee (Van Arsdale and TenBrink, 2000). This deep, unconsolidated sediment in the central and southern part of the embayment is an important source of local site effects, causing a complex mixture of amplification/deamplification of seismic waves at different period ranges (Hashash and Park, 2001; Wood and Baker, 2018; Woolery et al., 2016; Romero and Rix, 2005). Nevertheless, at the edge of the embayment where the sediment thickness is shallow, strong diffraction takes place due to the strong impedance contrast between soil column and shallow bedrock. This basin edge effect near the shallow part of the embayment results in longer duration ground motions (Kawase, 2003; Boore, 1999). The New Madrid Seismic Zone (NMSZ) is the major source of seismicity in the region, which is a series of three faults. Collectively, the local site effects from the deep sediments, basin edge effects from the shallow edges, and the presence of the NMSZ cause areas in the embayment to have some of the highest design ground motions in the United States (ASCE, 2017). Despite the NMSZ being one of the highest seismic hazard prone areas in the US, no large earthquake ground motions have been recorded in the embayment. In absence of locally recorded strong ground motions, the seismic velocity models of the embayment, especially down to bedrock could be helpful in understanding the spatial variability of the ground motion. Representative

estimates of the shear wave velocity (V_S) profiles in the embayment are of utmost importance for ground motion studies, which include but are not limited to back analyses for replicating recorded ground motions, and forward analyses to predict future strong ground motions. Numerous site response studies have demonstrated the influence of V_S profiles on the amplitude and frequency content of the surface ground motion (Rathje et al., 2010; Li and Assimaki, 2010).

Despite the large variation in sediment thickness and local site effects in the embayment, two single reference Vs profiles developed by Romero and Rix (2005) for the lowland and upland areas of the embayment are used for site response studies in the embayment due to the lack of site-specific deep V_S profiles (Hashash and Park, 2001; Romero and Rix, 2005). The overall site-specific V_S profile database for the embayment is sparse, with the majority of the available V_S profiles being 30 – 60 m deep (Liu et al., 1997, Street et al., 2004). Some seismic reflection/refraction studies are capable of capturing the velocity differences in deeper layers and inferring geologic layer boundaries (Street et al., 2004; Luzietti et al., 1992). However, these studies lack direct evidence of V_S for individual soil layers exceeding 150 m depth (Street et al., 2004). Rosenblad et al. (2010) developed eleven deep V_S profiles extending down to 200 – 250 m, characterizing down to a shallow impedance boundary in the embayment, but lacking the data down to the deep bedrock layer. Ramirez-Guzman et al. (2012) developed the Central United States Seismic Velocity Model (CUSVM) by combining results from borehole logs, and seismic reflection/refraction studies and extrapolated the results for the Central US, including the Mississippi embayment. However, below 100 m depth, reference V_S profiles and site-specific CUSVM V_S profiles show more than 50% difference (Himel and Wood, 2021a), emphasizing the need for additional site-specific deep Vs profiles to improve velocity models for the region and reduce uncertainties in modelling the deep V_S structure.

An effort to develop a deep V_S profile for the Mississippi embayment was made by Woolery et al. (2016) at the Central United States Seismic Observatory (CUSSO) (shown in Figure 4.1). A series of three boreholes with 30 m, 259 m, and 587 m depth constitutes the CUSSO vertical array, with accelerometers installed at the surface and at the bottom of each borehole. Walkaway seismic reflection/refraction, P-S suspension logging, and phase arrival time analysis were used to develop the V_S profile at this location. However, significant differences are observed between the suspension log and walkaway survey. A recent study at the CUSSO vertical array was conducted by Himel and Wood (2021) to study the reliability of surface wave methods (SWM) to properly characterize the deep soil column of the embayment down to bedrock. A combination of active and passive source surface wave methods were used to develop the SWM V_S profiles. A downhole V_S profile was also developed for the 587 m deep borehole for comparison as invasive methods are considered more reliable than the SWM. Despite the non-uniqueness issue of SWM (Cox and Teague, 2014), the developed SWM V_S profiles demonstrated comparable results with the downhole V_S profile and were able to capture site signatures from the experimental dispersion data, and fundamental period. This indicates SWM's competence in developing suitable V_S profiles at deep sites that can yield reasonable site response estimates (Griffiths et al., 2016a; Teague et al., 2018; Deschenes et al., 2018).

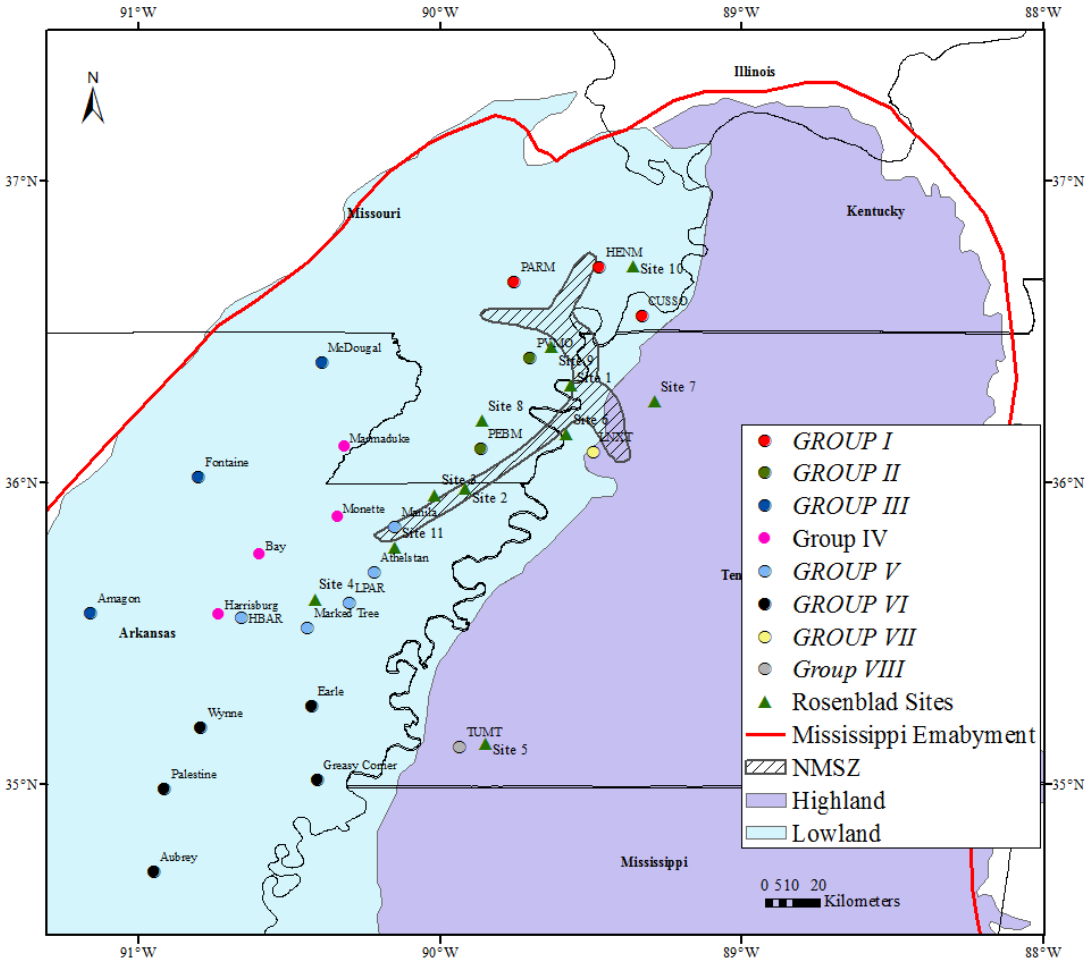

Figure 4.1 Map of the Mississippi embayment showing the 24 surface wave measurement sites along with the extent of lowland and upland area in the embayment, NMSZ and Crowley's ridge. Location of the related Rosenblad et al. (2010) study sites are also shown.

In this study, deep Vs profiles at 24 sites (including CUSSO) in the Mississippi embayment are developed following the SWM methodology by Himel and Wood (2021a). The acquisition and processing of the active and passive source surface wave data are discussed first. A demonstration of challenges associated with the non-uniqueness in the inversion process including mode identification and elimination of effective mode data is presented for an example site. The theoretical dispersion curves generated from the developed V_S profiles at the example site are compared with the recorded experimental dispersion data. Moreover, the theoretical ellipticity peak and theoretical transfer function (TTF) peak generated from the median V_S

profile are compared with the fundamental period of that site from horizontal to vertical spectral ratio measurements. These comparisons ensure that the SWM V_S profiles at the site are capable of capturing the site signatures. Finally, the developed SWM V_S profiles for all 24 study sites are presented and compared with reference V_S profiles, CUSVM site-specific profiles, and related V_S profiles from the literature.

4.3 Overview of the Mississippi Embayment Stratigraphy

The sediments in the Mississippi embayment range in age from Paleocene to recent Holocene and Pleistocene. As per CUSVM, geologic units in the Mississippi embayment are divided as Quaternary, Upper Tertiary, Lower to Middle Claiborne (LMC), Paleocene, Cretaceous, and Paleozoic era bedrock (Ramirez-Guzman et al., 2012). The Quaternary layer houses the Holocene and Pleistocene era alluvial surface deposits. The Holocene era deposits are found in the lowland, while the Pleistocene deposits are found in the upland part of the embayment Ramirez-Guzman et al. (2012) Romero and Rix, 2005) (see Figure 4.1). The Upper Tertiary layer consists of the Jackson formation and Upper Claiborne group, characterized with silts, clay, and some lignite (Van Arsdale and TenBrink, 2000). The LMC layer, also known as the Memphis sand/Sparta sand (depending upon location) is part of the Tertiary aged deposit but differentiated due to the velocity contrast with the Upper Tertiary layer. The Memphis sand is a very fine to coarse grained, light gray-white sand (Van Arsdale and TenBrink, 2000). The Paleocene layer houses the Wilcox and Midway groups and is composed of silt, clay, fine to coarse grained sand, and some minor limestone (Van Arsdale and TenBrink, 2000; Brahana et al., 1987). The Cretaceous layer consists of McNairy sand, Demopolis formation, and Coffee formation, composed mainly of sand, silt, and undifferentiated limestone (Street et al., 2004). The Paleozoic layer bedrock is composed of Knox Dolomite and forms the major impedance

boundary in the embayment. Another source of impedance contrast is observed at the interface of the Upper-Tertiary - LMC layer. The deposits above the LMC layer have a low V_S of 193 ± 14 m/sec compared with the Memphis sand's formation velocity of 685 ± 83 m/sec (Rosenblad et al., 2010). The presence of thick unconsolidated sediments along with the two impedance boundaries in the geologic structure adds significant uncertainty in ground motion propagation in the embayment (Hashash and Park, 2001).

4.4 Testing Sites

Surface wave measurements were carried out in two phases at 24 sites in Arkansas, Tennessee, Kentucky, and Missouri, as shown in Figure 4.1. In the first phase, measurements were made at fifteen sites non-seismic station sites, while in the second phase, measurements were made at seismic stations (CUSSO, HENM, PARM, PEBM, PVMO, HBAR, LPAR, LNXT, TUMT). The majority of the sites are situated in the lowland part of the embayment. The TUMT and LNXT sites are situated in the highland part. Based on similar site characterization results and geologic locations, the sites are divided into eight groups and shown accordingly on the map (see Figure 4.1). The locations of the Rosenblad et al. (2010) study sites are also shown in Figure 4.1 as some of the related Rosenblad et al. (2010) sites are compared with the Vs profiles developed in this study. Table 4.1 presents the coordinates of each site along with their estimated bedrock depth from the CUSVM (Ramirez-Guzman et al., 2012). Sites were selected based on their geologic location, accessibility, sufficient space for testing, and the ability to obtain necessary permission for testing. At the seismic station sites, measurements were taken in close proximity to the seismic stations. More details regarding the exact testing locations for each site are provide in the electronic supplement.

Table 4.1 Surface wave measurement site locations along with their bedrock depth from Ramirez-Guzman et al. (2012), except CUSSO, for which, bedrock depth sourced from Woolery et al. (2016).

Group	Site Name	Latitude	Longitude	Bedrock Depth (m)
Group I	CUSSO	36.552	-89.329	585
	HENM	36.716	-89.472	450
	PARM	36.664	-89.752	427
Group II	PEBM	36.113	-89.862	764
	PVMO	36.413	-89.699	591
Group III	Amagon	35.568	-91.156	350
	Fontaine	36.017	-90.799	291
	McDougal	36.399	-90.388	252
Group IV	Bay	35.762	-90.594	587
	Harrisburg	35.566	-90.730	701
	Marmaduke	36.119	-90.313	492
	Monette	35.886	-90.335	677
Group V	Athelstan	35.704	-90.217	858
	HBAR	35.553	-90.654	754
	LPAR	35.602	-90.300	840
	Manila	35.853	-90.147	813
	Marked Tree	35.520	-90.436	853
Group VI	Aubrey	34.711	-90.944	1114
	Earle	35.259	-90.423	1018
	Greasy Corner	35.016	-90.403	1069
	Palestine	34.987	-90.911	958
	Wynne	35.188	-90.790	853
Group VII	LNXT	36.101	-89.491	845
Group VIII	TUMT	35.123	-89.933	923

4.5 Testing Methodology

Active and passive source surface wave measurements were made at all 24 sites. The combination of active and passive source measurements ensures retrieval of both high and low frequency dispersion data, which in turn assure high resolution in the near surface and deep penetration depth, respectively. Active MASW (Park et al., 1999) testing was conducted using a linear array of 24, 4.5 Hz vertical (Rayleigh) and horizontal (Love) geophones with 2 m

geophone spacing (46 m long array). A 5.4 kg sledgehammer source was used to generate Rayleigh and Love waves from vertical and horizontal strikes, respectively. Multiple source offsets of 5, 10, 20, and 40 m from the first geophone were used to produce high quality data and minimize the influence of near-field effects. At each source offset, ten sledgehammer blows were stacked to improve the signal-to-noise ratio. P-wave refraction utilizing the same MASW array was conducted using a 2 m source offset to estimate the ground water table depth at each site. At some select sites, active MASW was conducted utilizing the University of Arkansas Vibroseis truck (Industrial Vehicles International T – 15000) as the seismic source. The vibroseis source is capable of producing longer wavelength data than the sledgehammer. Thus, can resolve deeper depths compared to a sledgehammer source. Only Rayleigh wave data were retrieved using the vibroseis with an array length ranging from 46 m (2 m geophone spacing) to 94 m (4 m geophone spacing). The same source offset distances were used for the vibroseis MASW testing as the sledgehammer MASW testing.

The passive source microtremor array measurements (MAM) (Tokimatsu, 1997) were carried out using circular arrays at all sites and L-shaped arrays in some select sites. Circular arrays of approximately 50 m, 200 m, and 500 m diameters were used at all sites. A 1000 m diameter array was used for some select sites where sufficient space was available. At the seismic station sites, nine three-component Trillium compact 20-sec broadband seismometers were used in each array, while ten seismometers were used for the non-seismic station sites. In each circular array configuration, one seismometer was placed in the center, and the rest of the seismometers were uniformly spaced around the circumference. At some sites, deviations from the typical layout were made due to site constraints. A centimeter accurate GPS unit was used to record the exact location of each seismometer. Ambient noise was recorded using each array for one hour to two

hours, with a longer recording time for larger diameter circular arrays. Nanometrics Centaur digitizers were used to record the data. The MAM data recorded using the circular array of seismometers were also used for the HVSR measurements. The L-array MAM measurements were carried out using 24, 4.5 Hz vertical geophones. A geophone spacing of 5 m was used, resulting in an approximate L-shaped array of 55 m × 60 m. Ambient noise for the L-array was recorded for 1 hour. A typical surface wave array setup is shown in Figure 4.2 for the Manila site.

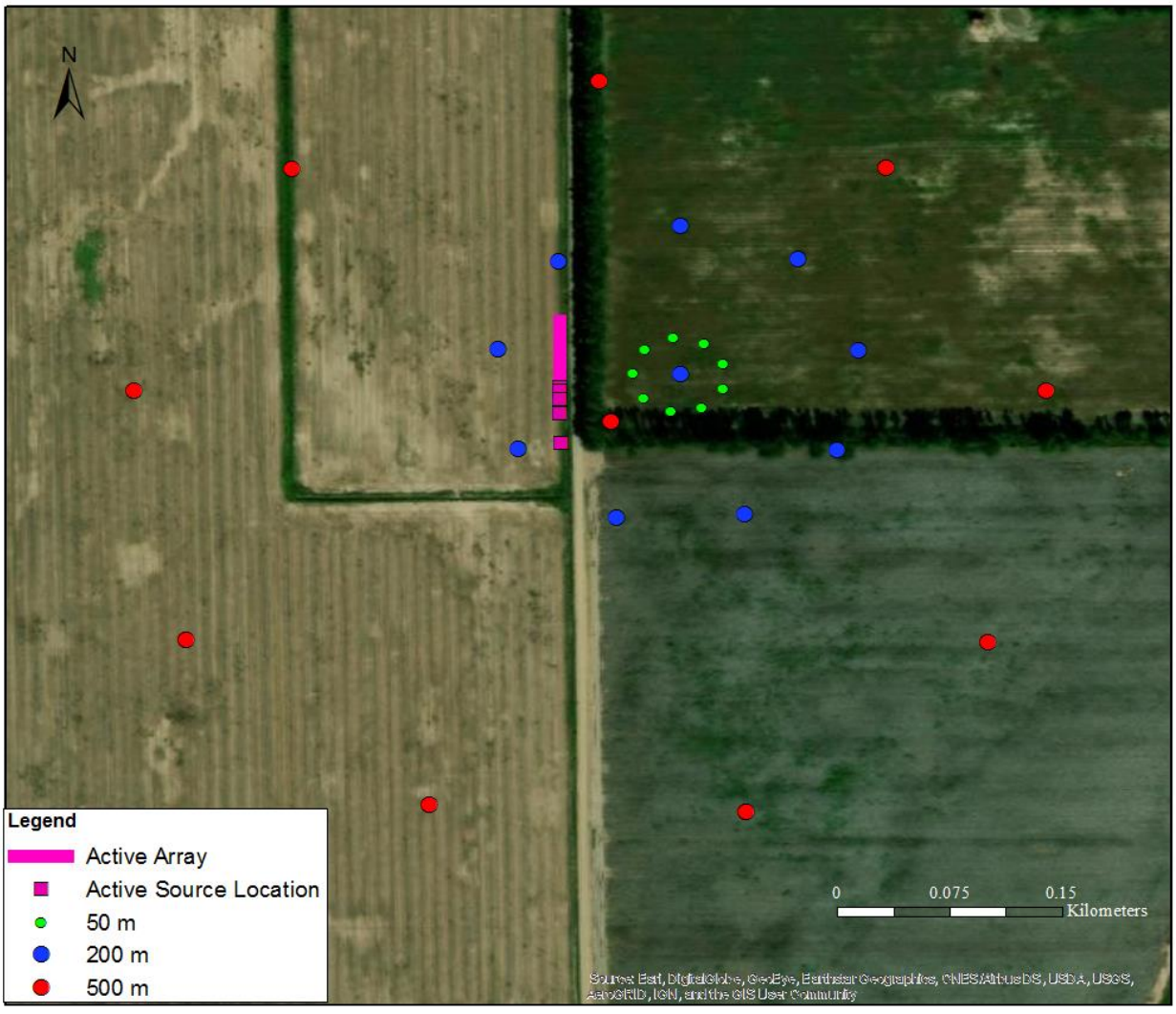

Figure 4.2 A typical surface wave array setup is shown with the three circular MAM arrays (50 m, 200 m, and 500 diameter) and active MASW array for the Manila site.

4.6 Data Processing

The data processing consists mainly of four major steps: 1) developing composite experimental dispersion data from active and passive SWM, 2) estimating the fundamental frequency of the site utilizing the horizontal to vertical spectrum ratio (HVSR) method (Nakamura, 1989), 3) P-wave refraction processing to estimate the water table depth, and 4) joint inversion of the composite experimental dispersion curves and site fundamental frequency to obtain Vs information.

The active source MASW Rayleigh (both sledgehammer and vibroseis) and Love data with multiple source offsets were processed using the Frequency Domain Beam Former method (FDBF) (Cox and Wood, 2011; Zywicki, 1999). The circular (both Rayleigh and Love) and L-array MAM data were processed using the High Resolution Frequency-Wavenumber (HRFK) method (Capon, 1967), and Frequency-Wavenumber (FK) method (Kelly, 1967; Harjes and Hanger, 1973), respectively. The circular MAM Rayleigh wave data were also processed using the Modified Spatial Auto-Correlation method (MSPAC) (Bettig et al., 2001). The MSPAC method acts as a cross-check to the HRFK and ensures reliable dispersion data estimates over a large frequency band (Foti et al., 2018). This method has been shown to be better capable of extracting low frequency data than the HRFK based methods (Foti et al., 2018). In addition, HRFK data can exhibit bias toward higher phase velocities when passive waves are propagating from a wide range of azimuths at the site (Asten and Boore, 2005). Considering advantages and disadvantages of HRFK and MSPAC, use of both approaches increases the confidence on resolved dispersion curves. In addition to use of multiple dispersion transformation methods, combined use the Rayleigh and Love wave data from the passive measurements ensures reduced non-uniqueness of shear wave velocity structure from inversion.

All dispersion data generally are inherently influenced by both epistemic and aleatory uncertainties. Understanding the intra method dispersion uncertainty along with uncertainties between inter method is still a topic of much ongoing research. For FK, HRFK, and FDBF, mean phase velocity and standard deviation at each frequency bin are calculated to estimate the intra method dispersion uncertainties. For MSPAC, manual selection of median, upper and lower bound of dispersion data phase velocities are made from a 3-D histogram of phase velocities created from spatial auto-correlation values. Dispersion data generated from each processing method are compared to observe differences and identify any potential data processing issues. However, given the possibility of different modes resolved by different transformation techniques, a direct combination of dispersion data to understand an overall uncertainty is not always the best approach. After carefully refining the experimental dispersion data from each method, individual Rayleigh and Love composite experimental dispersion data sets are prepared by adding all refined dispersion data. This composite experimental dispersion data set is utilized in the surface wave inversion. More details on the dispersion data processing and combining the active and passive source surface wave testing can be found in Wood et al. (2018) and Himel and Wood (2021).

Ambient data collected for the circular MAM were also used in the HVSR processing to compute the fundamental frequency of the site. Fundamental frequencies from each seismometers' HVSR peak frequencies and associated uncertainties are calculated. An average of all the fundamental frequencies and standard deviations are calculated to estimate a single site fundamental frequency and associated uncertainty. This frequency along with one standard deviation of uncertainty associated are utilized in the surface wave inversion for constraining the

bedrock depth. General guidelines from the SESAME project were followed for HVSR processing (SESAME, 2004).

The P-wave refraction data was processed to estimate the ground water table depth following Redpath (1973). P- wave arrivals at each receiver offset as a function of time were estimated from the linear geophone array. The time-intercept method was used to estimate the depth to the water table. The estimated depth to the water table is utilized in constructing the parameterizations for inversion.

A joint inversion of the fundamental frequency and composite dispersion curves was performed using the Geopsy software package, Dinver (Wathelet et al., 2020). Dinver utilizes a neighborhood algorithm method (Wathelet, 2008) to generate theoretical V_S profiles within user defined constraints. Parameters to constrain the inversion solution contain ranges of V_S, P-wave velocity (V_P), Poisson's ratio, density, and number/thickness of layers. The accuracy of V_S profiles generated in the inversion is highly dependent on the parameterization used in the inversion (Digiulio et al., 2012). Additionally, the parameterization aids the inversion by reducing the size of solution space, preventing generation of extraneous profiles and decreases processing time. The set of parameterizations for each site in this study were developed using ranges of V_S, Vp, Poisson's ratio and density from previous site characterization studies in the embayment (Woolery et al., 2016; Rosenblad et al., 2010; Ramirez-Guzman et al., 2012; Lin et al., 2014). Depth to bedrock was constrained in the inversion process as per the CUSVM bedrock depth at each site. However, there are other sources, such as, Dart (1995) that have compiled bedrock depth information for the Mississippi embayment. With soil profiles extending hundreds of meters deep, it is very difficult to measure the depth to bedrock precisely and as a result some discrepancies between Dart (1995) and CUSVM bedrock depth is observed. Nevertheless, sites

as deep as the ones found in the Mississippi embayment are generally insensitive in site response to bedrock depth changes within a reasonable bound (Cox et al., 2012). Bedrock V_S was allowed to have a parameterization range of 1600 – 3000 m/sec, which would allow the bedrock to adjust in conjunction with the overlying layers. This would ensure overall profile's ability to capture site signatures from the experimental fundamental frequency and dispersion characteristics. In each inversion trial, at least 500,000 theoretical V_S profiles are generated for each inversion run. Corresponding theoretical Rayleigh and Love wave dispersion curves generated from the theoretical V_S profiles are compared with the experimental dispersion curves to ensure that the modeled profiles are capturing the dispersion characteristics at the site. At the same time, theoretical ellipticity peaks, generated from the trial V_S profiles are compared with the fundamental frequency peaks from HVSR. Iterative comparison of theoretical Rayleigh fundamental mode ellipticity ensures that the bedrock V_S is properly modeled and the overall profile is able to capture the site signature from the experimental fundamental frequency (Scherbaum et al., 2003; Arai and Tokimatsu, 2005; Parolai, 2005). At each trial inversion, Dinver attempts to minimize the differences between the theoretical data and experimental recorded data. This overall 'closeness' between the experimental and theoretical results are quantified as misfit (Wathelet et al., 2004). In the Mississippi embayment, higher modes are excited at low frequencies due to a shallow impedance boundary. Superposition of multiple modes are expected due to the potential higher modes at particular frequencies. This superposition of multiple modes is termed as 'effective mode' (Socco et al., 2010). Identification and removal of effective mode data is vital for the inversion process as Dinver cannot utilize effective mode data. The effective mode data were identified from sudden phase velocity jumps, comparison of dispersion data from multiple methods, a-priori knowledge of subsurface

stratigraphy, use of proper parameterization, and iterative comparison of theoretical and experimental data after each inversion run. Another challenge of deep inversion is the identification and correct assignment of higher modes in the inversion. Assigning the wrong mode to dispersion data would negatively influence the resulting V_S profiles at the site. A two million model final inversion iteration for each site was conducted to ensure the inversion solution space was properly explored. A representative 1000 lowest misfit V_S profiles for each site were selected to calculate a median V_S profile for the site. This ensures a more representable profile is used rather than just selecting the single lowest misfit profile (Deschenes et al., 2018). More details on the inversion processing can be found in Himel and Wood (2021a).

4.7 Surface Wave Inversion Results

4.8 Manila Site

The Manila site is situated in Mississippi County, Arkansas with a bedrock depth of 813 m (Ramirez-Guzman et al., 2012). Being in the lowland part of the embayment, this site has Holocene age deposits at the surface along with geologic units commonly found in the embayment. The site is affiliated with Group V in this study.

HVSR curves calculated from the 50 m, 200 m, and 500 m arrays along with the calculated median HVSR curve are shown in Figure 4.3. The fundamental frequency from the median HVSR curve is determined to be 0.25 ± 0.02 Hz, which is associated with the soil/bedrock interface at this site. A secondary peak frequency around 0.8 Hz is also observed for this site, which is potentially associated with the shallow impedance boundary at this site (Himel, 2018; Gueguen et al., 2000; Field and Jacob, 1993). The fundamental frequency of 0.25 Hz was used in the joint inversion of the dispersion data and fundamental frequency. The secondary HVSR peak was used as a guide for developing the parameterization and in evaluating various

inversion runs to insure the secondary HVSR peak was observed in the resulting theoretical ellipticity (Himel, 2018).

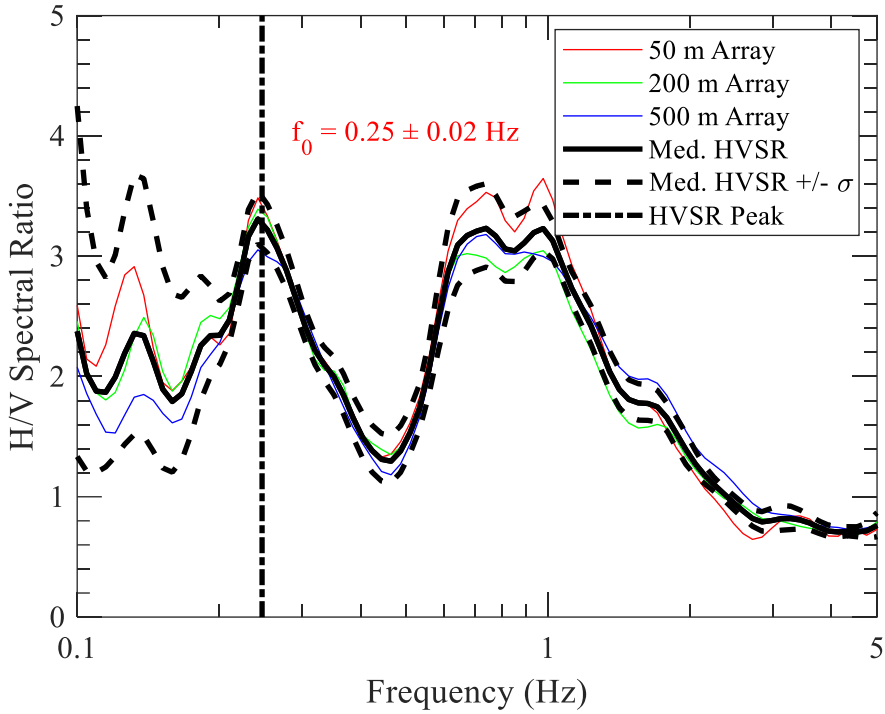

Figure 4.3 HVSR curves calculated for the 50 m, 200 m, and 500 m array from each seismometers in these arrays. A median HVSR curve calculated from the array results demonstrate the fundamental peak frequency around 0.25 Hz and a secondary frequency around 0.8 Hz.

The composite experimental dispersion data developed from surface wave measurements at the Manila site are shown in Figure 4.4a and b for the Rayleigh and Love wave data, respectively. The mean and +/- one standard deviation for each data point is shown. The array resolution limit ($k_{min}/2$ curve) from the 500 m circular array is also shown. The array resolution wavenumber limit, k_{min} is calculated based on the spatial distribution of sensors utilizing the Geopsy software package (Wathelet et al., 2008). For each frequency bin, the maximum resolvable phase velocity is calculated using $k_{min}/2$ (Woods and Lintz, 1973), and the results are shown with the $k_{min}/2$ curve. The active and passive data are in satisfactory agreement and

overlap in the 5 – 20 Hz for both the Rayleigh and Love data. The overlap of active and passive source data ensures each array captured similar dispersive characteristics at the particular overlapping frequency ranges. Standard deviations at lower frequencies are higher, an indication of higher uncertainties characterizing deeper depths. The MSPAC data points around 1.5 Hz, 1 Hz and 0.8 Hz exhibit flat dispersion curves, which could indicate transitioning from a higher/effective mode data to supposedly fundamental mode. Rayleigh and Love data demonstrate steep slopes around 1.8 Hz and 1 Hz, respectively. This could be an indication of dispersion data transitioning from fundamental to effective/higher mode data due to presence of a shallow stiff layer around this depth range. The estimated depth of this probable stiff layer from the Rayleigh data is around 130 m (500 m/sec at around 1.8 Hz)

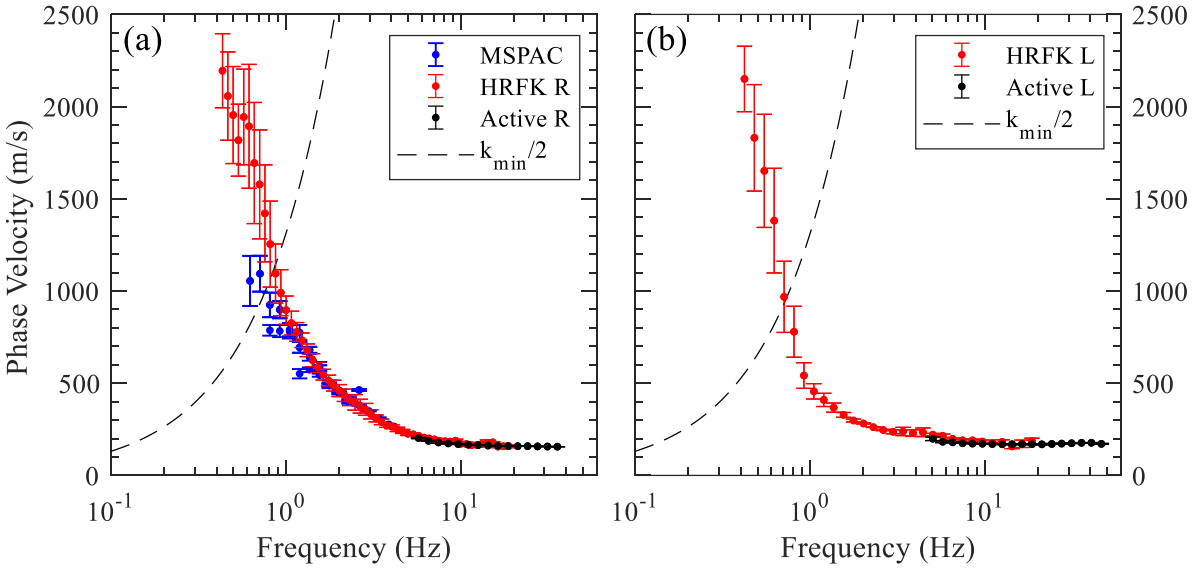

Figure 4.4 Composite experimental dispersion data from surface wave measurement at the Manila site for (a) Rayleigh and (b) Love wave. The array resolution limit for the 500 m circular (Kmin/2) shows the boundary for potentially less reliable data.

The theoretical dispersion curves associated with the 1000 lowest misfit V_S profiles (considered as 'best 1000' profiles) from the Manila site inversion results are shown for Rayleigh

and Love wave data in Figure 4.5a and b, respectively. Theoretical fit from the calculated median V_S profile is also shown. The fundamental, first higher, and second higher theoretical curves for Rayleigh are R0, R1, and R2, respectively. In the same fashion, Love modes are denoted with L0, L1, and L2. Identified fundamental, first higher, and second higher experimental dispersion points are shown with corresponding legends along with the identified effective mode data. A transition from fundamental to effective mode data is observed around 1.8 Hz for the Rayleigh wave data as expected from the composite dispersion curve. As discussed in the data processing section, some MPSAC data points around 1 Hz have lower phase velocities than their counterpart HRFK data and were identified as fundamental mode. The Rayleigh wave data from around 1 – 2 Hz were identified as effective mode data, which reached the first higher mode at around 2 Hz. This zone of complex propagation from 1 – 2 Hz is very close to both fundamental and first higher. If this effective mode data were erroneously considered as fundamental mode, it would have resulted in a stiffer layer than the representative velocity of the material present around this depth range (~130 m). Overall, comparison of multi method dispersion data, velocity jumps, and use of iterative and proper parameterization assisted in identifying the effective mode data in this frequency range. However, identification of effective mode data is still a topic of ongoing research. As a result, processing of surface wave dispersion data with potential effective mode is subjective of analyst's expertise and prior experience. Hence, analyses of surface wave data demands appropriate caution, expertise and application of engineering judgement driven by local geology. Another zone of complex propagation with effective mode data was identified from around 0.7 – 1 Hz from the HRFK Rayleigh data, which was identified as the second higher mode around 0.7 Hz. Some points beyond the largest array's (500 m) resolution limit were used to ensure resolution at deeper depths as the resolution limits are based on conservative estimates.

The Love wave experimental data demonstrate a clear effective mode propagation around 1 Hz. The Love wave effective mode data from around 0.5 – 0.7 Hz are very close to the first higher Love and were attempted to be fit as the first higher mode. However, they do not fit with the first higher mode of propagation, which could be due to shear strength anisotropy compared to the Rayleigh wave measurements and would result in a lower estimated Vs from Love waves than Rayleigh waves. Nevertheless, use of the combination of Rayleigh and Love complements each other and constrains the V_S model, reducing the non-unique characteristics of the surface wave method characterization. Dozens of inversion run iterations were carefully conducted with the Manila dataset considering various possible scenarios to achieve proper mode assignment and exclusion of effective mode data.

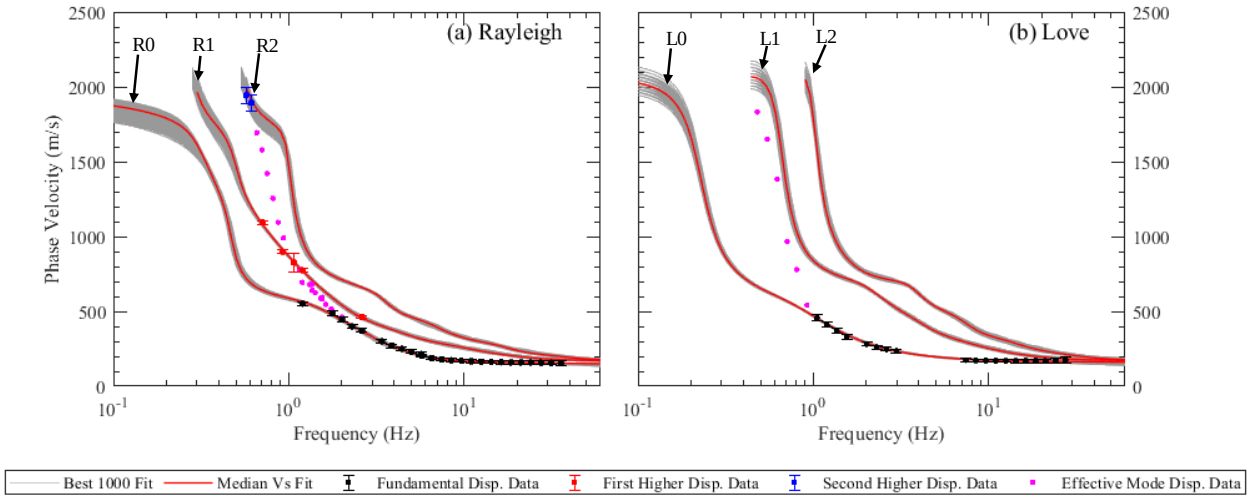

Figure 4.5 Experimental dispersion data and multimodal theoretical fit from surface wave inversion results at the Manila site for the (a) Rayleigh and (b) Love wave. Theoretical dispersion fit for '1000 best' fit V_S profiles are shown along with the theoretical fit from calculated median V_S profile. Identified fundamental, first higher and second higher Rayleigh and Love experimental data are shown along with the effective mode data. Calculated minimum misfit between the experimental and theoretical fit is 0.38 as per misfit equation from Wathelet et al. (2004).

V_S profiles obtained from the inversion of surface wave measurements at Manila are shown on a depth scale of 200 m and 1000 m in Figure 4.6a and b, respectively. The 1000 lowest misfit inversion V_S profiles, considered as the 'best 1000' profiles are shown along with their 5^{th} and 95^{th} percentile, and computed median from the 'best 1000' profiles. For comparison, site-specific V_S profile at Manila from CUSVM, Romero and Rix (2005) lowland V_S profile and V_S profiles from Rosenblad et al. (2010) Site 4 and Site 11 are also shown. Site specific geologic stratigraphy at Manila from CUSVM is superimposed on Figure 4.6a, and b. Reference V_S curves from Lin et al. (2014) for different soil types are shown in Figure 4.6a for comparison. Standard deviation of natural logarithm of V_S ($\sigma \ln V_S$) between the developed inversion profiles is shown in Figure 4.6c. The $\sigma \ln V_S$ quantifies the uncertainties between the developed V_S profiles.

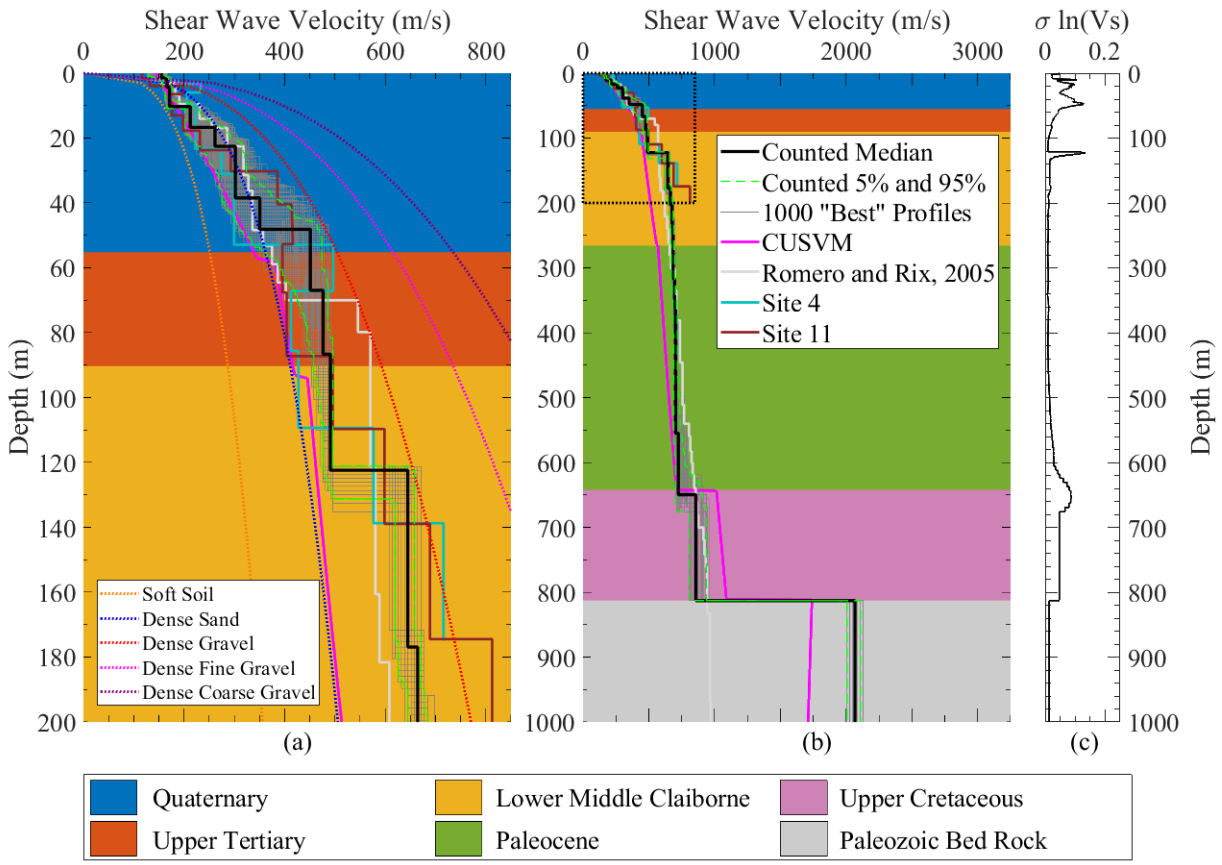

Figure 4.6 V_S profiles generated from surface wave inversion at Manila site are shown on a depth scale of (a) 200 m and (b) 1000 m. One thousand lowest misfit inversion V_S profiles, considered as the 'best profiles' are shown along with their 5th and 95th percentile, and calculated median. Site specific V_S profile at Manila from CUSVM, Romero and Rix (2005) lowland V_S profile and Rosenblad et al. (2010) Site 4 and 11 V_S profiles are shown for comparison. Reference V_S profiles for different materials from Lin et al. (2014) are shown in (a). Site specific geologic stratigraphy at the Manila site from CUSVM is superimposed on (a) and (b). Calculated $\sigma \ln V_S$ between the inversion V_S profiles is shown in (c) to demonstrate the uncertainties between the developed surface wave method V_S profiles.

For convenience in discussion, inversion profiles from this study, and Romero and Rix (2005) lowland profile would be denoted as SWM, and lowland (or highland in case of highland profile), respectively. Rosenblad et al. (2010) V_S profiles would be denoted with their corresponding site number (e.g., Site 4, Site 11).

All the developed SWM V_S profiles along with their median and related V_S profiles from the literature have similar shear wave velocities down to around 50 m. Shear wave velocities

stretch between the soft soil and dense sand reference curve in this depth range, which is typical of the surface alluvium and silt-clay mixture found in the Quaternary layer. The calculated SWM median and Site 4 V_S profiles have velocity jump around the Quaternary – Upper Tertiary interface, representing similar depth for the Quaternary layer as the site specific CUSVM geology at this site. The lowland V_S profile has a shallow impedance boundary around 70 m, which none of the other V_S profiles resolve. The CUSVM V_S profile has the impedance boundary from the LMC, i.e., Memphis sand around 95 m with a velocity jump from 430 to 445 m/sec. The SWM and Rosenblad et al. (2010) V_S profiles have thicker Upper Tertiary layers and do not have any velocity jumps down to approximately 110 m. Shear wave velocities within this range lay between the dense sand and dense gravel reference curves, which is consistent with the stiff clay and sand formations found in the Upper Tertiary. The SWM V_S profiles have a probable Memphis sand boundary from around 120 – 135 m, with a velocity of 600 – 660 m/sec, with the median V_S profile being at 122 m and 640 m/sec. The Rosenblad et al. (2010) sites have a similar depth to the Memphis sand around 110 m with a formation velocity around 600 m/sec. Both SWM and Rosenblad et al. (2010) V_S profiles have formation velocities at this impedance boundary between dense sand and dense gravel, which is consistent with the Memphis sand comprised of thick layers of sand mixed with gravel and clay lenses. Rosenblad et al. (2010) V_S profiles have very stiff layers below the probable Memphis sand depth, which none of the other V_S profiles, including the SWM V_S profiles resolve. The SWM and lowland V_S profiles have similar shear wave velocities from around 200 – 600 m. The CUSVM V_S profile being consistently softer than any other V_S profiles from around 20 – 600 m has as much as a 30% lower shear wave velocity over this depth range. The SWM V_S profiles resolved the Cretaceous layer from around 620 – 680 m with a velocity of 850 – 950 m/sec. The CUSVM V_S profile

resolved this layer interface at around 650 m with a velocity of 1000 m/sec. The bedrock depth being locked during inversion, SWM V_S profiles have similar bedrock depth as the CUSVM V_S profile at 813 m. However, the bedrock formation velocity of the SWM V_S profiles is in the range of 2000 – 2150 m/sec, whereas the CUSVM V_S profile has a V_S of 1730 m/sec.

The $\sigma \ln V_S$ profile (see Figure 4.6c) calculated to show the uncertainties and variabilities between the SWM V_S profiles demonstrate uncertainties in the near surface (down to 50 m), probable Memphis sand boundary, and Cretaceous boundary. This confirms uncertainties in characterizing the layer depths and formation velocities, especially at deeper depths. However, maximum $\sigma \ln V_S$ values observed are below 0.15, which is a reasonable uncertainty for intra method comparison (Garofalo et al., 2016a).

Comparison of the median HVSR, theoretical transfer function and theoretical ellipticity curves are shown in Figure 4.7. The transfer function was computed between the bedrock and ground surface from the median V_S profile using a MATLAB code from Teague (Teague, 2017). Theoretical Rayleigh wave fundamental mode ellipticity curve was generated from the median V_S profile using the Geopsy software package. The TTF and theoretical ellipticity fundamental peaks are in good agreement with the HVSR fundamental peak and within 4% of the fundamental peak frequency (0.25 Hz) at thee Manila site. Even though the HVSR second peak, around 0.8 Hz, was not used to constrain any shallow impedance boundaries associated with it, the ellipticity higher frequency peak is in reasonable agreement with the HVSR second peak. Theoretical ellipticity peaks being in good agreement with the experimental HVSR peaks implies that the depth to impedance boundaries were modeled properly in the median SWM V_S profile (Hobiger et al., 2013).

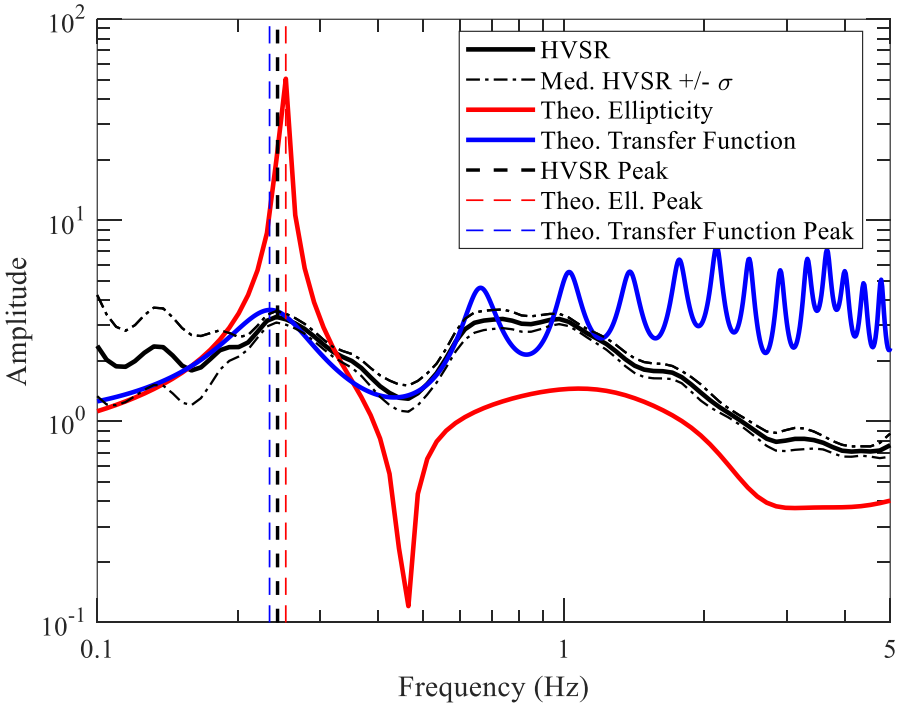

Figure 4.7 HVSR curve calculated from the surface wave measurements along with theoretical ellipticity and theoretical transfer function generated from the median V_S profile at the Manila site shown for comparison. Fundamental ellipticity peak and fundamental transfer function peak are within 4% of the HVSR fundamental peak frequency.

4.9 Group V_S Profiles

The tested sites are divided into eight groups based on the sites' similarities in geologic structure, shear wave velocities (especially down to the Cretaceous layer) and geologic location. In this section, site characterization results for one of the groups (Group V) is discussed in detail. Later, site characterization results for all the other groups are provided.

Sites that are organized in the Group V are Athelstan, Manila, Marked Tree, LPAR and HBAR. These sites stretch from Mississippi County to Poinsett County, Arkansas in the north-south direction and lie between Crowley's Ridge and the Mississippi River in the east-west direction. All of these sites fall in the lowland part of the embayment (see Figure 4.1). Site characterization results from Group V sites are shown in Figure 4.8 along with the Romero and

Rix (2005) lowland and Rosenblad et al. (2010) Sites 4 & 11 for comparison. Reference V_S profiles for different material types from Lin et al. (2014) are added for comparison in Figure 5.8a.

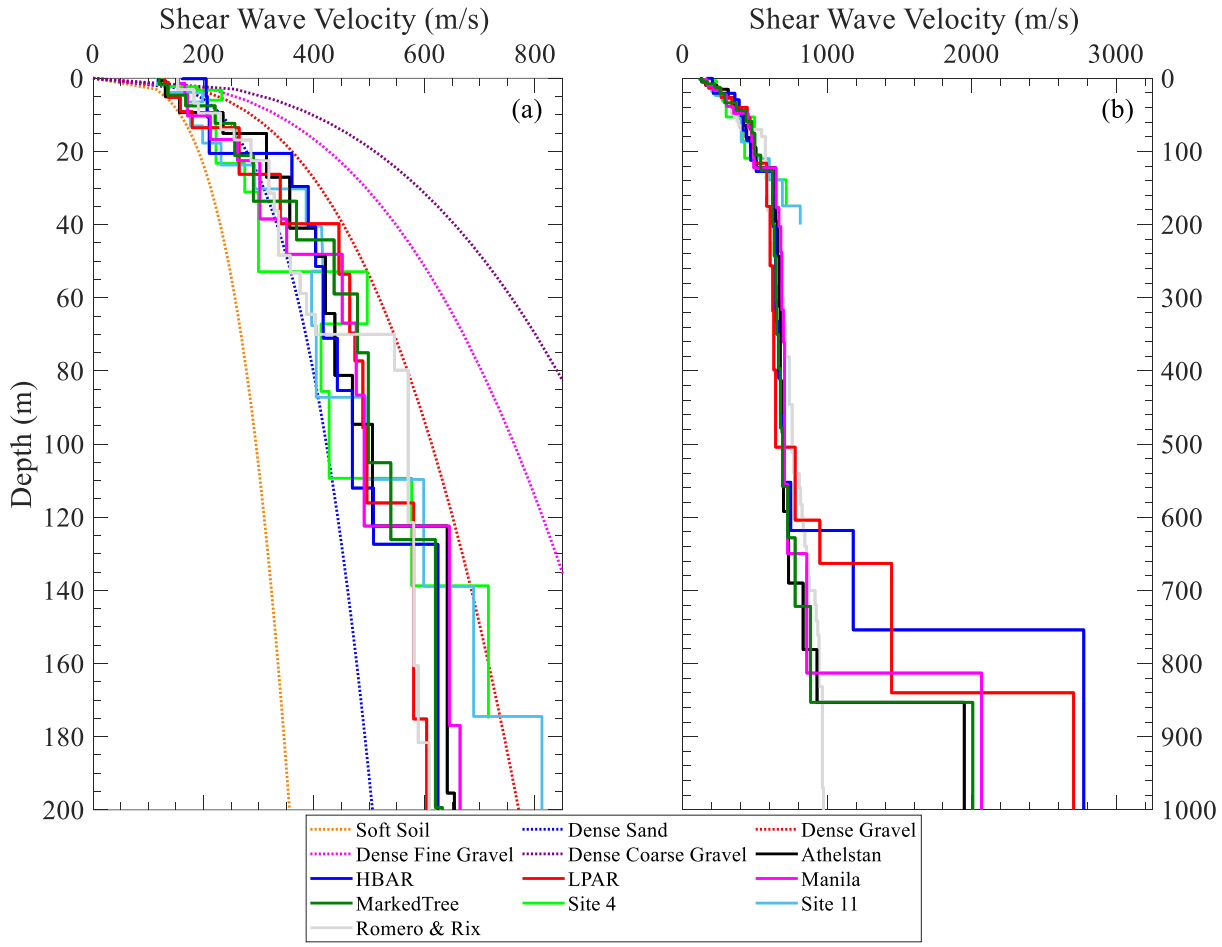

Figure 4.8 Median SWM V_S profiles shown for the sites in Group V along with V_S profiles from corresponding Romero and Rix (2005) lowland and nearby Rosenblad et al. (2010) sites are shown on a depth scale of (a) 200 m and (b) 1000 m. Reference V_S profiles for different materials from Lin et al. (2014) are also shown for comparison in (a).

All Group V SWM Vs profiles have shear wave velocities between the soft soil and dense sand curves to around 40 – 60 m depth and between dense sand and dense gravel reference curves down to around 100 – 125 m depth, inferring the Quaternary – Upper Tertiary and Upper Tertiary – LMC interfaces, respectively in these depth ranges. The Rosenblad et al. (2010) sites

are in good agreement with SWM profiles regarding the shear wave velocities and geologic layering in these depth ranges. The lowland profile also has a similar trend as the SWM and Rosenblad et al. (2010) profiles. However, the lowland profile has an impedance boundary around 70 m, which none of the other V_S profiles have. The SWM V_S profiles resolved the impedance boundary from the Memphis sand around 115 – 130 m, substantiated by the nearby Rosenblad et al. (2010) sites' V_S profiles. However, the Rosenblad et al. (2010) sites' deepest resolved layers have very high shear wave velocities compared to the other V_S profiles. All the SWM V_S profiles and the lowland V_S profile have similar trends from around 110 – 600 m. Even though the sites in Group V have very similar shear wave velocities and geologic layer depths in the probable Quaternary, Upper Tertiary, LMC, and Paleocene layers, they tend to have differences in formation velocities and depths to the Cretaceous and Paleozoic bedrock. However, this is expected as the Group V sites stretch in the east-west and north-south directions with variable bedrock depth from 750 to 850 m.

Median SWM V_S profiles for sites in Group I-VIII are shown in Figure 4.9a-h. Nearby Rosenblad et al. (2010) profiles are shown for comparison. The site-specific V_S profiles from SWM in a group have similar shear wave velocities and layer depths for the probable Quaternary, Upper Tertiary, LMC, and Paleocene layer. However, shear wave velocities and depths to the Cretaceous and Paleozoic bedrock differed between sites in a group due to the depth of these layers and uncertainty in the measured data. Groups I-II and IV-VIII have V_S profiles which have a shallow impedance boundary from the LMC layer interface. However, this boundary is not present in Group III sites. Some sites, such as the Harrisburg and Monette in Group IV and Greasy Corner in Group VI have a gradual increase of velocity rather than a sharp increase in Vs associated with the LMC layer depth. This may be a result of averaging 1000 V_S

profiles to calculate the median. For all groups, the LMC or Memphis sand layer in the SWM V_S profiles is resolved at a depth of around 50 – 175 m with an average formation velocity of 543 – 662 m/sec. Excluding the TUMT site in Group VIII, all other groups of V_S profiles have good agreement with the nearby Rosenblad et al. (2010) sites' shear wave velocities and layer depths. However, the deepest resolved layers at the Rosenblad et al. (2010) sites have 10 – 50% higher shear wave velocities than the resolved SWM V_S profiles.

Experimental site periods estimated from the HVSR test along with theoretical site periods from median V_S profiles' ellipticity and transfer function for each site are shown in Figure 4.10a. Average measured V_S in the top 30 m (V_{S30}) and down to the bedrock (V_{Savg}) for each site are shown in Figure 4.10b. The V_{S30} and V_{Savg} were calculated using the standard time-average equation. Experimental site periods for the study sites in the embayment range from 1.6 – 5.4 seconds, demonstrating longer periods for deeper sites. Theoretical site periods from the ellipticity and transfer function range from 1.6 – 5.2 and 1.5 – 5.6 seconds, respectively. Theoretical site periods match well with the experimental site periods for all sites, and are within 0.3 – 3.5% and 0.7 – 10% of the experimental site period for ellipticity and transfer function, respectively. The V_{S30} for the study sites range from 167 – 306 m/sec. Except for the PEBM site, all other sites fall in the site class D seismic site classification when only considering Vs30. The calculated highest V_{S30} of 306 m/sec is at TUMT, which is consistent with the stiff near-surface layers in the upland part of the embayment (Rosenblad et al., 2010). The PEBM site being situated in farmland and close to the flood zone of the nearby creek causes it to have soft near-surface sediments and results as a site class E. This is believed to be an outlier for the embayment in general, but consistent with the conditions at the PEBM station. The V_{Savg} of the

sediments above bedrock for the study sites range from 462 – 686 m/sec, demonstrating more variances between site to site than the site classifications estimated from V_{S30}.

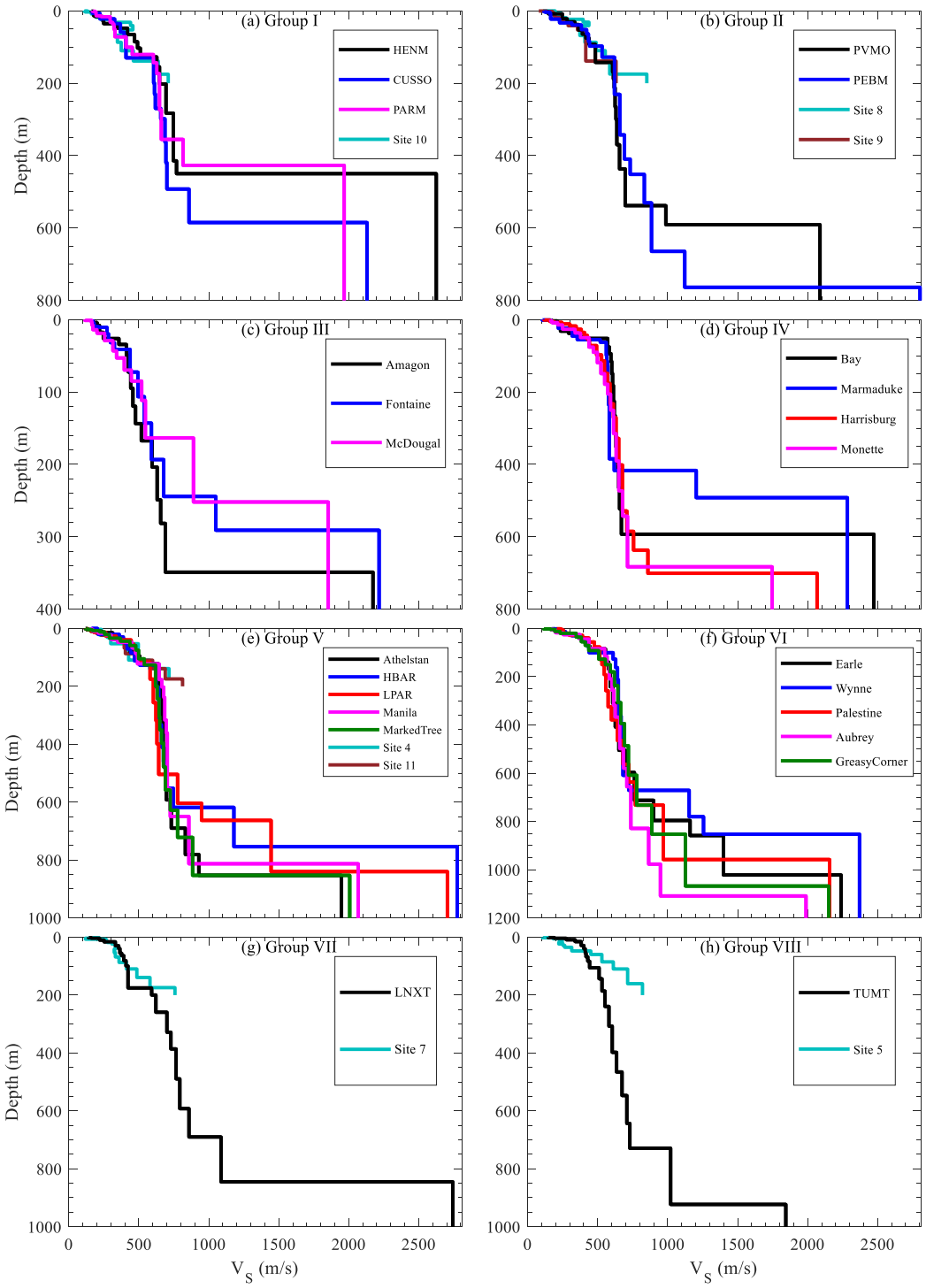

Figure 4.9 Median V_S profiles from SWM results shown for Group I-VIII in (a) – (h). Corresponding nearby Rosenblad et al. (2010) V_S profiles are shown for comparison.

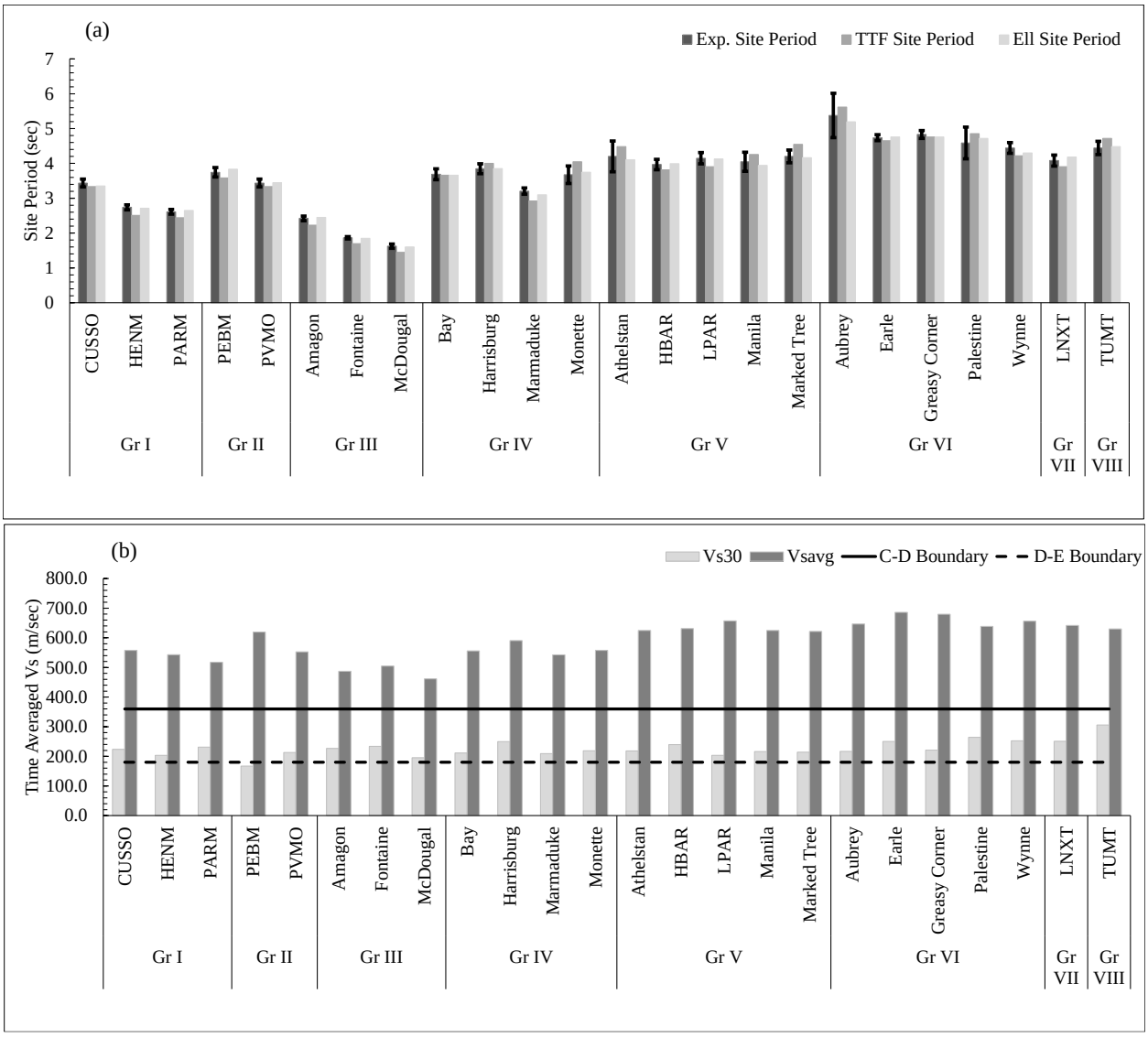

Figure 4.10 (a) Experimental site period from HVSR method with estimates of uncertainty of one standard deviation shown with error bars along with theoretical site periods from median V_S profiles' ellipticity and transfer function, (b) Time averaged V_{S30}, and V_{Savg} along with the C-D and D-E site class boundary line shown for all sites.

4.10 Discussion

This section contains the discussions on the following topics- (i) spatial variation of site period across the embayment and comparison of average shear wave velocities above bedrock, (ii) comparison of geologic formation velocities, (iii) differences observed with existing velocity

model and reference V_S profiles, and (iv) estimating a power-law relation between bedrock depth and site fundamental frequency.

4.11 Spatial variation of site period and comparison of V_{Savg}

To better understand the spatial variability of site period across the basin, a site period map for the Mississippi embayment is produced and shown in Figure 4.11a. The Kriging algorithm (Isaaks and Srivastava, 1989) is used for making interpolation between measured site periods across the embayment from this study, Himel (2018) and Langston and Horton (2014). Three measurement points from Langston and Horton (2014) (mk01, am03, m1es) are excluded from the interpolation to maintain consistency. Areas close to the western edge of the embayment is excluded due to limited measurement points. Overall, the site periods observed near the edge of the embayment are less than 2 second and gradually becomes longer for deeper sites towards the center of the embayment. Site periods observed in the center of the embayment are 4.5 – 5.4 seconds. Generally, good agreement is observed between the three data sources. Transition of site periods from shorter to longer are demonstrated to be closely related to the depth to the bedrock. However, additional measurement points are required near the embayment edge to accurately capture the rapid change in bedrock depth in this part.

Average shear wave velocities of the post-Paleozoic sediment, V_{Savg} is an important aspect of local seismic characteristic of the Mississippi embayment. Previous studies have used direct and indirect measurements to estimate V_{Savg} across the embayment. Chen et al. (1996) has used travel time difference measurements of direct and converted body waves to measure V_{Savg} at the PANDA station locations. Bodin et al. (2001) and Langston and Horton (2014) used linear and exponential models derived from the fundamental resonance period-sediment thickness relationship (see Equation 1), respectively to estimate V_{Savg}. In these last two studies, Equation 1

is used to indirectly estimate V_{Savg} by measuring the HVSR site period (T_0) and knowing the height of the soil column (H).

$$T_0=4H/V_{Savg} \quad (1)$$

To understand differences between the direct and indirect approaches, the V_{Savg} contour map by the Langston and Horton (2014) is shown in Figure 4.11b with V_{Savg} values directly calculated from the SWM median Vs profiles from this study using the travel time averaging method overlain on the map. Both the indirectly estimated contours and calculated V_{Savg} have similar trends with increasing V_{Savg} toward the center of the basin. This increase is associated with the higher overburden stresses in the unconsolidated sediments due to deeper bedrock depths toward the center of the basin. However, there is a systematic bias between the V_{Savg} determined using each approach.

To further investigate this bias, a comparison is made in Figure 4.12 between the V_{Savg} calculated from the median SWM Vs profiles in this study and V_{Savg} estimated using the Langston and Horton (2014) exponential model. In addition, V_{Savg} estimated from Bodin et al. (2001) linear model is shown for comparison. The Langston and Horton (2014) and Bodin et al. (2001) V_{Savg} points are calculated using the Equation 2 and 3, respectively. For calculating V_{Savg} using Equation 2 and 3, similar bedrock depths used in the SWM inversion models are utilized for consistency.

$$V_{Savg}=4He^{8.325*10^{-7}*H^2-0.00232*H-0.01796} \quad (2)$$

$$V_{Savg}=521.15+0.37459H \quad (3)$$

From Figure 4.12, a consistent 30-40% bias is observed between the calculated V_{Savg} and those points estimated using the Langston and Horton (2014) and Bodin et al. (2001) models. This overestimate of V_{Savg} using an indirect approach was also observed by Rosenblad et al.

(2010) where the Bodin et al. V_{Savg}-sediment thickness relationship (Bodin et al., 2001) overestimate V_{Savg} from 22 to 35% compared to the V_{Savg} estimated by both Rosenblad et al. (2010b) and Chen et al. (1996). This systematical overestimation of V_{Savg} by Bodin et al. (2001) and Langston and Horton (2014) is due to the use of an equivalent uniform layer thickness (i.e., assuming there is no increase in Vs with depth in the embayment) (2010b). This effect was first discussed by Dobry et al. (1976), who observed that the equivalent uniform layer approach does not consider the influence of velocity gradients in the subsurface leading to an overestimation of the $V_{Savg.}$ Therefore, this approach should not be used to determine V_{Savg} without considering velocity gradients, otherwise the V_{Savg} is overestimated in comparison to the true V_{Savg}

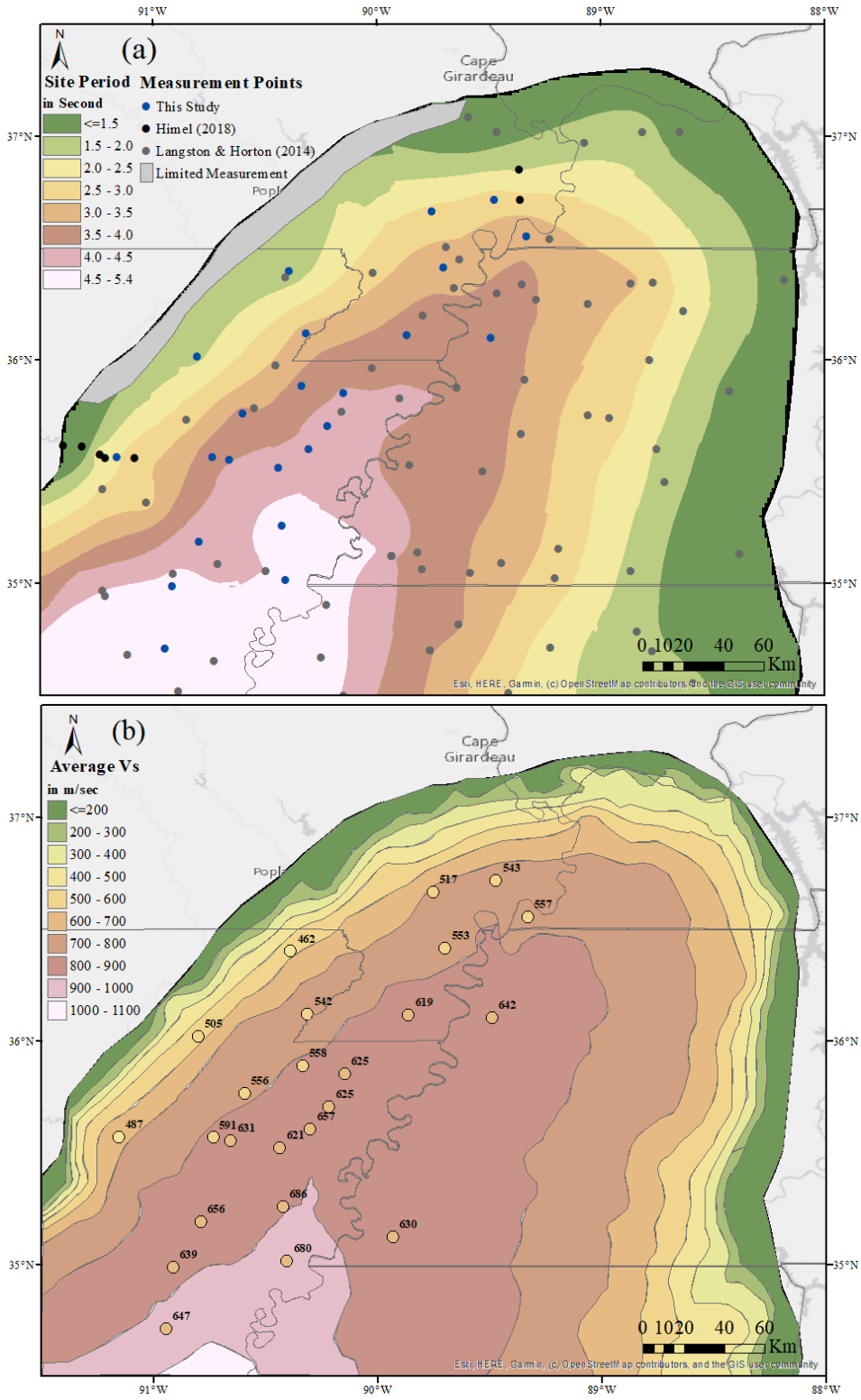

Figure 4.11 (a) Spatial variability of site period utilizing interpolation of measured data from this study, Himel (2018) and Langston and Horton (2014), and (b) comparison of V_{Savg} from surface wave measurements and from Langston and Horton's exponential model.

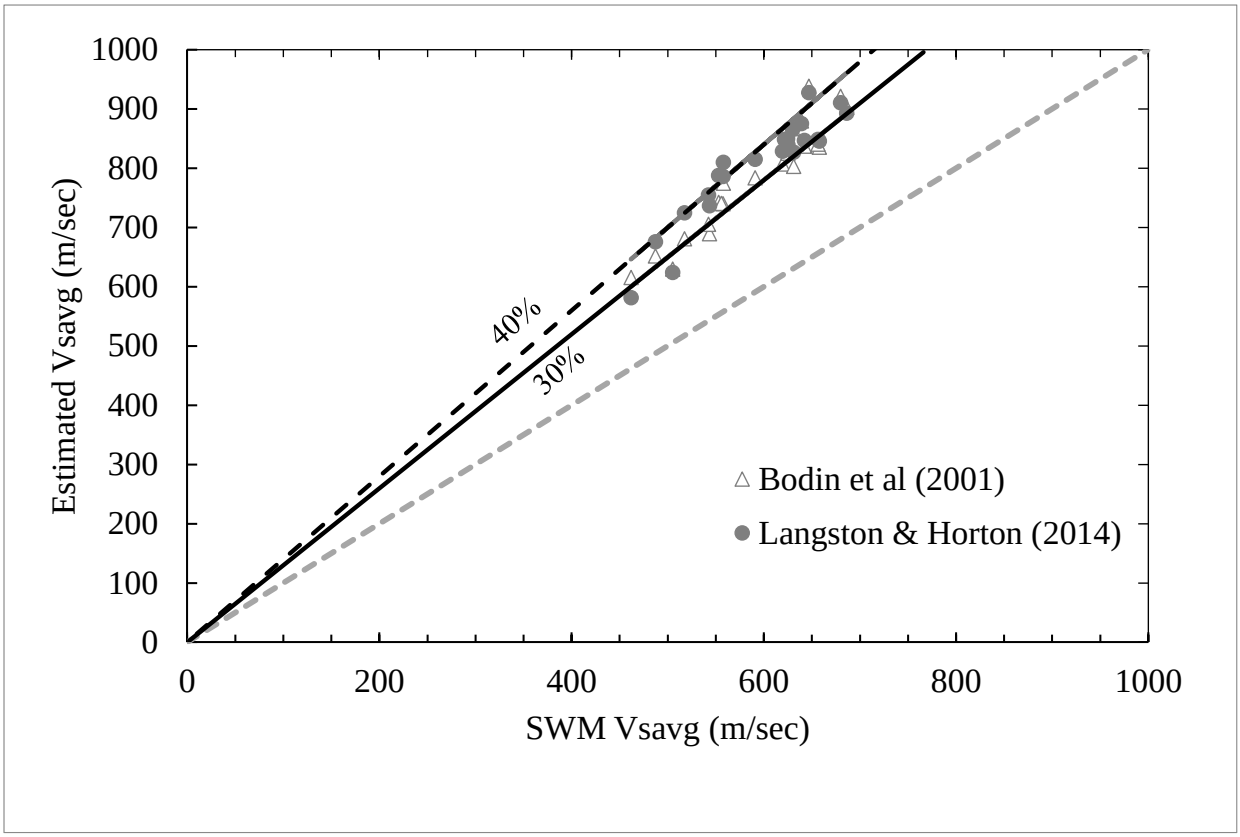

Figure 4.12 Comparison of V_{Savg} estimated from Bodin et al. (2001) and Langston and Horton's (2014) exponential model to the V_{Savg} calculated from SWM V_S profiles are shown. A 30% and 40% overestimation of each SWM V_{Savg} point is calculated and utilized to draw and extend 30% and 40% overestimation lines shown with solid black and dashed black lines, respectively.

4.12 Geologic Formation Velocity

This section discusses a comparison of formation velocities for geologic units commonly found in the Mississippi embayment. In addition to the Rosenblad et al. (2010) and Ramirez-Guzman et al. (2012), Gomberg et al. (2003) performed an extensive study on formation velocities of geologic units found in the Mississippi embayment to correlate with the lithology.

To perform the calculations for a geologic unit in the SWM profile, the whole thickness of the geologic unit is divided into 0.1 m thick segments starting from the bottom of the preceding unit's last layer to the top of the following unit's first layer to calculate an average formation velocity. This method to calculate the formation velocity gives an overall average of

the whole depth range of the geologic unit as the geologic units found in the SWM V_S profiles have multiple layers. The usual time average velocity equation is used for this purpose. Paleocene layers from SWM results do not show any distinguishable trend from the preceding LMC layer. Thus, the formation velocities of this layer are calculated by starting the 0.1 m thick segments from the CUSVM estimated Paleocene depths. Mathematical mean and standard deviation for each geologic unit's formation velocity is calculated from the individual unit's formation velocity results from all the study sites utilizing standard mathematical equations for mean and standard deviation. The same procedure was followed to calculate the formation velocities, their mean and standard deviation for the CUSVM V_S profiles. For the rest of the studies, these information were collected from the corresponding literature. Calculated formation velocities of the geologic units' from this study are shown with a box and whisker plot in Figure 4.13. Horizontal lines in each box and whisker plot graphically depict the minimum, first quartile, median, third quartile, and maximum of a particular geologic unit's formation velocity. Any outlier data are shown with a '+' sign. The range between the minimum and maximum, excluding any outliers for Quaternary, Upper Tertiary, Memphis sand, Paleocene, Cretaceous, and Paleozoic bedrock are 166 – 259, 326 – 475, 543 – 662, 456 – 774, 670 – 1445, 1735 – 2762 m/sec, respectively. The overlapping of the Memphis sand-Paleocene and Paleocene-Cretaceous layers' formation velocities is a demonstration of the uncertainties in site characterization for deeper layers.

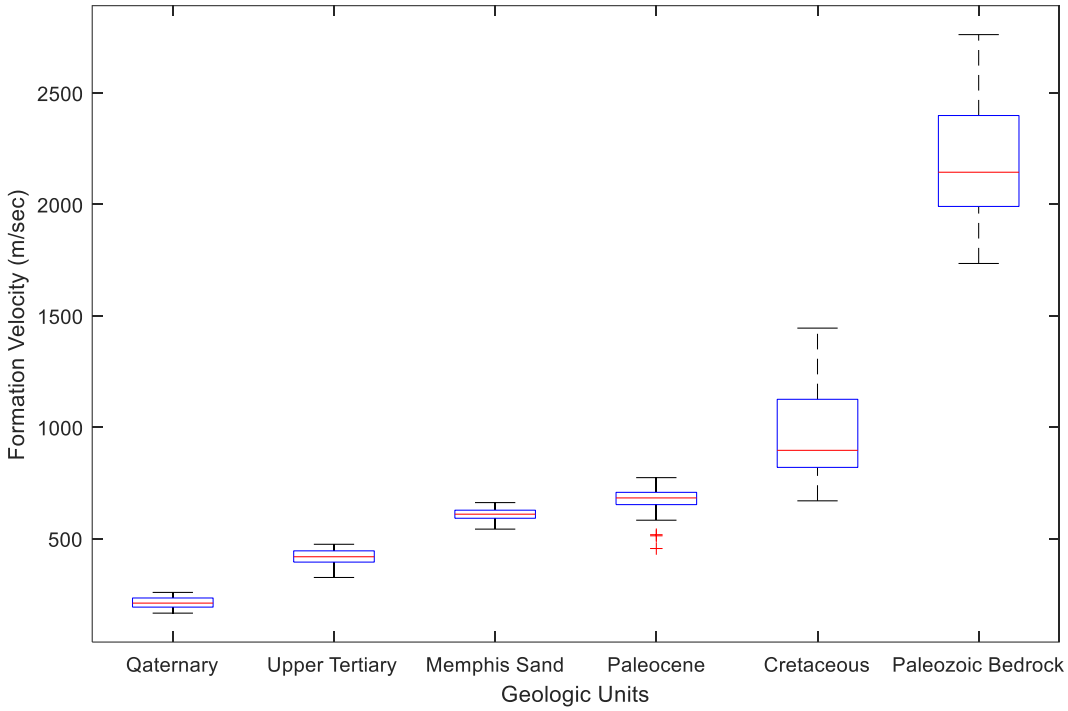

Figure 4.13 Formation velocities determined for the geologic layers found in the Mississippi embayment.

A comparison of the formation velocities from this study to the formation velocities estimated by Ramirez-Guzman et al. (2012), Rosenblad et al. (2010), and Gomberg et al. (2003) is provided in Table 4.2.

Table 4.2 Comparison of formation velocities for geologic units found in the Mississippi embayment with standard deviation shown in parenthesis.

Study	Formation velocity (m/sec)					
	Quaternary[a]	Upper Tertiary[b]	Memphis Sand	Paleocene	Cretaceous	Paleozoic Bedrock
This Study	214 (26)	418 (37)	607 (31)	665 (80)	967 (200)	2211 (301)
Ramirez et al. (2012)	239 (27)	397 (3)	497 (1)	635 (2)	1006 (96)	1824 (265)
Rosenblad et al. (2010)	193 (14)	399 (62)	685 (83)	-	-	-
Gomberg et al. (2003)	171 (24)	413 (105)	530 (134)	-	-	-

[a] Comprises of Alluvium (silt/clay, sand, sand/gravel) deposits near surface

[b] Comprises of Jackson, Cockfield and Cook mountain formation

The formation velocities determined in this study for the Quaternary and Upper Tertiary units are in overall good agreement with the previous studies. The Quaternary formation velocity (214 m/sec) falls in between the highest (239 m/sec) and lowest (171 m/sec) reported values by Ramirez-Guzman et al. (2012), and Gomberg et al. (2003), respectively. The Upper Tertiary formation velocity (418 m/sec) is 3.5% higher than the previous studies' average. The Memphis sand formation velocity determined in this study (607 m/sec) falls between the highest (685 m/sec), and lowest (497 m/sec) reported formation velocities for this unit by Rosenblad et al. (2010) and Ramirez-Guzman et al. (2012), respectively. As discussed previously, the Rosenblad et al. (2010) V_S profiles encountered some sharp increase in V_S within the Memphis sand unit, which none of the other studies observed. This has contributed to a higher average formation velocity for the Memphis sand unit by Rosenblad et al. (2010). The formation velocity for the Memphis sand reported by Ramirez-Guzman et al. (2012) is the lowest, with a very low standard deviation (1 m/sec) compared to the other studies. The deeper geologic units (e.g., Paleocene, Cretaceous, and Paleozoic bedrock) are resolved by Ramirez-Guzman et al. (2012) and this study. Both studies resolved these layers with reasonable average formation velocities. Overall, Ramirez-Guzman et al. (2012) has lower standard deviations, especially for the deeper geologic units in the embayment. On the other hand, average formation velocities from this study have increasing standard deviation with depth to the unit, which is pertinent to account for the uncertainties associated with the deeper unit's site characterization.

An interpolation of Memphis sand formation velocity using the Kriging algorithm and utilizing the measurement points from the study sites is carried out and shown in Figure 4.14. Previous work by Himel (2018) indicated the Memphis sand layer tends to become shallower

towards the north and west boundary of the embayment and ceases to exist at some point near the edge of the embayment. In this study, none of the Group III sites (Amagon, Fontaine, McDougal) resolved the Memphis sand layer. Therefore, areas west of the line connecting these sites (shown as no LMC zone in the figure) are estimated to have no Memphis sand. The upland area and areas in the north-west and south-west of the embayment are excluded from the interpolation due to limited measurements and no measurement points, respectively. The overall spatial variance indicates a stiffer Memphis sand formation in the central part of the embayment with formation velocities ranging from 600 – 650 m/sec and gradually becoming softer towards the boundaries of the embayment with formation velocities in the range of 490 – 525 m/sec. The depth to the Memphis sand layer also follows this general trend

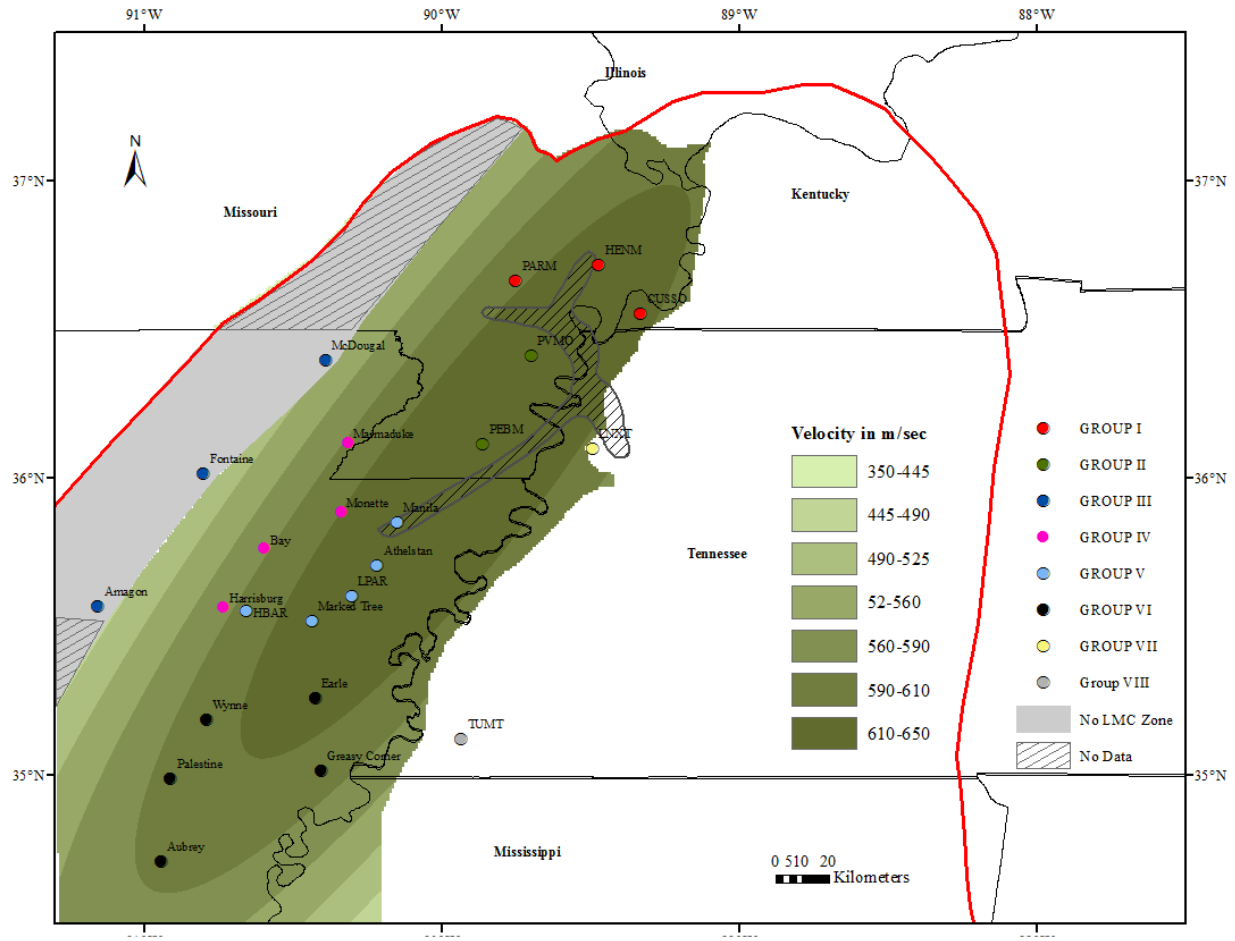

Figure 4.14 Spatial variance of the Memphis sand formation velocity across the Mississippi embayment using the Kriging algorithm. The Upland area and areas in the north-west and south-west of the embayment are excluded from the interpolation due to limited measurement and no measurement points, respectively.

4.13 Comparisons with previous V_S profiles

To understand the differences between the SWM V_S profiles and V_S profiles from previous studies (Romero and Rix, 2005; Ramirez-Guzman et al., 2012), percent differences are calculated at every 0.1 m depth increment using the following equation:

$$\% \text{ Difference} = \frac{(V_S \text{ of SWM} - V_S \text{ of Past Study})}{V_S \text{ of SWM}} * 100 \quad (4)$$

The percent difference plots between the SWM median V_S profiles and CUSVM V_S profiles for all sites in Group I-VIII are shown in Figure 4.15a-h, respectively. Other than some

exceptions observed, such as for Group III, the majority of the CUSVM V_S profiles have lower shear wave velocities than their corresponding SWM V_S profiles in the Quaternary, Upper Tertiary, LMC, and Paleocene layer with differences as higher as 35%. However, the CUSVM V_S profiles have higher shear wave velocities in the Cretaceous layer than the SWM resolved V_S profiles, which is more prominent for sites in the southern part of the embayment, such as for the Group VI sites. Much of the bedrock shear wave velocities resolved by the CUSVM are lower than the SWM resolved velocities by as much as up to 50%. The McDougal and HBAR CUSVM V_S profiles have 200% (at 13 m) and 90% (at 17 m) differences with their corresponding SWM V_S profiles, respectively due to a very shallow Memphis sand layer at around 6 m depth in the McDougal CUSVM, and shallow Quaternary-Upper Tertiary interface at around 5 m in the HBAR CUSVM. Both McDougal and HBAR sites are situated very close to the Crowley's Ridge (see Figure 4.1). As layer boundaries in the CUSVM are interpolated using the Kriging method (Ramirez-Guzman et al., 2012), the geologic layers' present and their depths at the HBAR and McDougal sites are influenced by the nearby sites from Crowley's Ridge. The Memphis sand layer resolved from the SWM V_S profiles are usually deeper than the Memphis sand layer resolved by the CUSVM profiles, except in Group IV, where the Memphis sand layers were resolved at relatively similar depths as the SWM V_S profiles.

Overall, many of the differences between the site-specific SWM and CUSVM are due to a lack of deep Vs information utilized in creating the CUSVM. The bedrock shear wave velocities in the CUSVM for the whole embayment are based on a few actual measurements near the NMSZ and Illinois basin and extrapolated to other locations as needed (Ramirez-Guzman et al., 2012). The CUSVM depends on estimated V_{S30} from the topographic slope for the shallow structure if no measured V_{S30} data is present nearby (Gomberg et al., 2003; Allen and Wald,

2007). The Kriging method is utilized to extrapolate geologic boundaries based on neighboring measurement sites for the target site. However, the lack of neighboring site measurements and an abrupt change in the neighboring sites' geology affects this process, as seen for the HBAR and McDougal sites. Another discrepancy observed between the SWM and CUSVM profiles is in the Cretaceous layer. Due to limited data on the Cretaceous layer boundaries, especially in the southern part of the embayment, extrapolation techniques had to be made for this layer in the CUSVM (Ramirez-Guzman et al., 2012). The effect of this extrapolation is seen in the percent differences for the Cretaceous layers, especially for the sites in the southern part (e.g., Group VI) where the CUSVM Cretaceous layers have a 30 – 40% higher V_S.

To calibrate and evaluate the performance of the modeled shear wave velocity structure in the CUSVM, a ground motion simulation was conducted using the M_W 5.4 Mt. Carmel, Illinois earthquake. As a result, many of the sites' fundamental frequencies from CUSVM velocity structures are capable of capturing site-specific recorded fundamental frequencies. However, the simulation demonstrated that the sites with increasing distance from the simulated seismic source have a slower arrival time as much as 5 sec at distant sites. This indicates shear wave velocities used in the CUSVM models are typically too low. This assumption is consistent with the results from this study, which indicate that majority of the site-specific CUSVM profiles have lower shear wave velocities in the Quaternary, Upper Tertiary, LMC, and Paleocene by as much as 35%. Another noticeable disagreement between the CUSVM and SWM profiles is in the depth to the shallow impedance boundary from the Memphis sand, a proper characterization of which might have a significant effect in the site response of a site (Himel et al., 2021b).

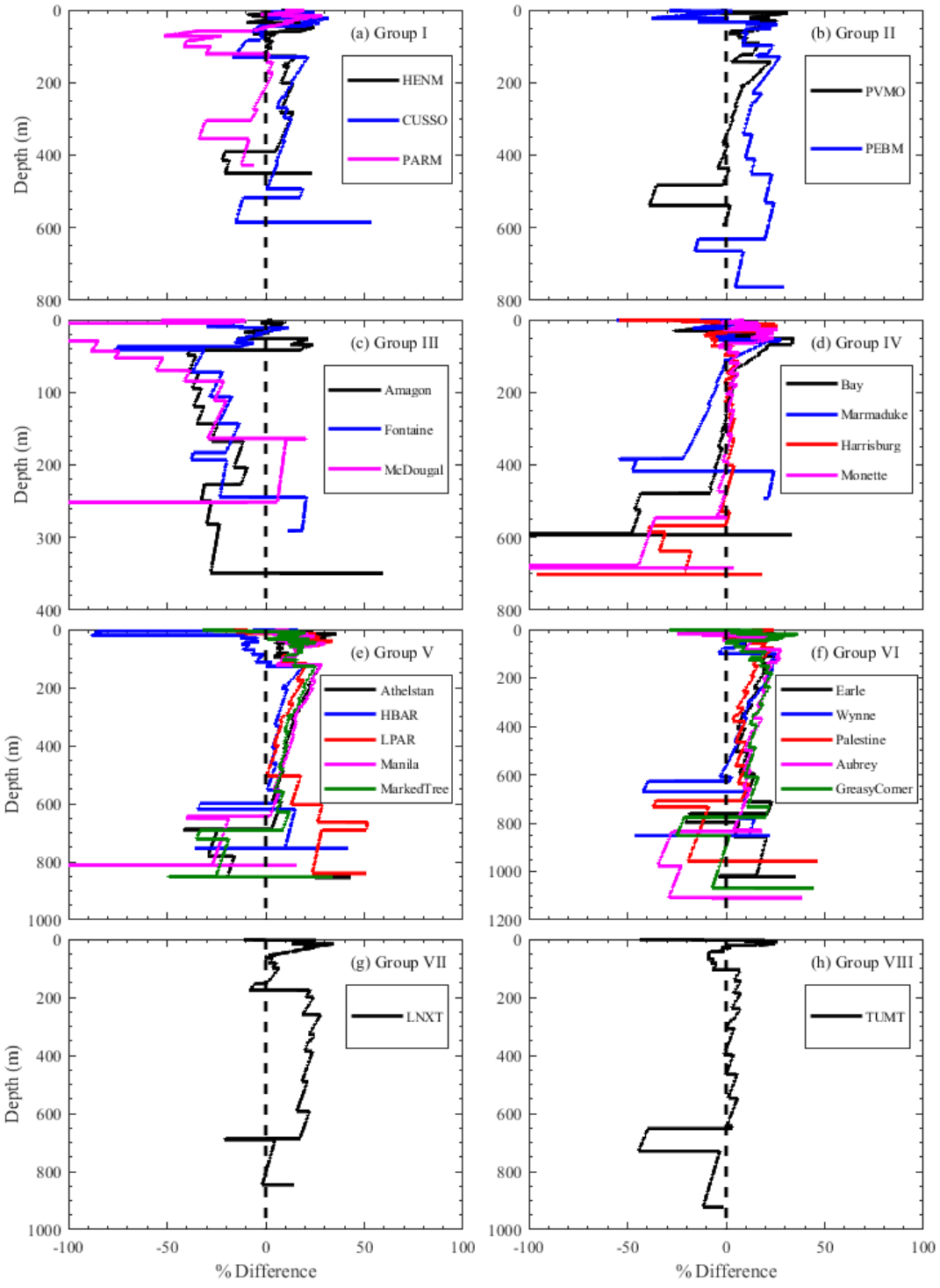

Figure 4.15 Percent difference between SWM Median VS profiles with corresponding CUSVM VS profiles shown for Group I-VIII in (a) – (h), respectively.

In addition to comparisons with the CUSVM, the percent differences between SWM V_S profiles and the Romero and Rix (2005) lowland, or upland profile are calculated using Equation 4 and shown for Group I-VIII in Figure 4.16a-h, respectively. The lowland profile is in general agreement with most lowland SWM sites, especially in the Upper Tertiary, and Paleocene layer, with percent differences ranging from 5 – 30%. A consistent percent difference for all the lowland sites is observed around 70 m due to the presence of an impedance boundary in the lowland V_S profile. As a result of this, all lowland SWM V_S profiles, except Group III, have 30 – 50% lower V_S at around 70 m. The lowland V_S profile does not resolve any distinguishable Cretaceous layer or any deep impedance boundaries above bedrock. Due to the absence of a distinct Cretaceous, and bedrock layer, all lowland SWM sites have 20 – 70% higher V_S in these layers than the lowland V_S profile. The LNXT and TUMT seismic station sites are the only study sites situated in the highland part. However, due to their differences in site characterization results, LNXT and TUMT are listed in Group VII and VIII, respectively. The highland V_S profile has 30 – 50% higher V_S than both LNXT and TUMT sites in the Upper Tertiary range. However, the LNXT Paleocene layer is in good agreement with the highland V_S profile, whereas the TUMT Paleocene layer is 10 – 30% softer than the highland V_S profile in this depth range. Both LNXT and TUMT SWM V_S profiles have 20 – 60% higher V_S in the Cretaceous and bedrock layers than the highland as the highland V_S profile does not have a distinct Cretaceous and bedrock layer. Nevertheless, the percent differences comparison indicate a better match between the highland SWM V_S profiles and highland V_S profile in the upper Mississippi embayment, and a greater mismatch in the lower embayment. This issue indicates the predicament of using a single reference V_S profile to be representative of the local geology of a large area, which can lead to critical misrepresentation of local site effects.

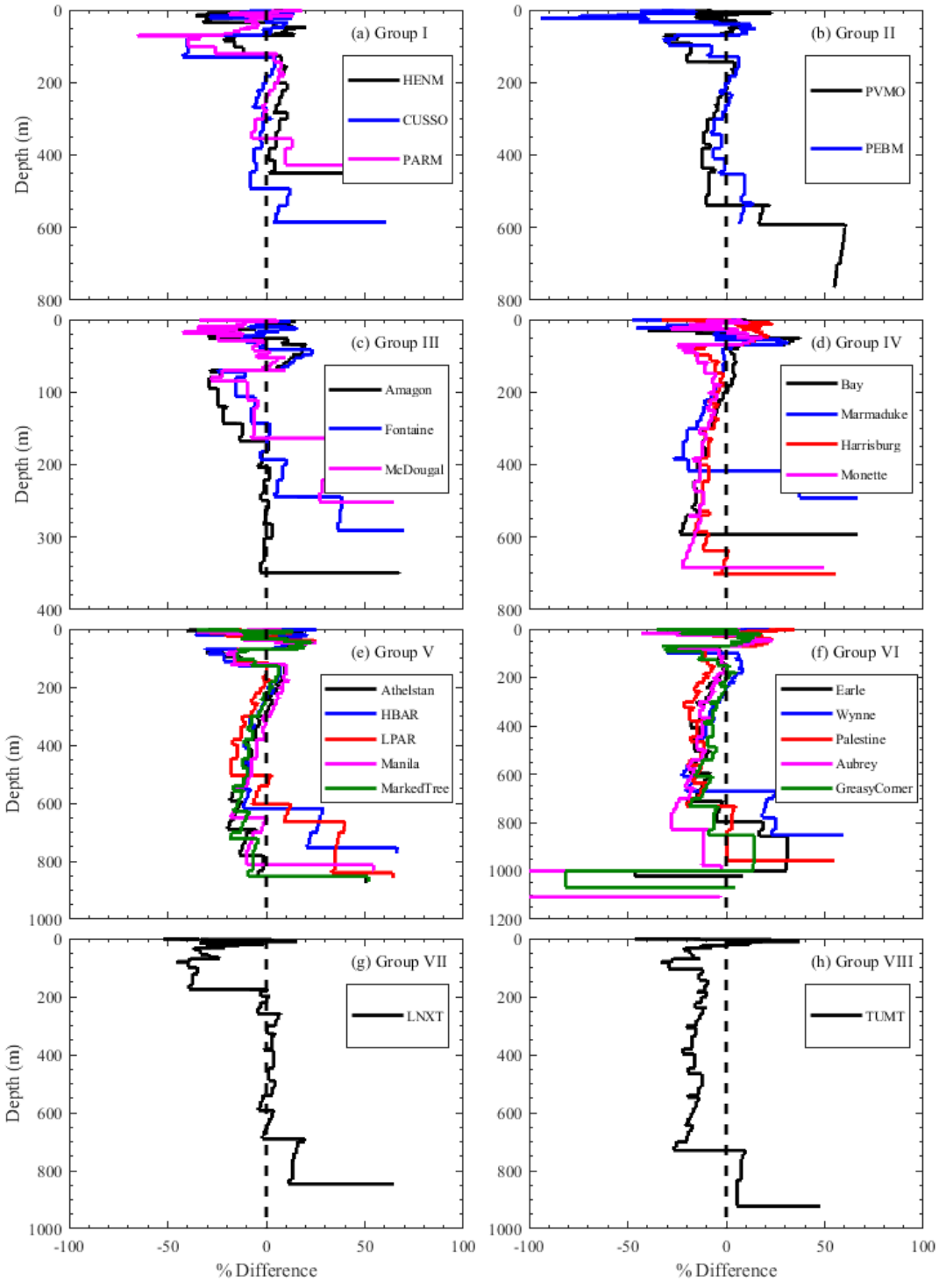

Figure 4.16 Percent difference between SWM Median VS profiles with the Romero and Rix (2005) lowland/upland VS profiles shown for Group I-VIII in (a) – (h), respectively.

4.14 Fundamental frequency, f_0-bedrock depth, H Relationship

The fundamental frequency from HVSR method has been used in many studies to map the bedrock depth in sedimentary basins (Ibs-von et al., 1999; Parolai et al., 2002). The fundamental frequency, f_0 and bedrock depth, H are shown to be related by a power-law function shown with Equation 5, where the constant a and exponent b are local geology dependent.

$$H=af_0^b \quad (5)$$

Ibs-von et al. (1999) and Parolai et al. (2002) used the power-law relationship shown in Equation 6 and 7 for mapping sediement thickness in the Rhine embayment (Germany) and Cologne area (Germany), respectively. However, no such relationships exist for the Mississippi embayment. A power-law fitting for Equation 5 is performed utilizing the fundamental frequency and corresponding bedrock depths used in this study and shown with Equation 8.

$$H=108\, f_0^{-1.551} \quad (6)$$

$$H=96\, f_0^{-1.388} \quad (7)$$

$$H=102\, f_0^{-1.459} \quad (8)$$

The developed power-law function in this study along with previous studies are shown in Figure 4.17. The calculated goodness-of-fit (R^2) between the measured and estimated points from power-law function demonstrate the highest R^2 (0.97) for Equation 8, which emphasizes the importance of local measurements for fitting the f_0-H power-law function. Based on the available measurement points, we recommend using Equation 8 for 250<H<1200 m in the Mississippi embayment. However, most depth to the bedrock studies in the Mississippi embayment have limited direct measurements and rely on interpolation between measrued bedrock depths. As a result, the developed power law relationship between fundamental frequency and bedrock depth could be refined with increasing knowledge on the depth to the bedrock in the Mississippi embayment.

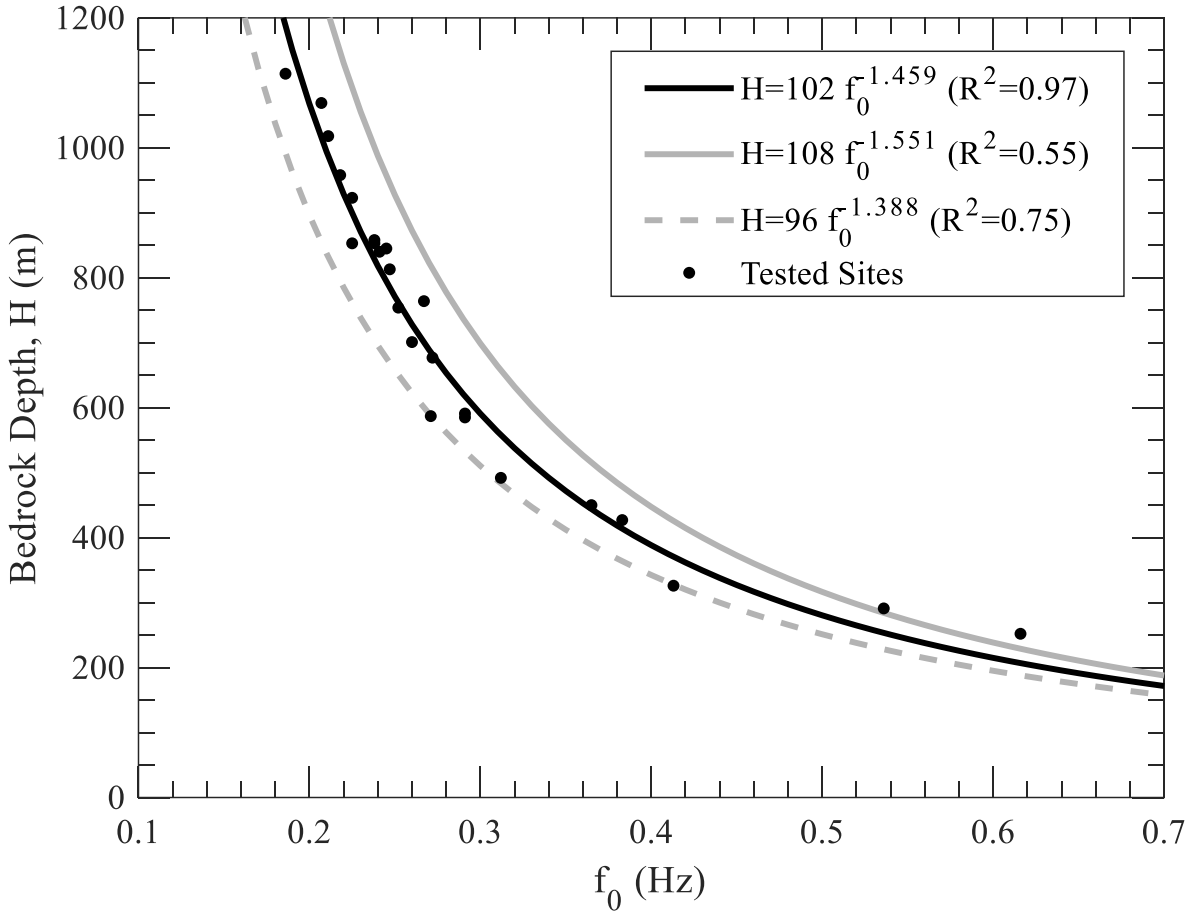

Figure 4.17 Power-law relationship developed between the fundamental frequency and bedrock depth for the Mississippi embayment. Fundamental frequencies from the HVSR test and bedrock depths utilized in the V_S inversion models are used here. The black solid, grey solid and grey dashed lines are power law fits from this study, Parolai et al. (2002), and Ibs-von Seht et al. (1999), respectively. The goodness-of-fit estimate (R^2) is shown in parenthesis for each equation.

4.15 Conclusion

In this study, deep shear wave velocity profiles are developed at 24 sites in the Mississippi embayment using a combination of active and passive source surface wave methods. An iterative multimodal joint inversion of surface wave data and fundamental frequency was conducted to develop shear wave velocity profiles to bedrock at each site. Iterative inversion runs were conducted to correctly assign modes of propagation and eliminate any effective mode

data. Parameterizations to constrain the inversion solutions were developed from a-priori related literature. Though not utilized in the joint inversion, a secondary HVSR peak frequency observed at many of the study sites were used as a guide to develop parameterization and later were used to evaluate V_S profile's ability to capture similar secondary peaks in the theoretical ellipticity. This insures the developed V_S profiles' capability to resolve any shallow impedance boundaries associated with the secondary HVSR peaks within reasonable bounds.

The developed shear wave velocity profiles captured the site signature from experimental dispersion data and fundamental site periods. Theoretical site periods generated from the median V_S profiles' ellipticity and transfer function are in the range of 0.3 – 3.5% and 0.7 – 10% of the experimental site periods, respectively, ensuring reasonable site response from the developed V_S profiles. Experimental site periods and estimated average shear wave velocity down to bedrock range from 1.6 – 5.4 second and 462 – 686 m/sec, with increasing values in the center part of the embayment and spatially decreasing values near the embayment border. Both site period and average shear wave velocity demonstrate a proportional relationship with the bedrock depth, i.e., deeper sites have longer site period and higher average shear wave velocity. Average shear wave velocities estimated based on a uniform layer resonance period tend to overestimate the average shear wave velocities by 25 – 40% compared to the values determined in this study. Calculated V_{S30} for the study sites range from 167 – 306 m/sec, with one exception, all study sites are in the seismic site class D classification. While the shallow V_{S30} measurements classify the majority of the sites in the embayment similarly, it fails to capture the overall deeper characteristics of the embayment sites, which changes spatially across the embayment. Average formation velocities for the commonly found geologic units in the embayment, Quaternary, Upper Tertiary, Memphis

sand, Paleocene, Cretaceous, and Paleozoic bedrock are 214, 418, 607, 665, 967, and 2211 m/sec, respectively.

The deep shear wave velocity profiles in this study were compared with existing V_S profiles from Rosenblad et al. (2010), Romero and Rix (2005) and site specific CUSVM profiles (Ramirez-Guzman et al., 2012). The developed V_S profiles had good agreement with the related Rosenblad et al. (2010) V_S profiles for layers above and slightly below the Memphis sand layer, but the Rosenblad et al. (2010) V_S profiles tended to overestimate the Vs compared to this study for layers near the max depth of their V_S profiles. The Romero and Rix (2005) Lowland and Highland V_S profile had reasonable agreement with the Vs profiles in this study with 5-30% differences being typical, but higher differences were observed around site specific layer interfaces of 20-70% due the generic natural of the Lowland and Highland V_S profiles. The CUSVM V_S profiles tended to have the largest differences between the V_S profiles in this study, consistently under predicting V_S for many sites and depths by 30% with some exceptions at particular sites and depths.

Overall, the current shear wave velocity models for the embayment lack information from sufficient site-specific shear wave measurements, especially from the deeper part of the embayment. This results in discrepancies in the shear wave velocity models. The developed shear wave velocity profiles from this study can fill the gap for deep site characterization information in the embayment. Use of these developed V_S profiles will be valuable in improving the performance of any existing velocity models, cultivating new models for the embayment, conducting site specific site response, and seismic hazard studies.

5. Chapter 5: An approach for developing site signature consistent deep shear wave velocity profiles for the Mississippi Embayment using generalized power-law functions

5.1 Abstract

A new approach is presented to develop site signature consistent deep shear wave velocity profiles (V_S profile) for the Mississippi embayment using generalized power-law functions. The approach utilizes 24 deep shear wave velocity profiles measured across the embayment to develop power-law shear wave velocity functions for the geologic units observed in the embayment. The velocity functions along with the layer interface boundaries are utilized to generate an initial V_S profile, whose Vs is then adjusted to be consistent with the fundamental site frequency (i.e., the site signature). Using the developed approach, model V_S profiles at 24 sites throughout the embayment are generated and compared to the corresponding measured Vs profiles. All modeled V_S profiles matched the site fundamental frequency within one standard deviation. Percent differences calculated between the modeled V_S profiles and measured V_S profiles demonstrated good agreement with less than a 10% difference at most depth ranges. However, differences of up to 30% are observed for near surface layers. The V_{Savg} of the modeled and measured V_S profiles have a strong association with a Pearson correlation coefficient of 0.95, while the V_{S30} of the modeled and measured Vs profiles have a Pearson coefficient of 0.49, indicating a weaker association. As an independent verification, model V_S profiles are generated at 11 Rosenblad et al. (2010) sites and compared with the measured V_S profiles at these sites. Percent differences calculated between the modeled and measured V_S profiles at the Rosenblad et al. (2010) sites are below 15% at most depth ranges, with a Pearson correlation coefficient calculated for V_{S150} of 0.75, indicating a strong association. With

reasonable layer interface models, this new approach can be used to develop an updated 3D shear wave velocity model for the Mississippi embayment.

5.2 Introduction

Local soil conditions (seismic velocity, density, layering, damping, etc.) influence seismic waves as they propagate from deeper bedrock layers to the ground surface. The modification of seismic waves due to localized site effects is called site response. The study of ground motion prediction, i.e., Ground Response Analysis (GRA) due to site response is critical for designing seismic resistant infrastructure. In many GRA studies, seismic response at the surface is assessed by simulating an input motion at bedrock through the local soil profile. Many recent efforts to validate 1D GRA to emulate empirical results from vertical array sites concluded that 1D GRAs fail to accurately predict recorded site response (Afshari and Stewart, 2019; Tao and Rathje, 2019; Teague et al., 2018). Three-dimensional GRA is believed to account for many of the short comings of 1D GRAs (De Martin et al., 2013). However, a 3D GRA requires spatial variability in shear wave velocity measurements (V_S profiles) in order to account for the lateral heterogeneity. Technical constraints and economic considerations are major impediments to deriving 3D V_S models for GRAs, limiting our ability to conduct 3D GRA studies. Vs profiles developed using any method are affected by aleatory variability and epistemic uncertainty. Despite this uncertainty, V_S profiles which accurately represent the resonance frequency of the site (i.e., the site signature) have been shown to produce reliable estimates of site response (Griffith et al., 2016; Himel and Wood, 2021; Teague et al., 2018). As an example, Teague et al. (2018) showed that site signature consistent surface wave method V_S profiles at the Garner Valley downhole array were able to predict site response more accurately than invasive V_S profiles from downhole and P-S suspension logging. Shear wave velocity

models (2D/3D) are predominantly based on sparsely measured data and are therefore significantly affected by aleatory variability and epistemic uncertainty reducing their benefits over 1D Vs profiles. However, 2D/3D V_S models which are adjusted to match local site signatures could lead to a cost-effective solution for site response studies over a large area.

The Mississippi Embayment, occupying a substantial area in the central United States, is characterized by deep unconsolidated sedimentary deposits and strong impedance contrasts within the soil column and at the Paleozoic bedrock boundary (Van Arsdale and TenBrink, 2000; Himel and Wood, 2022). Due to its complex three-dimensional geology, the Mississippi embayment is susceptible to ground motion amplification and has some of the highest design peak ground accelerations (PGA) in the nation (ASCE 2017). The presence of the New Madrid Seismic Zone (NMSZ) in the embayment and a 25 – 40% probability of a M_W 6+ earthquake in the next 50 years makes this region a high risk seismic hazard zone (Frankel et al., 2009). Regardless of high seismic hazard potential, no large earthquake ground motions have been recorded in the embayment. In the absence of locally recorded ground motions, reliable V_S profiles throughout the embayment are required to understand the spatial variance of seismic amplification in the embayment. Due to the lack of deeper V_S profiles, two reference V_S profiles from Romero and Rix (Romero and Rix, 2005) are typically used for site response studies in the embayment. The Central US Seismic Velocity Model (CUSVM) alleviated this issue in part by providing interpolated V_S profiles within the embayment and delivering continuous/3D site characterization information (Ramirez-Guzman et al., 2012). However, recent work by Himel and Wood (Himel and Wood, 2021a; Himel and Wood, 2022) conducted deep site characterization measurements at 24 locations across the embayment and observed up to 50% error between the measured and modeled shear wave velocities of different geologic units along

with inconsistencies in the depths to shallow impedance boundaries, leading to variability in the estimated local site response (Himel et al., 2021a; Himel et al., 2021b). This calls for a new approach to developing a 3D V_S model across the embayment that can better account for the site-specific spatial variability across the embayment.

In general, three approaches are used to develop 3D V_S models: (i) multiple spatial measurements, (ii) stochastic statistical models, and (iii) generalized parametric velocity equations. In the first approach, multiple invasive/non-invasive site characterization techniques are conducted and interpolated to develop a continuous 3D model. However, regardless of the type of direct measurements made, this approach requires a significant number of measurement locations, making this approach time consuming and a non-budget friendly option for engineering practice. The most simplistic statistical approach to account for uncertainty in soil properties when performing site response is to use upper and lower boundary V_S profiles, usually +/- 20% of the measured base profile (EPRI 2012). However, blind use of boundary V_S profiles have been shown to be ineffective for capturing site-specific site response, making this method inept for a 3D GRA study. More sophisticated stochastic statistical methods, such as Toro (Toro, 1995) and Monte Carlo simulations have yielded reasonable site response analysis in some studies, and have been shown to reproduce wave scattering effects (Nour et al., 2003). However, for highly heterogeneous sites, blind use of these statistical methods have yielded unreasonable ground motion predictions (Griffiths et al., 2016; Nour et al., 2003). In addition, numerous region/site specific inputs are required for a sophisticated statistical method, such as the Toro et al. (1995) method (e.g., layering model parameters, λ, c_1, c_2, c_3, and velocity model parameters, ρ_0, ρ_{200}, h_0, b, etc.), rendering these methods less useful for site-specific estimates. Generalized parametric velocity correlations are region specific and dependent on the stiffness of materials

found in a particular region. These parametric velocity functions along with regional layering interface models are used together to generate 2D/3D velocity models for a region. Different forms of velocity correlation functions, mostly of polynomial and exponential forms were used in previous studies. A USGS velocity model for the San Francisco bay area (Rodgers et al., 2008) and CUSVM for the central and eastern US (Ramirez-Guzman et al., 2012) utilized polynomial parametric velocity functions. Exponential parametric functions have been used for the Canterbury region, New Zealand (Deschenes et al., 2018; Lin et al., 2014) and southern California (Magistrale et al., 1996). However, with sufficient empirical constraints, no significant differences were observed between different forms of velocity functions (Thomson et al., 2020). Carefully curated parametric velocity correlations, though not directly generated from site experimental dispersion data, were observed to bear resemblance to dispersion characteristics of sites (Thomson et al., 2020). Apart from these aforementioned approaches, Hallal and Cox (Hallal and Cox, 2021) developed a method to generate pseudo 3D V_S profiles utilizing a geostatistical approach. In this approach, continuous 3D profiles are generated around the vicinity of a direct measurement site by scaling the layer thicknesses of the base profile to match the measured fundamental frequency from horizontal to vertical spectral ratio method (HVSR) (Nakamura, 1989). Implementation of this method for the Treasure Island and Delaney Park downhole array sites demonstrated good agreement with geologic cross sections. However, this approach allows layer thicknesses to vary while keeping the layer velocities the same. This could provide good spatial variability for engineering sites (hundreds of square meters), but for a large regional areas, such as the Mississippi embayment, where both layer thicknesses and velocities vary spatially, a different approach is required.

Based on the discussion above, a new approach to develop a 3D V_S model for the Mississippi embayment is described and evaluated in this article. The developed approach addresses the following issues: (i) development of generalized power-law velocity functions for local geologic units to account for the region specific material stiffness, (ii) utilizing spatially variable layer interfaces derived from previous studies, (iii) development of initial model V_S profiles for specific locations based on power-law velocity functions, mean formation velocity of geologic units, and derived layer interfaces at each location, and (iv) adjustment of initially modeled V_S profiles to capture the site signature. This model approach is tested at the 24 study locations from Himel and Wood (Himel and Wood, 2022), and 11 study locations of Rosenblad et al. (2010) utilizing layer interface models at these locations.

In this article, development of the power-law velocity functions is discussed first. The procedure to develop an initial V_S profile for one of the example sites (Athelstan) utilizing the developed power-law velocity functions, mean formation velocities from the Cretaceous and Paleozoic units, layer interfaces at the location from previous studies, and fundamental site frequency (f_0) is detailed. A workflow to adjust the modeled initial Vs profile to produce a final V_S profile that captures the site signature is discussed. Corresponding S_H wave theoretical transfer function (TTF) and theoretical fundamental mode Rayleigh ellipticity (TRE) for the initial and final V_S profiles are compared to the experimental f_0 for the example site. Percent differences of the modeled and measured V_S profiles at all 24 Himel and Wood (2022) study sites, and comparison of modeled and measured profiles' time averaged shear wave velocities down to the bedrock and for the top 30 m are shown. A Pearson correlation coefficient between the time averaged V_S of the modeled and measured Vs profiles are tested for this model approach and the CUSVM. Finally, the developed approach is utilized to generate deep V_S profiles at 11

Rosenblad et al. (2010) sites. A comparison of the generated V_S profiles and the measured Rosenblad et al. (2010) V_S profiles are made to validate the results from the developed approach.

5.3 Data source

The data for this article is based on study by Himel and Wood (Himel and Wood, 2022). The parametric power-law velocity functions, layer interface models and mean formation velocities used in this article are from these studies. Details of utilized shear wave velocity data, adopted geologic units for the embayment and the adopted geologic interface models are provided below.

5.4 Shear wave velocity data

Twenty-four deep V_S profiles from Himel and Wood (2022) are used in this article. Spatial distribution of the V_S profiles is shown in Figure 5.1. These measurement locations were grouped into eight groups due to similarities regarding geologic structure, shear wave velocities and geologic location (Himel and Wood, 2022). The V_S profiles were derived from a combination of active and passive source surface wave methods to ensure retrieval of both high and low frequency dispersion data. Active MASW using multiple shot locations for both Rayleigh and Love waves were used. Passive source microtremor array measurements (MAM) were carried out using circular and L-shaped arrays. A joint inversion of the active and passive dispersion data along with the site fundamental frequency was utilized to ensure that the generated V_S profiles capture the site signatures from both local dispersion and site fundamental frequency. This method was validated for the downhole array situated at CUSSO (Himel and Wood, 2021) and extended for the rest of the study sites. As the inversion process is highly non-unique, 1000 minimum misfit Vs profiles from a pool of 2 million inversion solutions were selected at each site location to calculate a median profile for that location. Each of the

calculated medians were tested to ensure that they captured local dispersion characteristics and site fundamental frequency within a reasonable uncertainty bound. For this article, the calculated median profiles are utilized to develop power-law velocity equations. More details regarding the actual measurements at these sites can be found from Himel and Wood (Himel and Wood, 2021; Himel and Wood, 2022).

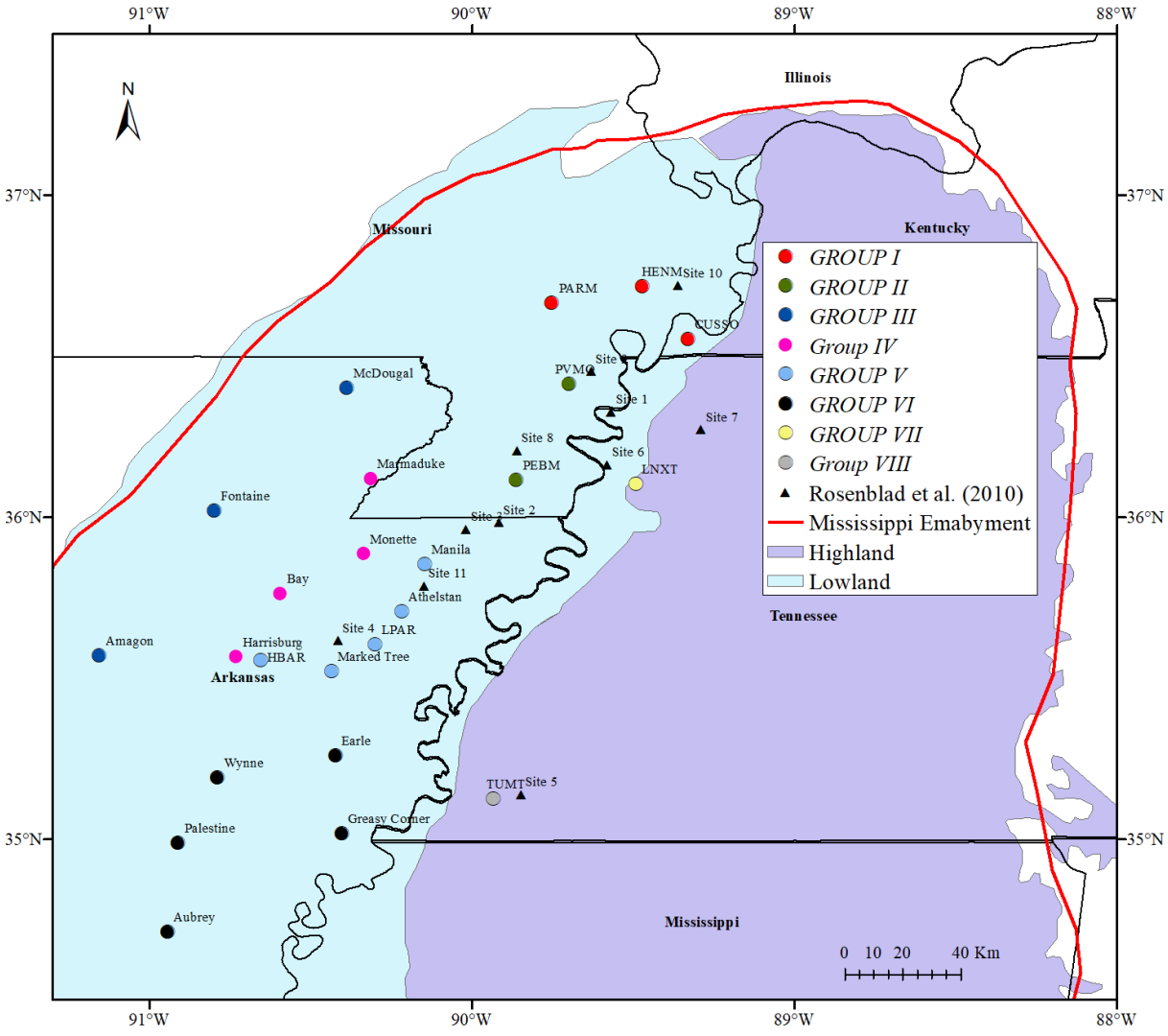

Figure 5.1 Spatial distribution of the 24 VS profiles used in this study from Himel and Wood (after Himel and Wood, 2022) is shown along with measurement locations from Rosenblad et al. (2010).

5.5 Adopted regional geologic units

The Mississippi embayment geology is generally described as a southward plunging syncline along the Mississippi river, with an overall basin-like structure (Mento et al., 1986; Brahana et al., 1987). An idealized cross section of the Mississippi embayment in the east-west direction crossing the Shelby County, Tennessee is shown in Figure 5.2 (modified after Ng et al., 1989). The structure of the embayment is well studied and described in previous studies, such as Brahana et al., Van Arsdale and TenBrink, and Street et al. (Brahana et al., 1987; Van Arsdale and TenBrink, 2000; Street et al., Street et al., 2004). Himel and Wood (Himel and Wood 2021; Himel and Wood, 2022) adopted the geologic units used in developing the CUSVM (Ramirez-Guzman, 2012) to be consistent with the existing model. In this article, similar geologic units are adopted. The geologic units adopted are the Quaternary (QT), Upper Tertiary (UT), Lower to Middle Claiborne (LMC), Paleocene (PL), Cretaceous (CR) and Paleozoic (PZ) era bedrock. The geologic units along with their corresponding chronological geologic layers and material types are provided in Table 5.1. The QT unit consists of the Holocene deposits in the lowland part and Pleistocene deposits in the highland part of the embayment, making the surface deposit layer in the highland stiffer than the lowland part (see Figure 5.1 for the extent of the highland and the lowland regions). The UT unit consists of the Jackson, Cockfield and Cook Mountain formations. The LMC unit, also known as Memphis sand and Sparta sand in some parts of the embayment, is a stiff layer of very fine to coarse grained sand. Due to rapid change in stiffness at the LMC top boundary, this unit creates an impedance boundary within the soil column. The shallow impedance boundary created by this unit influences local site response and as a result, accurate modeling of the depth to this unit is critical for GRA studies (Himel et al, 2021b). The PL unit consists of the Wilcox and Midway groups, which are spatially made up of several

formations across the embayment. The CR unit, situated above the PZ bedrock, contains the McNairy sand, Demopolis formation and Coffee formation. The PZ bedrock acts as the basement of the embayment and creates a deeper impedance boundary. The geologic units adopted here are geochronological, i.e., these units are sequentially deposited as no significant uplift has occurred over the periods in consideration. Because of the basin-like structure of the embayment, the adopted geologic units have a thicker structure in the deeper central part of the embayment and gradually becomes thinner near the edge (see Figure 5.2). The LMC unit follows the same trend and becomes deeper near the central part of the embayment, while diminishing near the edge (Himel, 2018).

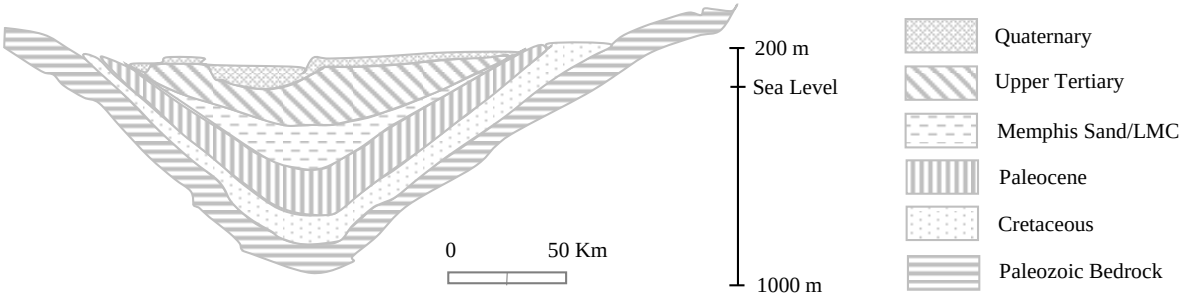

Figure 5.2 Typical geologic cross-section of the Mississippi embayment in the east-west direction crossing the Shelby County, Tennessee (modified after Ng et al., 1989).

Table 5.1 Adopted geologic units utilized for constructing the 3D velocity model.

Adopted Geologic Unit	**Chronological Geologic Layer**	**Material**
Quaternary (QT)	Holocene/Pleistocene	Alluvial surface deposits (fine to coarse grained quartz sand, chert gravel, and clay)
Upper Tertiary (UT)	Upper to Middle Eocene	Silt, clay, some seams of lignite
Lower to Middle Claiborne (LMC)	Lower Eocene	Fine to coarse grained, light grey-white sand
Paleocene (PL)	Paleocene	Silt, clay, fine to coarse grained sand, minor limestone

Adopted Geologic Unit	Chronological Geologic Layer	Material
Cretaceous (CR)	Cretaceous	Sand, silt, undifferentiated limestone
Paleozoic (PZ)	Paleozoic	Knox Dolomite

5.6 Adopted Geologic Interface Models

Geologic layer depths utilized in this study at the 24 Himel and Wood (2022) study locations are adopted from the layer interfaces resolved by Himel and Wood (Himel and Wood, 2021; Himel and Wood, 2022). In the inversion process used in the Himel and Wood studies, parametrization to constrain layer interfaces with a-priori knowledge from the literature along with vertical uncertainty bounds were utilized. Nevertheless, at many locations, geologic interfaces from the inversion differed from existing 3D models of the embayment (CUSVM), which was attributed to lack of direct measurement points used to create the CUSVM. However, the developed deep site characterization surface wave method (SWM) Vs profiles by Himel and Wood (Himel and Wood, 2021) were validated by vertical array downhole and P-S logging direct measurement results at the CUSSO site. The layer interfaces and shear wave velocities were shown to correlate well with the borehole results.

5.7 Development of power-law velocity equations

To develop power-law velocity equations for the geologic units in the embayment, the median V_S profiles at all 24 locations from Himel and Wood (2022) are utilized. Each of the median V_S profiles is broken up according to its geologic units' at each location. For the QT, UT, LMC, and PL units, shear wave velocity values at every 1 m depth increment from each of the median V_S profiles are selected to develop the power-law fits. To formulate a fit to the shear

wave velocity points of each geologic unit, a power-law equation of the following form from Lin et al. (Lin et al., 2014) is selected:

$$V_S = A_S * \left(\frac{\sigma_0'}{P_a}\right)^{n_s} \quad \text{Equation } 9$$

Where, V_S=Shear wave velocity in m/sec, A_S=shear wave velocity corresponding to effective mean stress of 1 atm, σ_0'=mean effective stress, P_a=Atmospheric pressure (1 atm=101325 Pa), n_S=exponent of normalized effective mean stress.

In Equation 9, σ_0' is a function of depth and material density (i.e., stiffness) present in the corresponding geologic unit. Hence, this parameter accounts for the increasing confining stress on the soil with depth. No aging parameter is used in the fitting equation as sediments in the Mississippi embayment are deposited sequentially as per their geologic age. Power-law fit velocity equations, and selected shear wave velocity points for the corresponding geologic unit along with median V_S profiles are shown in Figure 5.3a, b, c, and d for the QT, UT, LMC and PL unit, respectively. Reference V_S curves from Lin et al. (Lin et al., 2014) are shown for comparison. Power-law fitting parameters for the QT, UT, LMC, and PL units are provided in Table 5.2.

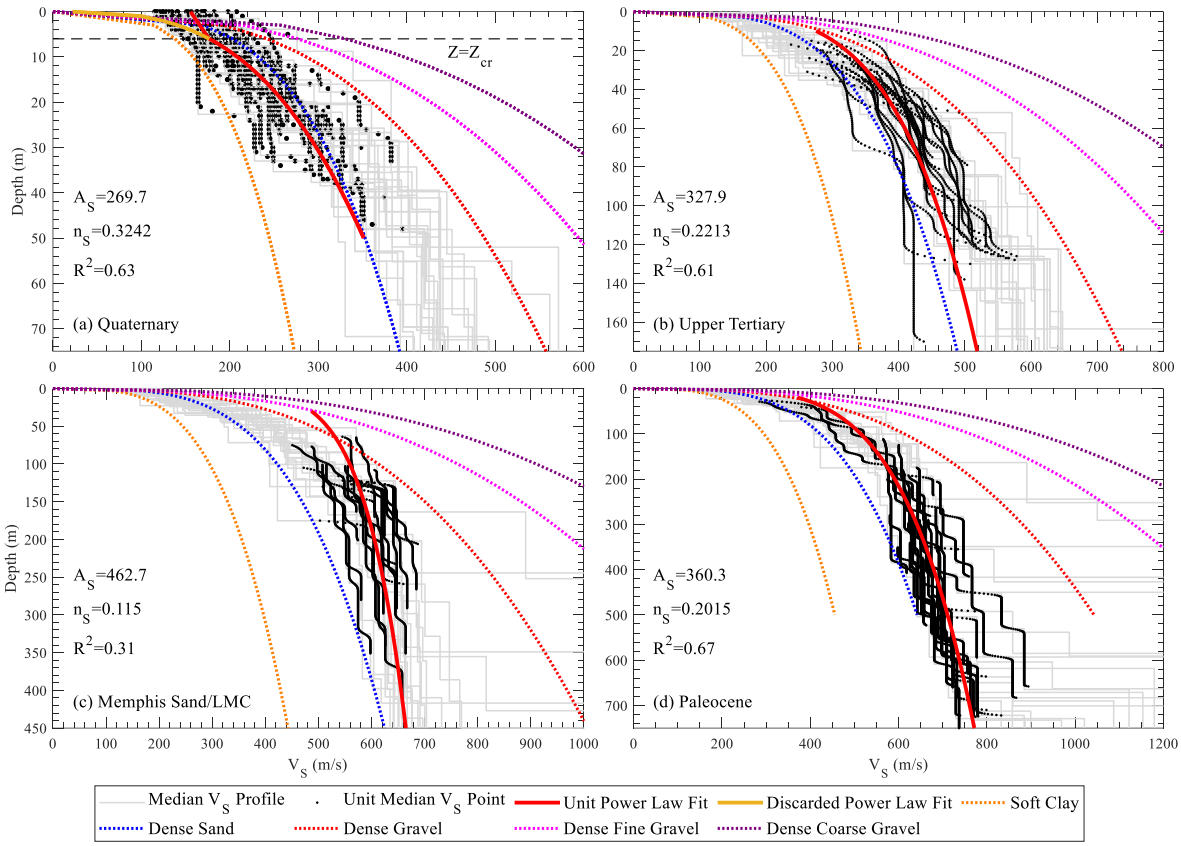

Figure 5.3 Median V_S profiles, selected shear wave velocity points at every 1 m incremental depth from each median V_S profiles, and corresponding power law fits are shown for the (a) QT, (b) UT, (c) LMC, and (d) PL . For the QT unit, the discarded fit for depths less than Z_{cr} is shown in (a). Reference V_S profiles for different materials from Lin et al. (2014) are shown for comparison.

Table 5.2 Power-law velocity equation fitting parameters for the QT, UT, LMC, and PL unit.

Geologic Unit	A_S (m/sec)	n_S	ρ (kg/m^3)
QT	267.7	0.3242	1700
UT	327.9	0.2213	1750
LMC	462.7	0.115	1800
PL	360.3	0.2015	1900

As shown in Figure 5.3a, while the power-law fit corresponds well with most of the shear wave velocity points, it fails to accurately predict soil stiffness at very shallow depths (shown as the ‘discarded power-law fit in Figure 5.3). Due to the nature of a power-law fit, it decreases exponentially and becomes zero at surface, which is not realistic for physical shear wave velocity, i.e., soil stiffness. To prevent this issue, a linear fit for the very shallow shear wave

velocity points near the surface is introduced based on the study from Rahimi et al. (2019). In this linear fit, a critical depth, Z_{cr} is defined, above which all shear wave velocity points are fit linearly by extrapolating the shear wave velocity at the Z_{cr} depth from power-law fit. Equation 10 and 3 from Rahimi et al. (2019) defines Z_{cr} and the linear fit for V_S for depths, $Z<Z_{cr}$. Here, γ_t=total unit weight, V_{S0}=shear wave velocity at the ground surface, $V_{S@Zcr}$=shear wave velocity at Z_{cr} depth from the power-law fit.

$$Z_{cr} = \frac{P_a}{\gamma_t} \qquad \textit{Equation 10}$$

$$V_S = V_{S0} + \left(V_{S_{@Zcr}} - V_{S0}\right) * \left(\frac{Z}{Zcr}\right) \quad \textit{for } Z<Z_{cr} \qquad \textit{Equation 11}$$

The power-law fit for the QT unit is within the soft clay and dense sand reference V_S curves from Lin et al. (2014), whereas the UT fit is between the dense sand and dense gravel reference curves. This is coherent with the material types constituting these two geologic units. The LMC and PL units' are both stiffer than their overlain units, which is consistent with the idea that young geologic units should have lower average velocities. However, the LMC and PL units have very similar power-law fits. This is also observed by Himel and Wood (Himel and Wood, 2021; Himel and Wood, 2022) as the PL unit had shown indistinct differences to the overlain LMC unit in the inversion solutions.

For the CR and PZ units, good power-law fits could not be achieved. Therefore, for these units, the mean formation velocities calculated by Himel and Wood (2022) are used for their corresponding layers in developing the initial V_S profile. Calculated mean formation velocities for the CR and PZ unit determined by Himel and Wood (2022) are 967 m/sec and 2211 m/sec, respectively with standard deviations of 200 m/sec and 301 m/sec, respectively. A histogram chart of formation velocities for the CR and PZ unit from all 24 sites along with the

calculated mean and standard deviation from Himel and Wood (2022) (Himel and Wood, 2022) is shown in Figure 5.4a, and b, respectively.

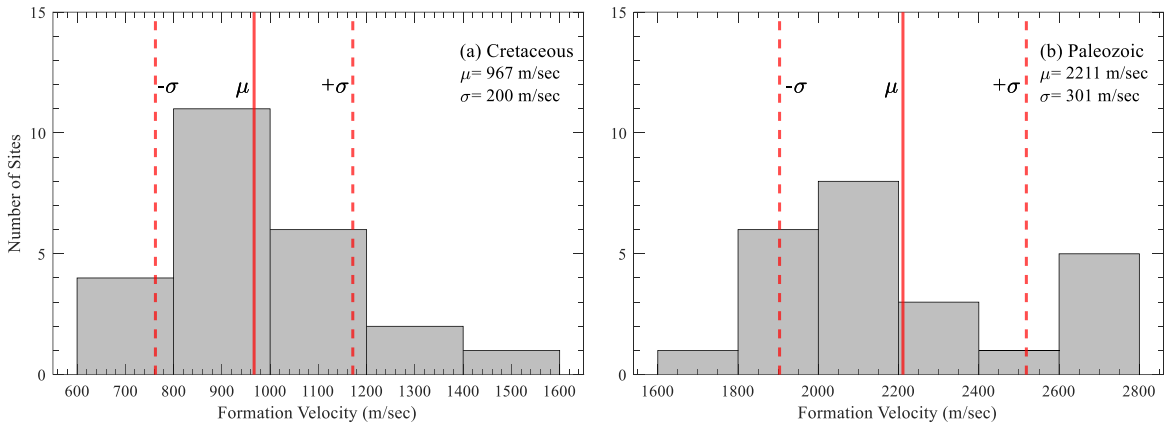

Figure 5.4 Calculated formation velocities from 24 study sites across the Mississippi embayment along with their mean and standard deviation shown for (a) CR unit, and (b) PZ unit (after Himel and Wood, 2022).

5.8 Development of the Initial V_S Profile

The following inputs are used to develop an initial V_S profile at a location: (i) layer interface model at that location, and (ii) velocity functions for the QT, UT, LMC, and PL units and mean formation velocities for the CR and PZ units. The first step to develop the initial profile is to discretize the continuous velocity functions into layers. The discretized profile will have multiple layers based on the geologic unit thicknesses and number of sub-layers (SL) within each layer. To avoid confusion, geologic unit thicknesses will be referred to as layers and divisions within a layer will be referred to as sub-layers hereafter. In the discretized profile, multiple SLs in a layer ensures gradual increase of material stiffness within a geologic unit, which is practical and observed in field condition as well. In this article, the following conditions were imposed to generate SLs within each geologic units: (i) First SL of the first layer is not allowed to be thinner than 1 m and a succeeding SL is made thicker than the preceding SL. (ii) A

layering ratio (LR) (Succeeding SL thickness/preceding SL thickness) of 1.3 for the QT, UT, and LMC unit and 1.5 for the PL unit is used. This allows for the shallower geologic units to have thinner SLs and deeper units to have thicker SLs. (iii) Number of SLs in a layer is calculated as per Equation 12, which is based on a geometric series and provided below. In Equation 12, H_0=thickness of the first SL in a layer, H=thickness of the layer, LR=layering ratio, n=number of SLs in the layer. For a known layer thickness (H, from the layer interface model) and LR, an iterative automated loop is run to calculate H_0 by varying n. The lowest value of n that satisfies condition (i) is taken as the number of SLs (n) within a geologic unit's layer. (iv) A single SL is used for the CR and PZ unit as a mean formation velocity is utilized for these two units instead of a velocity equation.

$$H_0 = H * \frac{1-LR}{1-LR^n} \qquad \textit{Equation 12}$$

To calculate shear wave velocity within a SL, mean effective stress (σ_0') at the middle of that SL is calculated and utilized in Equation 9 along with the fitting parameters of the corresponding geologic unit. For SLs in the QT unit situated within depth, $Z<Z_{cr,}$ shear wave velocity is calculated by Equation 11 in the middle of the SL. The calculated shear wave velocities at the middle of each SL are continued throughout that SL. An example of SL generation and assigning a shear wave velocity to an SL is provided in Figure 5.5. In this example, SL generation and assigning shear wave velocities based on the velocity functions at the middle of each SL is demonstrated for the QT unit at the Athelstan site. In the Athelstan geologic interface model, the QT unit is 15 m thick. Based on the conditions set to generate SLs, this layer is divided into 6 SLs, each thicker than the preceding SL. Shear wave velocity at the middle of each SL is calculated based on the corresponding velocity function. The velocity fitting curve (includes the linear fit down to Z_{cr} and power-law fit for the rest of the depth) is

shown for comparison along with the discretized profile for the QT unit. Utilizing the above-mentioned method, discretized profiles for the QT, UT, LMC, and PL unit is developed and shown in Fig. 6a, b, c, and d, respectively. All the segmental discretized profiles for the QT, UT, LMC, CR and PZ units are combined to form the initial V_S profile. The developed initial V_S profile following the mentioned methodology for the Athelstan site is shown in Figure 5.6e.

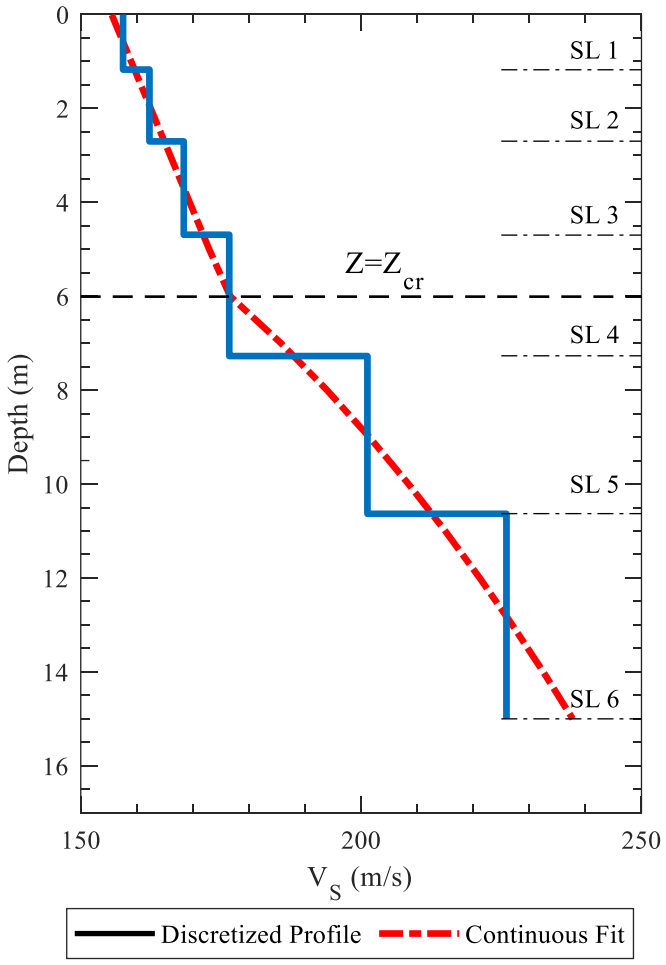

Figure 5.5 Discretized V_S profile derived from continuous fitting velocity functions for the QT unit at an example site, Athelstan. Layer thickness is divided into 6 SLs based on the preset conditions to generate SLs. The continuous velocity function fit is shown for comparison.

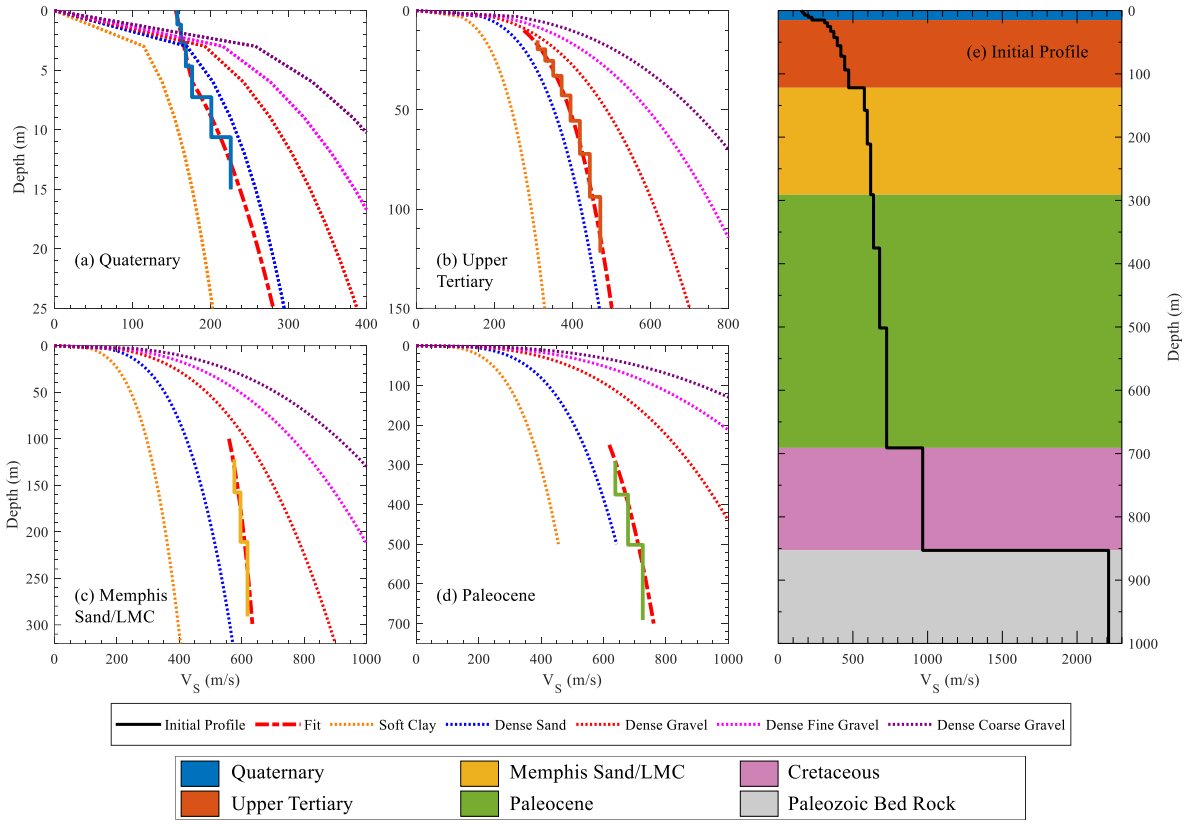

Figure 5.6 Discretized V_S profiles and corresponding velocity equation fits shown for the (a) QT, (b) UT, (c) LMC, and (d) PL unit. Reference V_S curves for different materials from Lin et al. (Lin et al., 2014) are shown for comparison. (e) Developed initial V_S profile.

5.9 TTF and TRE to Adjust V_S Profiles

Fundamental frequency peaks, TF_0 and Ell_0 from TTF and TRE, respectively are used as a tool to evaluate a V_S profile's performance in capturing local site response (i.e., the site signature from microtremor horizontal to vertical spectral ratio (MHVSR) measurements). In this section, discussion on adjusting the initial V_S profiles to capture the site signature by using TTF and TRE is presented. A schematic workflow of the method is shown in Figure 5.7. To proceed with the method, the characteristics of a V_S profile that influences its corresponding TF_0 and Ell_0 are important to discuss. For a multi-layered V_S profile, the corresponding TF_0 and Ell_0 are influenced by the following factors: (I) depth of the overall profile down to the major impedance

boundary, (II) layer thicknesses, (III) layer seismic velocity (both V_S and V_P) and density, and (IV) impedance contrast ratio $\left(IC = \frac{\rho_{\text{bedrock}} * V_{S\ \text{of bedrock}}}{\rho_{\text{soil}} * V_{S\ \text{of soil}}}\right)$ at bedrock. The bedrock Vs only influences the amplitude of TF_0 and does not have any effect on the frequency of TF_0 (Kramer, 1996). However, the frequency of the fundamental Rayleigh ellipticity has a strong dependence on the bedrock Vs (Malischewsky and Scherbaum, 2004).

For this study, the layer interface model and depth to bedrock are held constant for a given site and only adjustments to the V_S of soil layers are made so that TF_0 matches MHVSR f_0. The Vs of each soil layer is scaled up or down based on the ratio of the initial Vs profile TF_0 frequency and the measured MHVSR f_0. If the initial TF_0 is within 1σ of f_0, no adjustment is made to the Vs profile. While increasing/decreasing the shear wave velocities of each SLs, the change in the V_S of a particular layer is limited to 2σ of the geologic unit's formation velocity determined by Himel and Wood (2022).

Here, the linear TTFs are computed between the bedrock and ground surface using a MATLAB code from Teague (Teague, 2017 personal Comm.). The TREs for corresponding V_S profiles are computed in the Geopsy software package (Wathelet et al., 2008). To compute TREs, density, and P-wave velocity (V_P) for all SLs in the corresponding V_S profile is required. Density for a SL is taken from Table 5.2 for the SL's corresponding geologic unit. A saturated soil layer V_P of 1500 m/sec for SLs with $V_S < 750$ m/sec is used. For the SLs with $V_S > 750$ m/sec, including the bedrock layer, V_P is calculated based on corresponding V_S and a Poisson's ratio of 0.33.

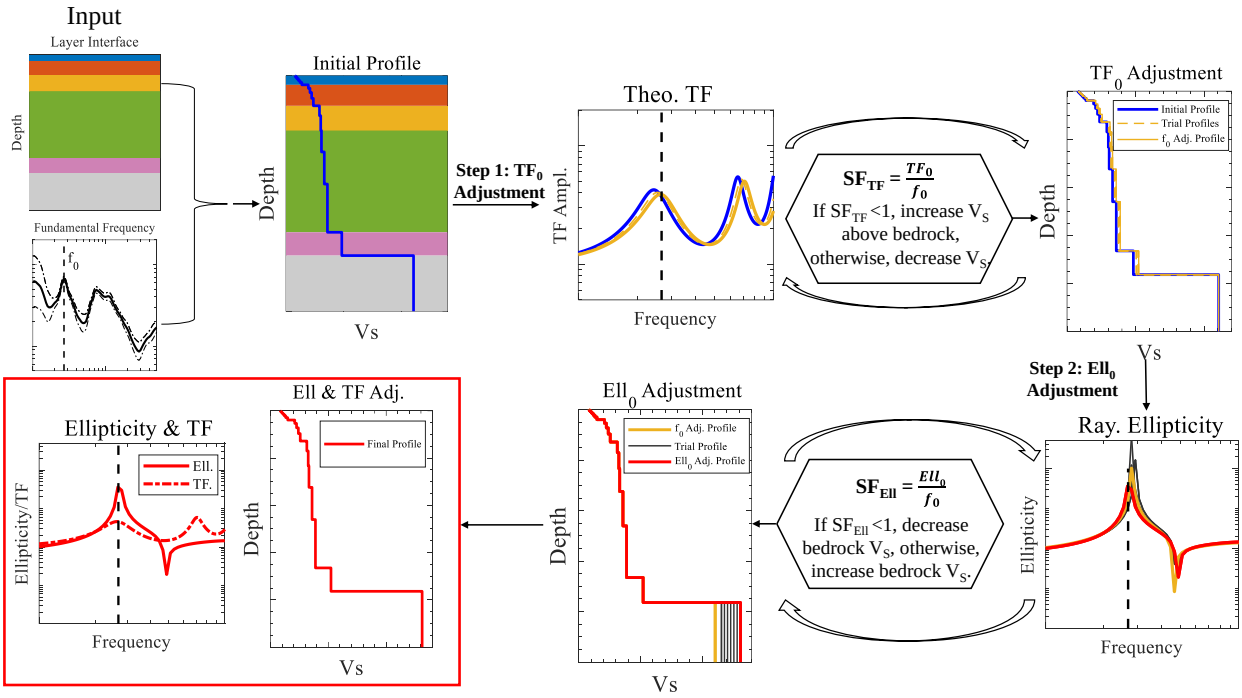

Figure 5.7 Schematic of an overall workflow of the developed approach to generate site signature consistent pseudo V_S profiles. Input for this approach are layer interface boundaries and measured f_0 at the site. The initial V_S profile is adjusted in steps 1 and 2 to match the T_{F0} and Ell_0 to the f_0, respectively.

In the second step (see Figure 5.8), the Vs of the bedrock is adjusted so that the Ell_0 of the Vs profile matches the MHVSR f_0 at the site. Similar to the previous step, a scaling factor is used for the adjustment and adjustments are made till the Ell_0 of the Vs profile is within 1σ of the MHVSR f_0 at the site. When adjusting the bedrock V_S, an allowable velocity range from 1700 to 2900 m/sec is used, which is the measured bedrock V_S range from Himel and Wood (Himel and Wood, 2022).

5.10 Site Signature Consistent Pseudo V_S Profile at Athelstan, Arkansas

Utilizing the approach in Sections 3.3, a site signature consistent pseudo V_S profile for an example site, Athelstan, Arkansas is developed and shown in Figure 5.8. The initial V_S profile,

trial V_S profiles from step 1 and 2, and the adjusted final profile are shown for (a) top 200 m, and (b) down to the bedrock in Figure 5.8. The median inversion V_S profile generated at this location from Himel and Wood (2022) is also shown for comparison. The layer interface model used to generate the initial V_S profile at this location is shown in Figure 8 (c). Overall, both the initial V_S profile and final Vs profile are in good agreement with the median inversion Vs profile, with final V_S profile within 10% of the measured profile for most depth ranges. The largest differences between the final and measured profiles are observed at very shallow depths and in the deeper CR and PZ layers up to 20%. While the median inversion profile has two SLs in the CR layer, one single SL is used to model the CR unit in the initial V_S profile, which consequently rolled over to all the trial profiles and the final profile.

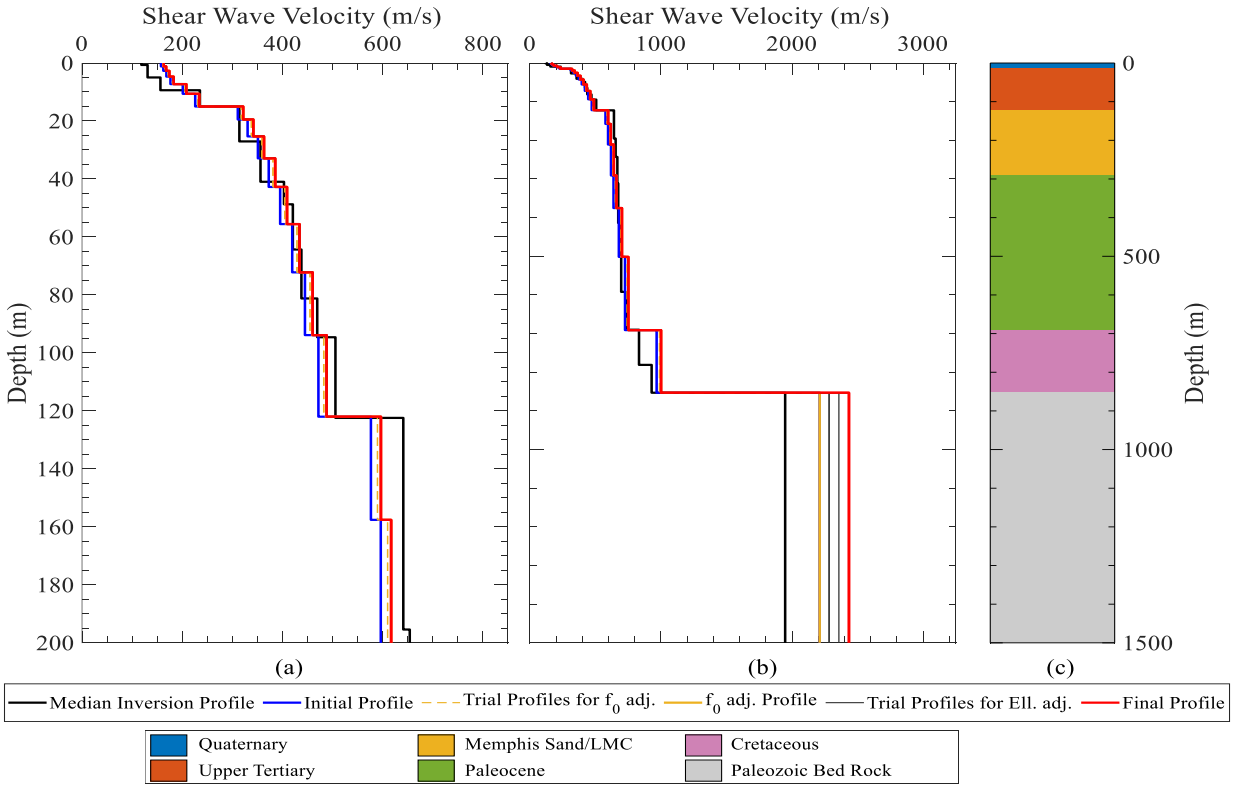

Figure 5.8 The initial V_S profile, trial profiles from step 1 and 2, and the final profile shown for the Athelstan, Arkansas site down to (a) 200 m, and (b) bedrock. Corresponding layer interface model used for this location is shown in (c).

Corresponding TF_0 and Ell_0 of the candidate V_S profiles from Figure 5.8 are shown in Figure 5.9a and b, respectively. Experimental MHVSR f_0 at this location is also shown for comparison.

From Figure 5.9a, the TF_0 corresponding to the median inversion profile, initial profile, and final profile are 0.22 Hz, 0.23 Hz, and 0.24 Hz, respectively, whereas the MHVSR f_0 is 0.24 Hz at this location. From Fig 9b, the Ell_0 corresponding to the median inversion profile, initial profile, MHVSR f_0 adjusted profile and the final profile are 0.25 Hz, 0.23 Hz, 0.25 Hz, and 0.24 Hz, respectively.

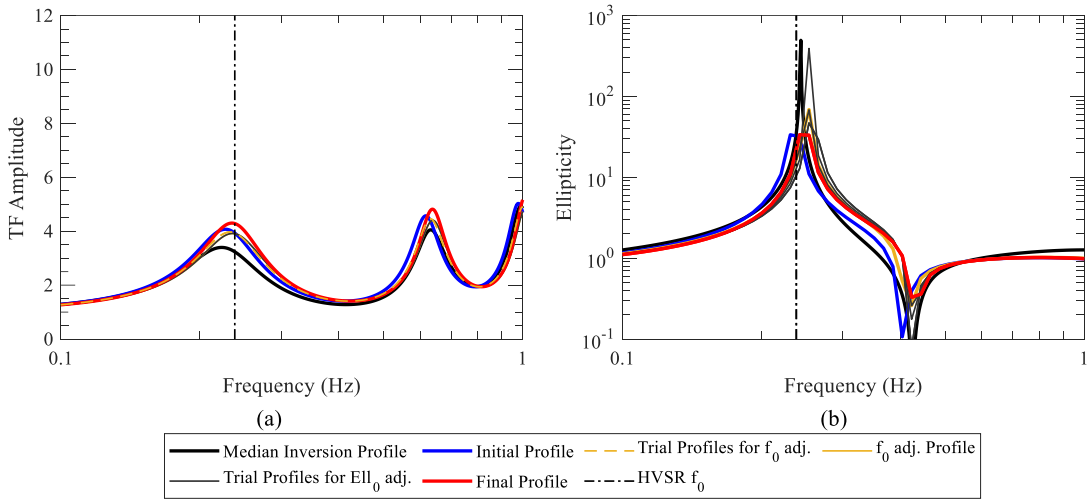

Figure 5.9 (a) TF_0 and (b) Ell_0 shown for the candidate V_S profiles in Figure 5.9. Experimental f_0 at the site is shown for comparison.

5.11 Comparison of modeled and measured V_S Profiles

To better understand the differences between the modeled and measured V_S profiles, percent differences at every 0.1 m depth increment are calculated for all 24 Himel and Wood (2022) study sites using Equation 13 and are shown in Figure 5.10 a – h for the Group I – VIII, respectively. A similar figure was presented by Himel and Wood (2022) (Himel and Wood,

2022) to observe the differences between the measured inversion profiles and modeled CUSVM profiles at these 24 sites.

$$\% \text{ Difference} = \frac{(V_S \text{ of measured} - V_S \text{ of modeled})}{V_S \text{ of measured}} * 100 \qquad \text{Equation 13}$$

Overall, percent differences between the modeled and measured profiles are within 10% for most of the depth ranges, while exceptions are observed for the shallow, and very deep layers of all groups and most depth ranges for the Group III sites. Percent differences for the shallow layers ranged from 5% to as much as 50% for some sites, which is reasonable as generic velocity equations cannot account for abrupt spatial changes in the shallow depths from site to site. For the deeper layers, such as the CR and PZ, percent differences ranged from 5% to 40%, which is attributed to the way CR is modeled with one single sublayer and a single mean formation velocity, and because PZ layers being adjusted to match Ell_0 to the f_0. For the Group III sites, corresponding TF_0 for the sites' inversion measurements were approximately 5% to 10% higher than the f_0, which implies that the inversion V_S profiles in this group are relatively stiffer than what the f_0 is suggesting. This explains the higher percent differences between the modeled and measured sites in this group. The CUSVM modeled profiles at these sites were observed to have 30% to 50% lower V_S at most depth ranges than the measured inversion Vs profiles, indicating an overall spatial bias throughout the embayment (Himel and Wood, 2022). While the modeled V_S profiles in this study have some specific differences in the shallow and deep layers, no generic trend of spatial bias is observed.

In order to provide independent verification, the developed model approach is used to generate Vs profiles at 11 sites where Rosenblad et al. (2010) developed Vs profiles in the Embayment (see Figure 5.1). To generate model V_S profiles at the Rosenblad et al. (2010) sites,

layer interface model information provided by Rosenblad et al. (2010) is used for the QT, UT, LMC and PZ unit, while information from the CUSVM is used for the PL and CR unit. Geologic layers Alluvium, Upper Claiborne and Memphis sand used in Rosenblad et al. (2010) are attributed to the QT, UT, and LMC, respectively to use in the model V_S generation. While the V_S profiles from Rosenblad et al. (2010) do not extend down to the bedrock, these site characterization results have been observed to be reliable down to approximately 150 m to 250 m (Wood et al., 2019; Himel and Wood, 2022). In order to compare results from the approach in this article to the Rosenblad et al. (2010) Vs profiles, model V_S profiles are generated at the 11 Rosenblad et al. (2010) sites. A percent difference between the modeled and measured V_S profiles for Sites 1 – 11 are shown in Figure 5.11. Similar to the percent differences observed between the modeled and measured V_S profiles for the 24 Himel and Wood (2022) study sites, modeled V_S profiles at most Rosenblad et al. (2010) sites are within 15% of the measured Vs profiles, except at the deeper layers below 150 m. Exceptions to this are observed for Site 5, 8 and 10, with differences of up to 50% at some depth ranges. Increased differences at deeper depths between the measured and modeled Vs profiles could be attributed to higher average formation velocities resolved for the Memphis sand layer by Rosenblad et al. (2010) (Himel and Wood, 2022). Overall, comparison between the modeled and measured V_S profiles at the Rosenblad et al. (2010) sites show no signs of spatial bias and are in good agreement.

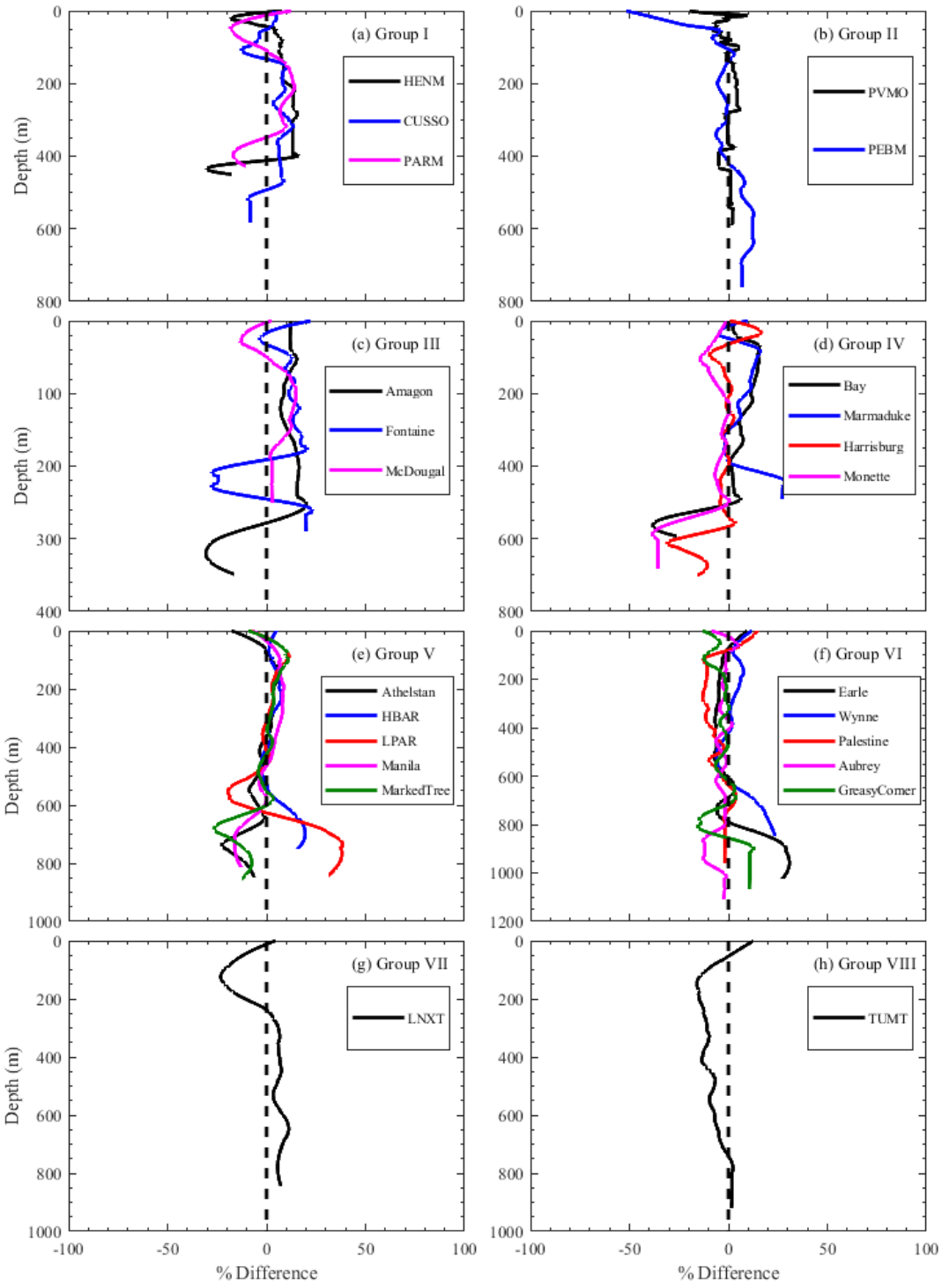

Figure 5.10 Percent differences calculated between the modeled and measured inversion profiles for all 24 Himel and Wood (2022) study sites grouped as Group I – VIII and shown in (a) – (h), respectively.

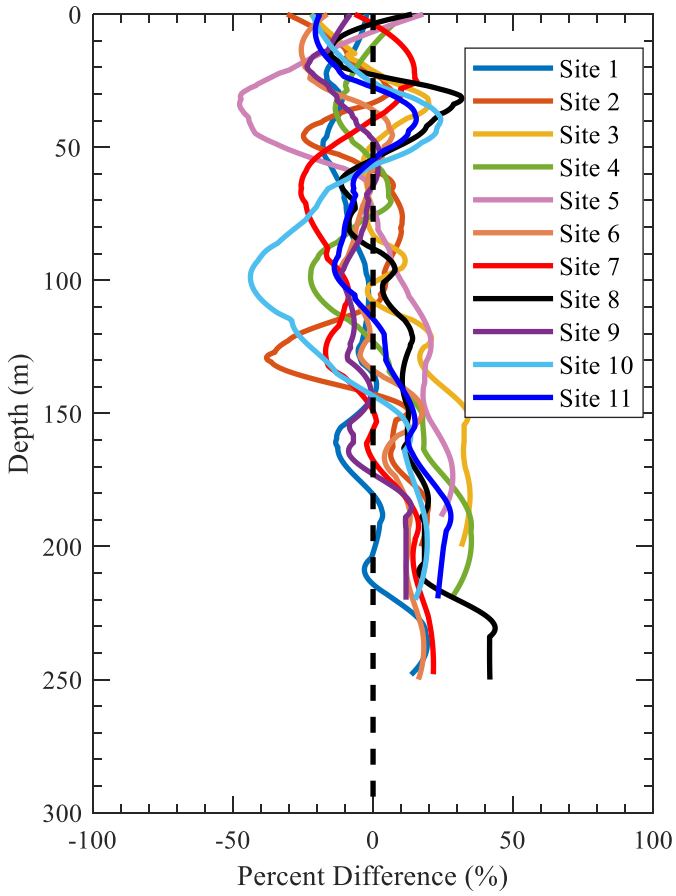

Figure 5.11 Percent differences calculated between the modeled and measured inversion VS profiles for the Rosenblad et al. (2010) study sites.

To better understand the overall agreement between the modeled and measured Vs profiles, the time averaged shear wave velocity down to the bedrock (V_{Savg}) and down to 30 m (V_{S30}) is calculated for the modeled V_S profiles and measured inversion Vs profiles. A comparison of V_{Savg} and V_{S30} between the modeled and measured inversion Vs profiles at the 24 Himel and Wood (2022) study sites are shown in Figure 5.12a, and b, respectively.

From Figure 5.12a, the V_{Savg} comparison between the modeled and measured inversion Vs profiles are in good agreement with most modeled V_S profiles' V_{Savg} within 5% of measured V_S profiles. The V_{Savg} from the modeled profiles ranged from 445 – 700 m/sec, while it ranged

from 460 – 690 m/sec for the measured inversion profiles. Differences between the modeled and measured profiles' V_{Savg} ranged from 0.5 – 8.5%, with average percent difference below 4%, indicating a very good agreement between the modeled and measured profiles throughout the embayment.

From Fig 12b, while the V_{S30} comparison between the modeled and measured inversion profiles are still in good agreement with average percent difference between modeled and measured V_{S30} below 8%, they are not as good as the V_{Savg} comparisons. The V_{S30} from the modeled profiles ranged from 201 – 280 m/sec, while it ranged from 167 – 305 m/sec for the measured inversion profiles. Differences between the modeled and measured profiles' V_{S30} ranged from 0.3 – 44%. This broad range of differences between modeled and measured V_{S30} indicates very good agreement is observed for some of the modeled sites, while some demonstrate significant differences. For example, the PEBM site's modeled and measured Vs profiles' calculated V_{S30} are 190 m/sec and 167 m/sec, respectively. The PEBM inversion profile's low V_{S30} was attributed to the measurement site being situated in a flood zone of nearby creek causing it to have soft surface sediments. However, this site specific very shallow local soil condition is not well modeled by the generic velocity equations at this particular site. This suggests that the velocity equations, though able to predict general trend of shallow site characterization well, can fail to accurately predict some site specific soil conditions.

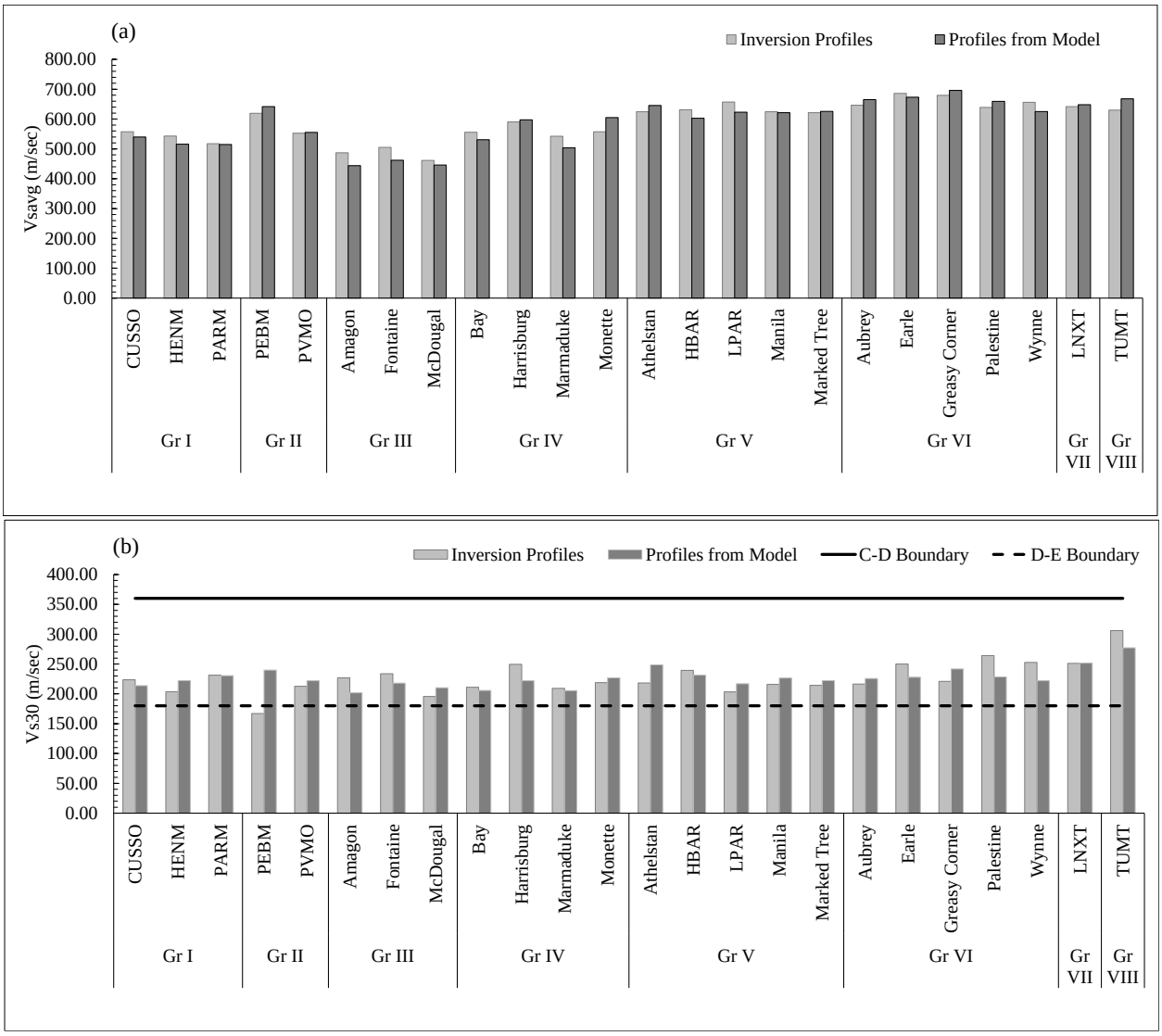

Figure 5.12 Comparison of time averaged (a) V_{Savg}, and (b) V_{S30} between the modeled and measured inversion profiles at the 24 Himel and Wood (2022) study sites.

The Pearson correlation coefficient, r, is calculated between the modeled and measured time averaged shear wave velocities to quantify how well the models and actual measured results correlate for the 24 Himel and Wood (2022) study sites. For this, Pearson correlation coefficient between (a) V_{Savg} model and V_{Savg} inversion, (b) V_{S30} model and V_{S30} inversion, (c) V_{Savg} CUSVM and V_{Savg} inversion, and (d) V_{S30} CUSVM and V_{S30} inversion are calculated and shown in Figure 5.13a, b, c, and d, respectively. The Pearson coefficient can range from +1 to -1, with

+1 implying highest positive correlation. In general, a positive Pearson coefficient above 0.5, 0.3 – 0.5 and below 0.3 indicates very strong, medium and weak correlation, respectively. Here, the Pearson coefficient between the modeled and measured V_{Savg} is 0.95, indicating a very strong positive correlation between the modeled and measured shear wave velocities. However, the Pearson coefficient between the modeled and measured V_{S30} is 0.49, demonstrating a weaker correlation than the overall profile. This illustrates that though the overall modeled and measured Vs profiles are very well correlated, shallow characterization of the models are not always in good agreement with the measured inversion results. The Pearson correlation between the CUSVM modeled and measured V_{Savg} is 0.16, demonstrating a very weak association between these two data sets. Similarly, the Pearson coefficient between the CUSVM modeled and measured V_{S30} is 0.18. Moreover, Pearson coefficient is calculated for the Rosenblad et al. (2010) sites' time averaged V_S down to 150 m (V_{S150}). The Pearson coefficient between the modeled and measured V_{S150} at the Rosenblad et al. (2010) sites is 0.75, whereas a Pearson coefficient of 0.34 is calculated for the CUSVM modeled Vs profiles at the same sites. These statistics suggest that the developed approach to model V_S profiles across the embayment is correlating better with the measured V_S profiles than the previously modeled CUSVM V_S profiles.

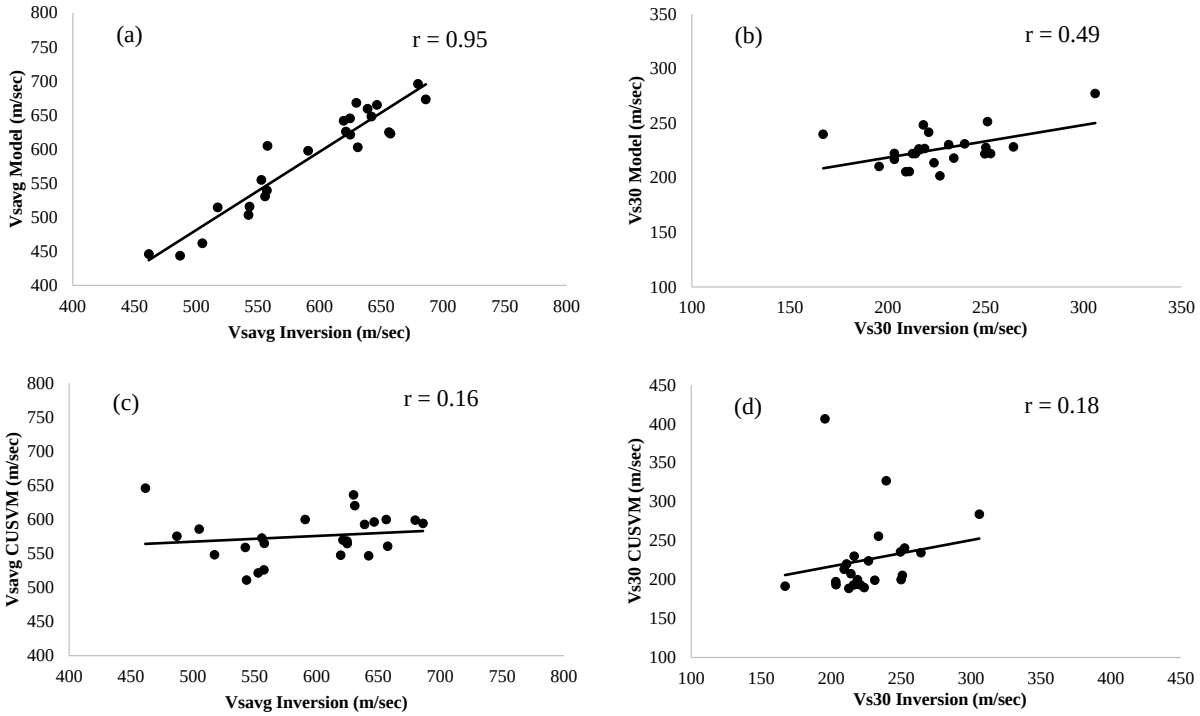

Figure 5.13 Pearson correlation coefficient calculated between the (a) V_{Savg} Model and V_{Savg} inversion, (b) V_{S30} Model and V_{S30} inversion, (c) V_{Savg} CUSVM and V_{Savg} inversion, and (d) V_{S30} CUSVM and V_{S30} inversion.

5.12 Conclusion

While accounting for 3D variability in subsurface condition in deep basin like structures, such as the one found in the Mississippi embayment is critical for seismic design, hazard assessment, and ground motion analysis, it is challenging both technologically and economically. In this paper, a new approach is developed to generate site signature consistent pseudo 3D V_S profiles in the embayment. In this approach, parametric velocity functions for the geologic units found in the embayment are developed using data from 24 deep Vs profiles across the embayment. These parametric velocity functions, along with layer interface boundaries at a location are used to form an initial V_S profile at that location. This initial V_S profile is adjusted to capture the site signature from locally measured fundamental frequency (typically using MHVSR). Using the developed approach, model V_S profiles at 24 Himel and Wood (2022) study

sites and 11 Rosenblad et al. (2010) sites across the embayment are generated using the velocity functions, corresponding layer interface model and locally measured fundamental site frequency. Comparing the modeled and measured V_S profiles, following conclusions can be drawn:

- While differences in layering and shear wave velocities may persist, the developed approach is capable of emulating measured V_S profiles capturing the overall characteristics of a site.

- Near surface characterization using generic velocity functions may not provide good near surface results for sites with unique conditions, such as very soft alluvial material.

- The presented approach is capable of generating model V_S profiles, which generally have Vs within 10% to 20% of site-specific measured Vs profiles and within 1σ of the measured fundamental site frequency.

- The Pearson correlation coefficient between the model and measured Vs profiles indicates good association between the Vs profiles even with independently measured Vs profiles.

- Better correlation with measured Vs profiles is observed for the modeled Vs profiles using the presented approach than CUSVM modeled Vs profiles. No particular spatial bias in the modeled V_S profiles using this approach is observed, such as observed in the CUSVM V_S profiles.

Overall, this method for generating pseudo Vs profiles can be implemented in a 3D shear wave velocity model as the core method to generate site signature consistent V_S profiles. Additional elements of the 3D model are a continuous layer interface model, and a measured or

estimated fundamental frequency. This model and velocity functions will be implemented in the Mississippi Embayment to develop a more accurate 3D velocity model of the Embayment.

6. Summary, Conclusion and Future Recommendation

6.1 Summary

6.1.1 Development of SWM technique for deep site characterization

- A combination of active and passive source surface wave measurements were made at the CUSSO site. Joint inversion of the surface wave data and site fundamental frequency is conducted to develop a site signature consistent deep V_S profile.
- Downhole measurements at the CUSSO borehole arrays are conducted using a sledgehammer and vibroseis sources. A downhole V_S profile at the CUSSO site is developed.
- A comparison between the SWM and downhole V_S profile is shown. Time averaged shear wave velocity calculated from the SWM, and downhole profile are 558 m/sec and 553 m/sec, respectively, which are within 8 – 9% of the average shear wave velocity recorded from earthquake phase arrivals.
- Theoretical dispersion curves associated with the SWM and downhole V_S profile fit well with the experimental dispersion data with a misfit ranging from 0.24 – 0.57, whereas the CUSVM V_S profile at this location has a misfit of 1.49.
- Corresponding fundamental peaks from theoretical transfer function for the SWM and downhole V_S profiles are within 4% of the fundamental peak from empirical transfer function. Fundamental Rayleigh ellipticity peaks of the corresponding candidate V_S profiles are within 1% of the experimental HVSR f_0.

6.1.2 Site response impact of properly characterizing the Memphis sand layer

- A suite of pseudo V_S profiles is developed by varying the Memphis sand depth and formation velocity from the base V_S profile adopted from the downhole measurement at CUSSO.
- Linear and non-linear site response analyses using the pseudo and base V_S profiles are conducted.
- Varying the velocity of the Memphis sand impacts the amplification of the surface motion up to 12%. However, no influence on the frequency/period of amplification is observed due to a change in the Memphis sand velocity.
- Varying the depth to the Memphis sand layer influences the first harmonic frequency of resonance up to 12% from the base V_S profile's first harmonics in the linear analysis. In the non-linear analysis, 10 – 30% difference below 1.0 sec period is observed in spectral acceleration for the pseudo V_S profiles and the base V_S profile, whereas this difference increased up to 45% in the 1 – 2 sec period range.

6.1.3 Deep shear wave velocity profiles at 24 study sites from surface wave measurements

- Active and passive source surface wave measurements are conducted at 24 sites (including CUSSO) across the Mississippi embayment.
- Deep V_S profiles are generated at the 24 study sites using SWM. Multimodal joint inversion of experimental dispersion data and fundamental frequency at each site is conducted to develop site signature consistent V_S profile. A median V_S profile is calculated at each site from the best 1000 minimum misfit V_S profiles from a pool of 2 million inversion solutions.

- All developed SWM V_S profiles capture site signature from experimental dispersion data and fundamental frequency within one standard deviation.
- Comparison between the CUSVM V_S profiles and measured SWM V_S profiles is shown. The modeled CUSVM V_S profiles have lower shear wave velocities than their corresponding measured SWM V_S profiles ranging from 30 – 50%, indicating spatial bias across the embayment.
- Time averaged shear wave velocity down to the bedrock for the 24 developed V_S profiles ranged from 462 – 686 m/sec, with higher average velocities for deeper sites and vice versa. Site periods for the 24 study sites ranged from 2 – 5 sec, with longer site periods for the deeper sites and vice versa.
- Average formation velocities calculated for the geologic units Quaternary, Upper Tertiary, Memphis sand, Paleocene, Cretaceous, and Paleozoic bedrock are 214, 418, 607, 665, 967 and 2211 m/sec, respectively.

6.1.4 Approach for developing site signature consistent V_S profiles from power-law functions

- Power-law velocity functions for the geologic units found in the Mississippi embayment are developed utilizing the deep V_S profiles from 24 study locations across the embayment.
- Initial model V_S profile for a location is developed utilizing the velocity functions, mean formation velocity of the geologic units and layer interface information at that location.
- The initial model V_S profile is adjusted by scaling up or down the layer shear wave velocities to match the fundamental transfer function peak to the experimental HVSR f_0. Similarly, bedrock V_S is adjusted to match fundamental peak ellipticity to the HVSR f_0.

- All modeled V_S profiles for the 24 study sites have theoretical transfer function peaks within one standard deviation of the measured fundamental frequency.
- Comparison between the modeled and measured V_S profiles at the 24 study sites are shown. Most modeled V_S profiles are within 10% of the measured V_S profiles at all depth ranges. However, differences of up to 30% are observed in near surface layers.
- Time averaged V_S is calculated down to bedrock, V_{Savg} and for the top 30 m depth, V_{S30} for the modeled and measured V_S profiles. Differences between the modeled and measured V_{Savg} ranged from 0.5 – 8.5%, with average percent difference below 4%. Differences between the measured and modeled V_{S30} is very broad and ranged from 0.3 – 44%, with average difference below 8%.
- Pearson correlation coefficient is calculated for V_{Savg} and V_{S30} between the modeled and measured V_S profiles. Pearson correlation coefficient for the V_{Savg} and V_{S30} are 0.95 and 0.49, respectively. For the CUSVM V_S profiles, the calculated Pearson correlation coefficient between modeled and measured V_{Savg} and V_{S30} are 0.16 and 0.18, respectively.
- Using the developed approach, model V_S profile at 11 Rosenblad et al. (2010) sites are generated. Most of the modeled V_S profiles at the Rosenblad et al. (2010) sites are observed to be within 15% of the measured V_S profiles at most depth ranges down to 150 m. Time averaged V_S down to 150 m, $V_{S150,}$ is calculated for the modeled and measured V_S profiles at the Rosenblad et al. (2010) sites. Pearson correlation coefficient for the V_{S150} between the modeled and measured Rosenblad et al. (2010) sites is 0.75.

6.2 Conclusion

The conclusions that are drawn from this dissertation are as following:

6.2.1 Utilizing SWM for deep site characterization

While SWM site characterization is inherently non-unique, careful curation of SWM inversion solution combining both experimental dispersion characteristics and fundamental frequency can provide comparable site characterization result as invasive methods. Deep site characterization using SWMs is challenging due to the lack of low frequency energy, identification of modes of wave propagation, and presence of effective mode dispersion data. However, utilizing both active and passive source surface wave measurements ensures proper layer characterization at shallow depths and enough resolution at deeper depths, respectively. The below conclusions are made from the results of this dissertation:

- Array size is a critical aspect of surface wave measurements. Previously, a passive array of 3 ~ 4 times the diameter of the resolved depth was suggested. Nevertheless, array size of 0.5 ~ 1 times the diameter of the target resolution depth is found to be sufficient when resolving dispersion data utilizing multiple transformation techniques, such as the MSPAC and HRFK.
- While the HRFK method is capable of resolving low frequency data on the order of 0.1 Hz, most of the very low frequency data resolved are effective or higher mode, making the use of this low frequency data difficult and requiring experienced analyst to understand.
- Although parameterization plays an important role in SWM site characterization, both blind and guided approaches provides comparable results when parameters are prepared carefully utilizing engineering judgement and local geology.

- The blind approach of developing SWM parameterizations might not be able to detect velocity reversals in very deep layers. Iterative parameterization should be used when velocity reversals are likely.
- If available, a-priori information should be utilized to prepare parametrization. This could lead to less computational effort in the inversion process.
- The S_H wave transfer function and fundamental mode Rayleigh ellipticity works as a tool to assess a V_S profile's capacity of capturing the local site signature. Regardless of the SWM's non-uniqueness, filtering out inversion V_S profiles based on their theoretical peaks provides robust and comparable results as invasive methods.

6.2.2 Site response impacts of shallow impedance boundary

The shallow impedance boundary found in the Mississippi embayment from the Memphis sand has a variable depth to the layer across the embayment. Depending on the over-consolidation stress above the Memphis sand layer, velocity variation is also observed. While shallow impedance boundaries are observed to be responsible for seismic amplifications at particular frequencies, the Memphis sand is still poorly characterized. Based on the results of this dissertation, following conclusions are made regarding this issue:

- Shear wave velocity of the Memphis sand layer primarily influences the first harmonic peak amplification and does not affect the frequency range of the amplification. Incorrect assignment of shear wave velocity to this layer will result in inappropriate amplification due to the shallow impedance boundary.
- Depth to the Memphis sand layer has a more significant impact on site response than the shear wave velocity of this layer as varying the depth influences both the frequency range for amplification and surface spectral acceleration.

- Varying the depth or shear wave velocity of the Memphis sand layer has greater influence in periods ranging from 1 – 2 second. This implies that poor characterization of the Memphis sand layer would have adverse affect on important infrastructure, such as public transportation bridges and skyscrapers with natural frequency within 1 – 2 second range and may lead to inaccurate seismic design loads. Therefore, careful characterization of the shallow impedance boundary is essential for avoiding potential hazardous or economic penalties due to under-designing or over-designing of infrastructure.

6.2.3 Deep V_S profiles in the Mississippi embayment

While the CUSVM model provided a 3D model of the Mississippi Embayment, differences in layer velocity and layer interface depths are observed between the measured SWM V_S profiles and CUSVM V_S profiles. Based on the results of this dissertation following conclusions are made on this issue:

- Deep V_S profiles modeled by the CUSVM tend to have lower shear wave velocities for deeper layers, particularly for layers below the Upper Tertiary unit. Due to a lower overall stiffness of the CUSVM V_S profiles, when used in site response analysis, they can result in lower surface spectral acceleration due to higher damping.
- Modeled V_S profiles from the CUSVM tend to have differences in layer interface depths when compared to the measured inversion profiles, particularly for the Memphis sand layer. Overall, CUSVM V_S profiles have shallower Memphis sand layer depths than the measured SWM inversion V_S profiles. Inaccurate characterization of the Memphis sand at shallower depths might lead to over-prediction of surface spectral acceleration below a 2 second period and under-prediction above a 2 second period as per the results from chapter 3, which could lead to over-designed or under-designed structures, respectively.

6.2.4 Approach to develop 3D model for the Mississippi embayment

Conclusions from the results of modeled V_S profiles from the developed approach are as following:

- Velocity functions for geologic units can provide valuable information regarding geologic layer stiffness if sufficient data is used to develop the velocity functions. However, velocity functions may have limited applicability outside a region as they are derived from regional material stiffness data. Velocity functions developed in this dissertation from 24 deep V_S profiles are observed to emulated measured V_S profiles when used in conjunction with representative layer boundaries.

- A layering ratio approach to define sublayers within each geologic layer prevented development of any velocity contrasts within the layer. Layering ratio of 1.3 and 1.5 were used in this dissertation for the shallow and deep layers, respectively, which is observed to fit very well with measured SWM V_S profiles in the Mississippi embayment.

- Modeling of the near surface layers using the generalized velocity functions is not always fruitful. Velocity functions bearing general trend of geologic unit's stiffness may fail to accurately characterize the very shallow layers with specific conditions as observed in the results of this dissertation.

- While the models from the developed approach might have differences in layering and shear wave velocities compared with the measured V_S profiles, the overall modeled V_S profile has same linear site response as the measured V_S profile.

- Modeled V_S profiles from the developed approach are better correlated to the measured V_S profiles than the CUSVM V_S profiles, indicating a need to develop a new 3D shear wave velocity model for the Mississippi embayment.

6.3 Recommendations for Future Research

While this dissertation details many issues regarding surface wave methods and deep site characterization, more research is needed in regards to the surface wave method technique, layer interface models, and 3D shear wave velocity models for the embayment. Proposed topics for future study are as follows:

- Surface waves at very low frequency is often propagated with effective/higher modes, identification of the correct mode is critical for inversion process but difficult. Identification of the effective and higher mode data is still subjective and requires prior experience. A systematic investigation of mode identification method is required to eradicate subjectivity of analyst.
- Deep site characterization using SWM is often limited by the availability of low frequency energy and relies on the quality of resolved dispersion characteristics at low frequencies. Reliability of the resolved low frequency energy and their dependence on the transformation technique is crucial for representative site characterization. A future study could be conducted to examine the performance of different broadband sensors' capability capturing low frequency energy as well as different transformation techniques' resolving the low frequency dispersion data.
- Parameterization is critical for deriving representative site characterization solutions from surface wave inversion. In this dissertation, comparable results were achieved for both the guided and blind approach parameterization. However, a velocity reversal was not detected in the blind approach. Research to develop systematic parameterization in absence of a-priori knowledge is crucial for surface wave methods' universal applicability.

This future research could include dispersion curve's features, such as gradient, phase velocity range, frequency range of interest while developing a systematic approach.

- The developed approach in this dissertation to model site signature consistent deep V_S profiles requires further study to implement this approach in a new 3D velocity model for the embayment. In addition to the developed approach, elements of this new 3D model could be a continuous layer interface model and a mesh of fundamental frequency to enable the model to interpolate fundamental frequency and layer interfaces at any target location within the Mississippi embayment. This fundamental frequency and layer interface will be used in conjunction with the developed approach to generate a site signature consistent pseudo deep V_S profile at a target location. Depending on availability, following user inputs could be allowed in the 3D model to have more site-specific characteristics in the developed V_S profiles: layer interface model/fundamental frequency/V_S measurement of top 30 m.

7. Reference

American Society of Civil Engineers (ASCE), 2017. Minimum design loads and associated criteria for buildings and other structures, ASCE 7-16, Reston, VA.

Aki K (1957) Space and time spectra of stationary stochastic waves, with special reference to microtremors. Bull Earthq Res Inst 35:415–456

Afshari, K., and Stewart J. P., 2019. Insights from California vertical arrays on the effectiveness of ground response analysis with alternative damping models, *Bulletin of the Seismological Society of America* **109(4)**, 1250–1264.

Bard PB-Y, Campillo M, Chavez-Garcia FJ, Sanchez-Sesma F, 1988. A theoretical investigation of large- and small-scale amplification effects in the Mexico City valley, *Earthq Spectra* **4**, 609–33.

Bodin, P., Smith, K., Horton, S., Hwang, H., 2001. Microtremor observations of deep sediment resonance in metropolitan Memphis, Tennessee, Engineering Geology 62, 159-168.

Bonnefoy-Claudet, S., Kohler, A., Cornou, C., Wathelet, M., Bard, P.-Y., 2008. Effects of love waves on Microtremor H/V ratio, Bull. Seism. Soc. Am 98(1), 288-300.

Boore, D. M., 1999. Basin Waves on a Seafloor Recording of the 1990 Upland, California, Earthquake: Implications for Ground Motions from a Larger Earthquake, *Bull. Seism. Soc. Am.* **89(1)**, 317-324.

Bazzurro, P. and Cornell, A. (2004). Nonlinear Soil-Site Effects in Probabilistic Seismic-Hazard Analysis, BSSA, 94(6): 2100-2123.

Bakun, W.H. and Hopper, M.G. (2004). "Magnitude and locations of the 1811-1812 New Madrid, Missouri and the 1886 Charleston, South Carolina, Earthquakes", Bulletin of the Seismological Society of America, 94(1), 64-75.

Brahana, J.V., Parks, W. S., and Gaydos, M. W., 1987. Quality of Water from Freshwater Aquifers and Principal Well Fields in the Memphis Area, Tennessee, USGS Water- Resources Investigations Report 87-4052, Reston, VA.

Cox, B.R., Ellis, T.B., and Griffiths, S.C., 2012. Site-Specific Ground Motion Analyses for Transportation Infrastructure in the New Madrid Seismic Zone, MBTC 3032.

Cox, B.R., Wood, C.M., Teague, D.P., 2014. Synthesis of the UTexas1 Surface Wave Dataset Blind-Analysis Study: Inter-Analyst Dispersion and Shear Wave Velocity Uncertainty, in *Proceedings, Geo-Congress 2014 Technical Papers*, Atlanta, Georgia, pp. 850–859.

Cramer, H., 2006. Quantifying the uncertainty in site amplification modeling and its effects on site specific seismic-hazard estimation in the upper Mississippi Embayment and adjacent areas, Bulletin of the Seismological Society of America 96, 2008–2020.

Deschenes, M.R., Wood, C.M., Wotherspoon, L.M., Bradley, B.A., and Thomson, E., 2018. Development of Deep Shear Wave Velocity Profiles in the Canterbury Plains, New Zealand, *Earthquake Spectra* **34**, 1065 - 1089.

De Martin, F., S. Matsushima, and H. Kawase (2013). Impact of geometric effects on near-surface Green's functions, *Bull. Seismol. Soc. Am.* **103**, 3289–3304.

DiGiulio, G., Savvaidis, A., Ohrnberger, M., Wathelet, M., Cornou, C., Knapmeyer-Endrun, B., Renalier, F., Theodoulidis, N., and Bard, P. Y., 2012. Exploring the model space and ranking a best class of models in surface-wave dispersion inversion: Application at European strong motion sites, *Geophysics* **77(3)**, B147–166.

Electric Power Research Institute (EPRI), 2012. *Seismic Evaluation Guidance: Screening, Prioritization and Implementation Details (SPID) for the Resolution of Fukushima Near-Term Task Force Recommendation 2.1: Seismic*, EPRI Rep. 1025287, Palo Alto, CA, 206.

Field, E., and Jacob, K., 1993. The theoretical response of sedimentary layers to ambient seismic noise, *Geophys. Res. Lett.* **20**, 2925–2928.

Foti, S., Lai, C., Rix, G., and Strobbia, C. (2014). "Surface Wave Methods for Near-Surface Site Characterization. Boca Raton, FL: CRC Press.

Frankel, A.D., Applegate, D., Tuttle, M.P., and Williams, R.A., (2009). Earthquake hazard in the New Madrid Seismic Zone remains a concern: U.S. Geological Survey Fact Sheet 2009–3071, 2 p.

Garofalo, F., et al., 2016. InterPACIFIC project: Comparison of invasive and non-invasive methods for seismic site characterization. Part I: Intra comparison of surface-wave methods, *Soil Dynamics and Earthquake Engineering* **82**, 222 – 240.

Griffiths, S. C., Cox, B. R., Rathje, E. M., and Teague, D. P., 2016a. Mapping dispersion misfit and uncertainty in VS profiles to variability in site response estimates, *Journal of Geotechnical and Geoenvironmental Engineering* **142**(11), 04016062 1-12.

Griffiths SC, Cox BR, Rathje EM, Teague DP. (2016b) Surface wave dispersion approach for evaluating statistical models that account for shear wave velocity uncertainty. J Geotech Geoenviron Eng 2016;142(11):04016061.

Guo, Z., Aydin, A., 2016. A modified HVSR method to evaluate site effect in Northern Mississippi considering ocean wave climate, Engineering Geology 200, 104-113.

Guéguen, P., Chatelain, J.-L., Guillier, B., and Yepes, H., 2000. An indication of the soil topmost layer response in Quito (Ecuador) using HVSR spectral ratio, *Soil Dyn. Earthq. Eng.* **19**, 127–133.

Hallal, M. M., Cox, B. R., 2021. An H/V geostatistical approach for building pseudo-3D Vs models to account for spatial variability in ground response analyses Part II: Application to 1D analyses at two downhole array sites, *Earthquake Spectra*, **37(3)**, 1931-1954.

Hashash , Y. M. A., Kottke A. R., Stewart J. P., Campbell, K. W., Kim B., Moss, C., Nikolaou, S., Rathje E. M., Silva, W. J., 2014. Reference Rock Site Condition for Central and Eastern North America, *Bulletin of the Seismological Society of America* **104 (2)**, 684–701.

Hashash, M.A., Park, D., 2001. Non-linear one-dimensional seismic ground motion propagation in the Mississippi Embayment, *Engineering Geology* **62**, 185-206.

Himel, A., 2018. Utilizing the HVSR Second Peak for Surface Wave Inversions in the Mississippi Embayment, Masters Thesis, Department of Civil Engineering, University of Arkansas, Fayetteville, AR.

Himel, A. K., Wood, C. M., 2021a. Developing an Updated Set of V_S Profiles for the Central United States Seismic Observatory with Estimates of Uncertainty between Different Methods, *Soil Dynamics and Earthquake Engineering* **143**.

Himel, A. K., Wood, C. M., Rahimi, S., 2021b. Site Response Impacts of the Memphis Sand Layer within the Mississippi Embayment, in *Proceedings, Geo Extreme 2021*, Savannah, Georgia.

Himel, A. K., Wood, C. M., 2022. Deep shear wave velocity profiles in the Mississippi embayment from surface wave measurements, *Soil Dynamics and Earthquake Engineering* **158**.

Heisey, J.S., Stokoe, K.H and Meyer, A.H. 1982. Moduli of pavement systems from Spectral Analysis of Surface Waves. Transportation Research Record, No. 852, Washington D.C., pp 22-31.

Kawase, H., 2003. Site Effects on Strong Ground Motions. International Handbook of Earthquake and Engineering Seismology, Part B, W. H. Lee, H. Kanamori, P. C. Jennings, and C. Kisslinger, eds., Academic Press, 1013-1030.

Kramer, S. L., 1996. *Geotechnical earthquake engineering*. Upper Saddle River, N.J.: Prentice Hall.

Langston, L. and Horton, S. (2014). Three-Dimensional Seismic-Velocity Model for the Unconsolidated Mississippi Embayment Sediments from H/V Ambient Noise Measurements. BSSA, 104(5) 2349-2358.

Lin, Y. C., Joh, S. H, and Stokoe, K. H., 2014. Analyst J: Analysis of the UTexas 1 Surface Wave Dataset Using the SASW Methodology, Geo-Congress 2014 Technical Papers: Geo-Characterization and Modeling for Sustainability. GSP 234. 2014.

Liu, H. -P., Hu, Y., Dorman, J., Chang, T.-S., and Chiu, J. M., 1997. Upper Mississippi Embayment Shallow Seismic Velocities measured in situ, *Eng. Geol*. **46**, 313–330.

Li, W., and Assimaki, D., 2010. Site- and Motion-Dependent Parametric Uncertainty of Site-Response Analyses in Earthquake Simulations, *Bull. Seism. Soc. Am.* **100**(3), 954–968.

Malischewsky, P. G., Scherbaum, F., 2004. Love's formula and H/V-ratio (ellipticity) of Rayleigh waves, *Wave Motion* **40 (1)**.

Mayoral, J. M., et al., 2019. Site effects in Mexico City basin: past and present, *Soil Dynamics and Earthquake Engineering* **121.**

Magistrale, H., McLaughlin, K., Day, S., 1996. A geology-based 3D velocity model of the Los Angeles basin sediments. *Bull Seismol Soc Am* **86**, 1161–6.

Mento, D.J., Ervin, C.P., McGinnis, L.D., 1986. Periodic energy release in the New Madrid seismic zone, *Bull Seismol Soc Am* **76**, 1001-1009.

Nakamura, Y., 1989. A method for dynamic characteristics of subsurface using microtremors on the ground surface, Quick Report of Railway Technical Research Institute, 30, 25-33.

Nazarian, S., and Stokoe, K.H. 1984. In situ shear wave velocities from spectral analysis of surface waves. *In* Proceedings 8th world conf. on earthquake engineering. **3**, pp 31-38.

Ng, K. W., Chang, T. S., Hwang, H., 1989. Subsurface conditions of Memphis and Shelby County. Technical Report NCEER-89-0021, National Center for Earthquake Engineering Research, State University of New York at Buffalo, Buffalo, NY.

Nogoshi M. and T. Igarashi, (1971). On the amplitude characteristics of microtremor (part 2) (in Japanese with english abstract). Jour. Seism. Soc. Japan, 24, 26-40.

Nour, A., Slimani, A., Laouami, N., Afra, H., 2003. Finite element model for the probabilistic seismic response of heterogeneous soil profile, *Soil Dynamics and Earthquake Engineering* **23(5)**, 331–348.

Park, C.B., Miller, R.D. and Xia, J., 1999. Multichannel analysis of surface waves, *Geophysics* **64(3)**, 800-808.

Park, C.B., Miller, R.D., Ryden, N., Xia, J., and Ivanov, J., (2005). "Combined use of active and passive surface waves." Journal of Engineering and Environmental Geophysics (JEEG), Vol. 10 (3): 323-334.

Ramírez-Guzmán, L., O., Boyd, S., Hartzell, R., Williams, 2012. Seismic velocity model of the central United States (Version 1): Description and simulation of the 18 April 2008 Mt. Carmel, Illinois, Earthquake, *Bull. Seism. Soc. Am.* **102**, 2622-2645.

Raitt, R. W., 1954. Seismic refraction studies of Bikini and Kwajelein Atolls. *Geological Survey Professional Paper*, 260-K.

Rahimi, S., Wood, C. M., Bernhardt-Barry, M., Himel, A. K., 2019. Updated Reference Shear Wave Velocity Curves for Near-Surface Site Characterization, in *Proceedings, Geo-Congress 2019*, Philadelphia, Pennsylvania.

Romero, S.M., Rix, G.J., 2005. Ground Motion Amplification of Soil in the Upper Mississippi Embayment, *Report No. GIT-CEE/GEO-01-1*, National Science Foundation Mid America Center, Atlanta.

Rathje E. M., Kottke A. R. and Trent W. L., 2010. Influence of input motion and site property variabilities on seismic site response analysis, *Journal of Geotechnical and Geoenvironmental Engineering* **136**(4), 607- 619.

Rodgers, A., Petersson, N. A., Nilsson, S., Sjogreen, B., McCandless, K., 2008. Broadband waveform modeling of moderate earthquakes in the San Francisco Bay Area and preliminary assessment of the USGS 3D seismic velocity model, *Bull Seismol Soc Am* **98**, 969–88.

Rosenblad, B., Bailey, J., Csontos, R., and Van Arsdale, R., 2010. Shear Wave Velocities of Mississippi Embayment Soils from Low Frequency Surface Wave Measurements, *Soil Dynamics and Earthquake Engineering* **30**, 691 – 701.

SESAME, 2004. Guidelines for the implementation of the H/V spectral ratio technique on ambient vibrations: measurements, processing and interpretation, 62 pp.. http://sesamefp5.obs.ujfgrenoble.fr/Delivrables/Del-D23

Socco, L.V., Foti, S., and Boiero, D., 2010. Surface-wave analysis for building near-surface velocity models — Established approaches and new perspectives, *Geophysics* **75** (5), A83 – A102.

Street, R., Woolery, E. W., & Chiu, J.-M., 2004. Shear-wave Velocities of the Post-Paleozoic Sediments across the Upper Mississippi Embayment, *Seismological Research Letters* **75**(3), 390–405.

Tao, Y., and Rathje, E., 2019. Insights into modeling small-strain site response derived from Downhole Array data, *Journal of Geotechnical and Geoenvironmental Engineering* **145(7)**, 04019023.

Teague DP, Cox BR. (2016). Site response implications associated with using non-unique Vs profiles from surface wave inversion in comparison with other commonly used methods of accounting for vs uncertainty. Soil Dyn Earthq Eng 2016;91:87–103.

Teague DP, Cox BR and Rathje EM (2018) Measured vs. predicted site response at the Garner Valley Downhole Array considering shear wave velocity uncertainty from borehole and surface wave methods. Soil Dynamics and Earthquake Engineering 113: 339–355.

Teague DP, Cox BR, Bradley B, Wotherspoon L. Development of Deep Shear Wave Velocity Profiles with Estimates of Uncertainty in the Complex Inter-Bedded Geology of Christchurch, New Zealand. Earthq Spectra 2018. http://dx.doi.org/10.1193/041117EQS069M.

Thomson, E.M., Bradley, B.A., Lee, R.L., Wotherspoon, L.M., Wood, C.M., Cox, B.R. (2020). Generalised parametric functions and spatial correlations for seismic velocities in the Canterbury, New Zealand region from surface-wave-based site characterisation, Soil Dynamics and Earthquake Engineering, Vol. 128, January 2020, 105834.

Tokimatsu, K., Shinzawa, K., and Kuwayama, S. (1992). "Use of short-period microtremors for Vs profiling." Journal of Geotechnical Engineering, Vol. 118 (10): 1544-1558.

Toro, G., 1995. *Probabilistic Models of the Site Velocity Profiles for Generic and Site Specific Ground Motion Amplification Studies*. Technical Rep. 779574, Brookhaven National Laboratory, Upton, NY, 147.

Van Arsdale, R.B., TenBrink, R.K., 2000. Late Cretaceous and Cenozoic Geology of the New Madrid Seismic Zone, *Bull. Seism. Soc. Am.* **90**, 345–356.

Wathelet, M., 2008. An improved neighborhood algorithm: parameter conditions and dynamic scaling, *Geophysical Research Letters* **35**, L09301.

Wood, C., Ellis, T., Teague, D., Cox, B. (2014). Analyst I: Comprehensive Analysis of the UTexas1 Surface Wave Dataset. 2014 Geo-Congress: Geo-Characterization and Modeling for Sustainability. Feb. 23-26, 2014, 820-829.

Wood, C. M., and Baker, E. R. B., 2018. Cost Savings of Implementing Site-Specific Ground Motion Response Analysis in the Design of Short-Period Mississippi Embayment Bridges, *Earthquake Spectra* ***34*****(3)**, 1155–1175.

Wood C., Himel, A., (2019). Development of Deep Shear Wave Velocity Profiles at Seismic Stations in the Mississippi Embayment, USGS Project report, https://earthquake.usgs.gov/cfusion/external_grants/reports/G18AP00078.pdf

Woolery, E.W., Wang, Z., Carpenter, N.S., Street, R. Brengman, C., 2016. The Central United States Seismic Observatory: Site Characterization, Instrumentation, and Recordings, *Seismological Research Letters* **87(1)**, 215-218.

Yoon, S., and Rix, G. (2004). "Combined active-passive surface wave measurements for near-surface site characterization. Proc., Symposium on the Applications of Geophsics to Engineering and Environmental Problems, Vol. 17, Denver, CO: 1556-1564.

Zywicki, D.J. (2007). "The impact of seismic wavefield and source properties on ReMi estimates." Proc., Geo-Denver 2007, Innovative Applications of Geophysics in Civil Engineering, Geotechnical Special Publication 164 (CD-ROM), ASCE, Reston, VA.